SYRACUSE UNIVERSITY RESEARCH CORPORATION

A STATISTICAL ANALYSIS OF SITING ERROR IN RADIO DIRECTION-FINDING

DSD R-161

Prepared Under
Office of Naval Research
Contract NOnr 4798(00)
for U.S. Marine Corps
(R and D Project CS 454 and CS 471)

30 August 1967

"DISTRIBUTION OF THIS DOCUMENT IS UNLIMITED"

DEFENSE SYSTEMS DIVISION

A STATISTICAL ANALYSIS OF SITING ERROR IN RADIO DIRECTION-FINDING

DSD R-161

Prepared Under
Office of Naval Research
Contract NOnr 4798(00)
Contract Authority No. NR-259-051/2-18-66
for
U.S. Marine Corps
(R and D Project CS 454 and CS 471)

Laurence A. Lyons

30 August 1967

DEFENSE SYSTEMS DIVISION

SYRACUSE UNIVERSITY RESEARCH CORPORATION

"DISTRIBUTION OF THIS DOCUMENT IS UNLIMITED"

BLANK PAGE

TABLE OF CONTENTS

TABLE OF CONTENTS (continued)

LIST OF ILLUSTRATIONS

LIST OF ILLUSTRATIONS (continued)

LIST OF ILLUSTRATIONS (continued)

LIST OF TABLES

PREFACE

Choosing a beachhead site for HF D/F in support of an amphibious operation usually involves a choice among mediocre or even poor locations. The number of suitable sites is restricted by both the need for security and the limitations imposed by D/F requirements themselves. The latter requirements may be broken up into two general categories:

a) Physical characteristics (i.e., is it large enough and sufficiently clear and level for antenna erection?) and

b) Electrical characteristics (i.e., are there nearby scattering objects such as hills, equipment, etc.?).

As severe as these limitations are, there is at present no formal site classification scheme, nor a tactically usable method of electrical site evaluation. It is clear that the electrical characteristics must be determined before any meaningful classification can be made.

The purpose of this report is to present a quantitative basis for site classification (see Table P-I) and a significantly simplified method of measuring the electrical characteristics of certain sites. The body of the report deals with the method of measurement. This method seems highly promising on a theoretical and scale-model experimental basis, but for final validity awaits spot-checking at HF frequencies.

Table P-I gives some examples of the physical sizes required for some given antennas. For example, the Wullenweber requires a nearly 1,000-foot diameter and the AN/TRD-21 requires 75 feet just

PHYSICAL PARAMETERS

Clear Diameters (in feet)	Examples
300 - 1000	Wullenweber
100 - 300	Doppler
30 - 100	Adcock
10 - 30	Elevated H
3 - 10	Whip

ELECTRICAL PARAMETERS

k^2	Examples
$3\text{-}10^{-3}$ - 10^{-3}	Null depth of 28 - 33 dB
10^{-2} - $3\text{-}10^{-3}$	Null depth of 23 - 28 dB
$3\text{-}10^{-2}$ - 10^{-2}	Null depth of 18 - 23 dB
10^{-1} - $3\text{-}10^{-2}$	Null depth of 13 - 18 dB
$3\text{-}10^{-1}$ - 10^{-1}	Null depth of 8 - 13 dB

TABLE P-I PHYSICAL AND ELECTRICAL PARAMETERS

for the antenna elements. Examples are also given for the electrical parameter, k^2, which is a ratio of average scattered power to direct power. This parameter was related to null depth of a figure-eight pattern, not only to make the classification less arbitrary, but also to give the user more of a "feel" for its meaning. A null depth of 20 dB may be considered average for most siting conditions, while 30 dB indicates a good location and a minimum of scattering obstacles. Similarly, a 10 dB null depth would indicate a relatively poor D/F site. The method of converting k^2 into equivalent null depth is given in Appendix A.

The currently available method of determining the electrical character of a site is extremely complicated and time-consuming under the best of circumstances. In order to test a D/F site, one must move a transmitter around the receiving antenna at a given distance and take readings for each azimuthal position at all frequencies of interest. The disadvantages here are obvious. Keeping a known distance from the antenna of several thousand yards is impossible under beachhead constraints. Even if it were feasible to maintain a fixed distance, the allowed azimuthal positions would fall far short of those required.

The new technique described in this report will enable a transmitter at one or two fixed positions to scan the frequencies of interest and extract the same information as is obtained by the more cumbersome procedure. Chapter 4 of this report gives the general experimental techniques. A practical guide to the field use of this method may be summarized as follows:

1) Place a target transmitter approximately 100 wavelengths distant from the site.

2) Sweep the transmitter over a one-octave band centered on the frequency of interest.

3) Continuously record the received field strength (measured with a whip) at the site as a function of frequency.

4) Construct a moving average field strength by averaging, at each frequency, the field strength over a 0.1 octave band centered on that frequency.

5) Take the ratio of the measured field strength to the moving average field strength at 40 equispaced points over the octave band.

6) Determine the variance of these 40 samples. This is the value of k^2.

The actual numbers given are somewhat arbitrary and other choices may be found to be satisfactory. Steps 4 through 6 may be quickly performed with a special portable device. While this device is not yet available, a diagram is shown in Figure P-1.

Having obtained the electrical parameter, it is feasible to assign a physical parameter on the basis of available site diameter as shown in Table P-I. For conciseness, we may assign coded labels to all of the parameters in Table P-I and regroup them as shown in Table P-II. On the basis of this table, one may now speak of a D/F site as belonging to one of 25 categories; e.g., A-3, B-1, D-5, etc. This removes

A3518

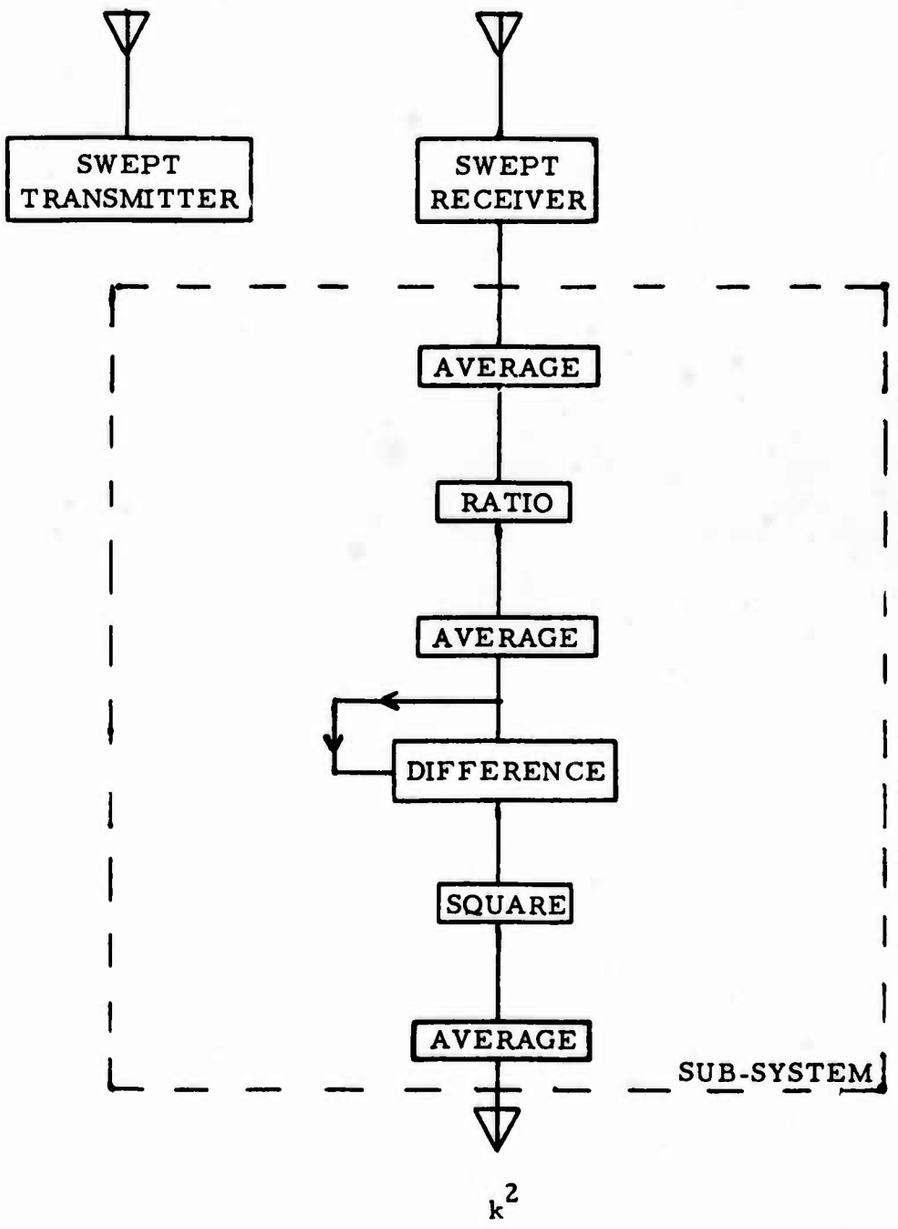

FIGURE P-1 A POSSIBLE AUTOMATIC METHOD OF ELECTRICAL CHARACTERIZATION OF HF D/F SITES

Physical		Electrical	
Code	Diameter (feet)	k^2	Code
A	300 - 1000	10^{-3} - $3\text{-}10^{-3}$	1
B	100 - 300	$3\text{-}10^{-3}$ - 10^{-2}	2
C	30 - 100	10^{-2} - $3\text{-}10^{-2}$	3
D	10 - 30	$3\text{-}10^{-2}$ - 10^{-1}	4
E	3 - 10	10^{-1} - $3\text{-}10^{-1}$	5

TABLE P-II SITE PARAMETERS

the use of such qualitative terms as "good" and "poor." Although each category defines a range of values for each parameter, they are well-defined and subject to experimental verification.

The work described in this report covers the theoretical justification of the model used and provides experimental verification for a scaled-down model. The materials used were chosen to correspond to actual conditions at HF. Ultimately, the scheme will require full-scale verification in the HF region, as well as the collection of enough data to further verify the statistical nature of the study.

JAMES CARMICHAEL

A STATISTICAL ANALYSIS OF SITING ERROR IN RADIO DIRECTION-FINDING

by

Laurence Anthony Lyons

A. B., Harvard University, Cambridge, Massachusetts, 1960

M. E. E., Syracuse University, Syracuse, New York, 1964

Dissertation

Submitted in partial fulfillment of the requirements for the degree of Doctor of Philosophy in Electrical Engineering in the Graduate School of Syracuse University, May, 1967

APPROVED:_____

DATE:_____

ACKNOWLEDGMENTS

My interest in radio direction-finding evolved into the work presented here through many invaluable discussions with my advisor, Dr. A. T. Adams. I am deeply indebted to him for his guidance and encouragement.

I wish to express my thanks to the management of the Syracuse University Research Corporation and particularly to Dr. B. E. Simmons, for the support given my efforts.

My wife has been a continual source of strength and confidence during the completion of this study.

I am grateful to the secretarial staff of the Syracuse University Research Corporation and Mary Jo Fairbanks of the Electrical Engineering Department for their assistance in preparing this manuscript. Mr. A. H. Berical of the Syracuse University Research Corporation provided much help in the mechanical design of the experimental apparatus.

This work was sponsored by the Office of Naval Research and the U.S. Marine Corps under Contract NOnr 4798(00).

ABSTRACT OF THESIS

Reradiation from various parts of the site is a significant cause of direction-finding error in the HF (1 – 30 MHz) band. Previous investigators have considered the errors introduced by one or two localized reradiators (e.g., towers, small objects). Only a small minority of sites is characterized by the presence of such obstacles. In this work a statistical model of a site is devised to analyze the effect of extended reradiators (e.g., hills, buildings) or D/F accuracy. Such a model applies to the majority of D/F sites encountered in practice.

In the model a series of assumptions leads to an explicit expression for the probability density distribution of the electric field amplitude at the direction-finder as each of two quantities is varied:

A) the azimuthal position of a target transmitter;

B) the frequency of a target transmitter.

If the derived density distribution is expressed as a function of the ratio of the total electric field amplitude (scattered waves plus direct wave) to the direct wave amplitude, the distribution, in each case, becomes a one-parameter Rice distribution. It is suggested that this parameter be employed as a single-number criterion for evaluating D/F sites. The parameter, which is the ratio of the mean square power in the scattered waves to the power in the direct wave, may be determined by calculating the variance of a number of samples of the received electric field amplitude (normalized to the direct wave). These samples may be taken over angle, with the transmitter frequency fixed, or, equivalently, over frequency, with the transmitter position fixed.

The validity of the statistical model was examined theoretically and experimentally. In the theoretical work, the case of scattering from perfectly conducting hemispherical bosses on a conducting plane was found to be well described by the statistical model. In the experimental work, the case of scattering from irregularly shaped obstacles on an imperfectly conducting earth was also adequately described by the model.

The new results contained in this work are as follows:

1) The application of statistical methods to D/F site selection. Although the theory employed has appeared in the literature on ionospheric propagation and rough-surface scattering, the assumptions leading to the theory had to be justified and reinterpreted in the context of this problem.

2) The introduction of a single-parameter evaluation of a site. Current methods of site evaluation are rule-of-thumb procedures, which do not possess a firm analytical basis. The single parameter proposed is a physically acceptable measure of site quality and can be directly related to the accuracy of a specific direction-finder on a given site.

3) The equivalence of measurements at various angles of arrival (A, above) to measurements at various frequencies (B, above). This is probably the most useful single result of the investigation. The IEEE recommends a rough technique for site selection, which depends on an examination of the fluctuations in the received power as a target transmitter is moved in a circular path about the site. For large radius circles, this

is generally a difficult procedure. The simplified procedure recommended in this work involves examining the fluctuations in received power as the frequency of a fixed position target transmitter is varied.

4) A means of correcting for the presence of a few obstacles in the vicinity of the direction-finder. The means suggested becomes cumbersome for more than three obstacles, but it is an improvement over present methods, which can correct for only one obstacle.

Chapter 1

INTRODUCTION

Radio direction-finding has been investigated for over seventy-five years. The earliest known direction-finder, the rotatable loop, was first used by Hertz in 1888. In various forms, it is still in use today. Since the principle of its operation and some of its limitations are common to many modern D/F systems, it is perhaps worthwhile to describe it briefly.

The small loop is a directional antenna. When it is used as a receiving antenna, it may be employed, in theory, to determine the direction of arrival of a plane wave of arbitrary polarization by orienting it so that no voltage is induced in it. The plane of the loop then coincides with an equiphase surface and the axis of the loop is parallel to the Poynting vector. This property of the loop caused it to be used at first as a direction-finder for vertically polarized ground waves. The loop was mounted with its axis parallel to the ground and was rotated about a vertical axis until a null was achieved. Although the early loops did not perform as well as has been described, because of interactions between the antenna and the feed structure, later loops did, after the introduction of the balanced, shielded, loop.[1]

A much more serious limitation to the performance of the loop, and most D/F systems, comes from multipath propagation. This effect was first noticed when the loop was sufficiently far from the transmitter to receive both ground-wave signals and sky-wave signals reflected from the ionosphere. Since the phenomenon was more notice-

able at night, because of the lowered height of the ionosphere, it became known as "night effect." It arises in the following way: A loop mounted with its axis parallel to the ground will null on a vertically polarized sky wave, when the axis of the loop lies in the plane of incidence (the vertical plane containing the wave normal). It will not null, however, when the sky wave is even partially horizontally polarized. In general, sky waves do have horizontally polarized components. Thus even if the sky wave and the ground wave have the same azimuthal angle of arrival (which is not always true either) the loop will not give a satisfactory indication of this angle.

The initial solution to this problem lay in constructing a direction-finding antenna that would respond only to the vertically polarized component of the wave. The Adcock[2] system, as it is called after its inventor, does just this. In one form it consists of two vertical electric dipoles placed parallel to each other so that they and the support structure form the letter H. The dipoles are connected 180° out of phase and the structure is rotated about the center of the cross bar of the H. If the spacing between the dipoles is small enough (less than 1/4 wavelength) the receiving pattern has, in azimuth, the form of a rotating figure 8. The D/F is performed on the nulls with some auxiliary antenna to remove the 180° ambiguity. So if the ground wave and sky wave have the same azimuthal angle of arrival the Adcock is capable of determining it.

If these two waves do not have the same azimuthal angle of arrival, however, the bearing indication given by the Adcock may have a large systematic error. In fact all D/F systems which, like the Adcock,

employ directional antennas of small aperture, are subject to it. It was first described and its cause explained in 1923 by Heiligtag.[3] Recently Hayden[4] reviewed its derivation. A summary of his presentation follows: In Figure 1-1 is shown the standing wave field produced by two vertically polarized plane waves whose wave normals lie in the plane of the paper and have a 30° angle between them. The equiphase surfaces of this field are corrugated (or, if the two waves are of equal strength, broken). From the figure it can be seen that the normal to the phase front varies from a direction between the wave normals (but closer to the normal to the stronger wave), to a direction outside the angle between the wave normals (but away from the normal to the weaker wave). At present all small aperture D/F systems give an indicated bearing which is equal to, or very nearly equal to, the normal to the equiphase surface. Thus the indicated bearing of such a system is significantly dependent on where it is placed.

One answer to this problem is to construct a large aperture system which will average out the "wrinkles" in the wavefront to give a true bearing indication. In principle, this is what the Wullenweber[5] system, the cyclical-differential-phase system[6] and the Doppler[7] system do. Another approach is to average over the bearings of a number of spatially dispersed small aperture systems. Both of these methods are expensive to implement, however, so considerable effort has gone into the analysis of multipath propagation, with the hope that cheaper and less involved D/F systems will result.

Because multipath propagation in the ionosphere is the major source of error in the HF (1 - 30 MHz) band, considerable effort[8-15] has gone into investigating it. The bulk of this work is necessarily experimental,

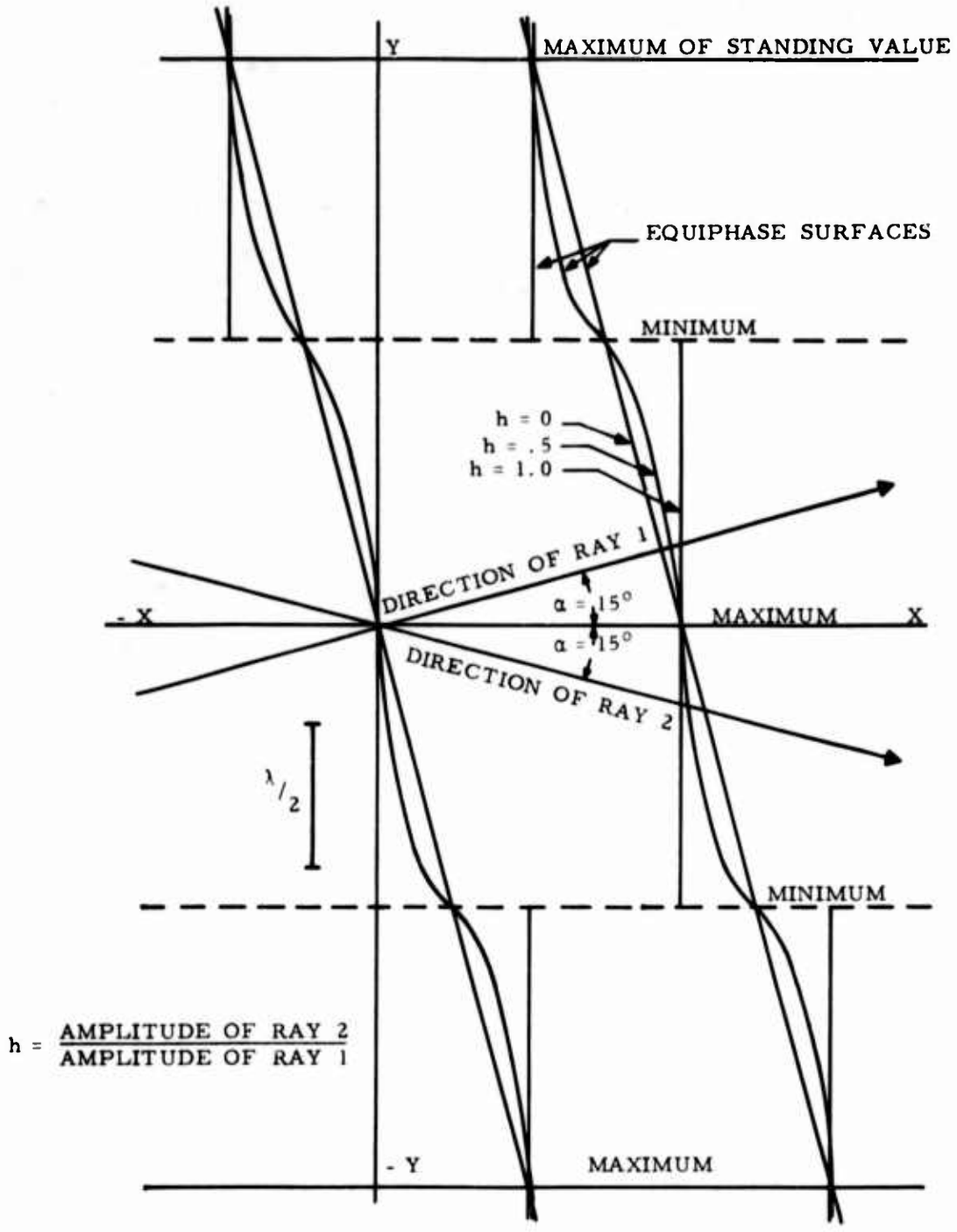

FIGURE 1-1 WAVE INTERFERENCE FIELD FOR RAY SEPARATION OF 30°

since the mechanisms involved are quite complicated. Useful results have followed, particularly in the substitution of time averaging for space averaging. The dynamic nature of the ionosphere makes this a profitable procedure. Relatively little effort, however, has gone into the second source of multipath propagation, namely, the reflection of electromagnetic waves from surface obstacles in the vicinity of the direction-finder.

Siting error, as it is called, has been overshadowed by the larger errors due to multipath propagation in the ionosphere, but it is by no means insignificant. It is the major source of D/F error in the VHF and UHF bands and it is important in the HF band for short range (0 - 50 miles) direction-finding. The work to follow will concentrate on the latter area, but it is equally applicable to the VHF and UHF areas as well.

Previous investigators[16-25] have concentrated on the effect of bearing accuracy of one or two "point reflectors" (i.e., structures whose major dimension is much smaller than a wavelength, or thin vertical towers) in the vicinity of the direction-finder. The comparatively simple nature of the reradiated field from a "point" source or a linear reflector parallel to the polarization vector leads to explicit expressions for the expected bearing error in their presence. Needless to say, sites where one or two dominant point reflectors constitute the major source of reradiation are very much in the minority. Far more common are sites characterized by several, more or less, extended sources of reradiation (i.e., buildings, hills, clumps of trees). Any object whose horizontal dimensions are large will have a complex

induced current distribution on and within it. The reradiated fields are correspondingly complex. This work attempts a unified analysis of sites possessing obstacles of this type and, by adopting a statistical model, arrives at a single parameter useful in evaluating them. This parameter can be measured quickly and accurately on a given site, through a new method presented here.

The statistical techniques given have not been applied to direction-finding before. Their advantage is two-fold.

1. The problem of site evaluation is given a more logical solution, in place of the rule-of-thumb methods in use at present.
2. The preliminary measurement procedure necessary for site selection is considerably simplified.

It is hoped that the conclusions presented will provide a practical guide for engineers engaged in choosing D/F sites.

Chapter 2

DEVELOPMENT OF AN ANALYTICAL MODEL OF A D/F SITE

A. Hypothesis to Explain D/F Errors

About twenty years ago, various investigators, encouraged by their success with shipboard direction-finders, were examining the possibility of "calibrating" a D/F site by plotting measured errors in bearing against angle of arrival (for a fixed frequency). One of these investigators, W. Ross,[1] performed a series of experiments on several sites to determine if calibration were feasible. The sites he selected were, in general, very good, as far as could be judged by visual inspection; i.e., the direction-finding stations were situated in the middle of fairly flat terrain. Small hills and folds in the ground were present, but, from past experience, did not appear to be sufficient reason to reject the site. The procedure he followed was to examine the size of the bearing error as a function of each of three variables, namely, azimuthal position of a target transmitter, frequency, and distance between the direction-finder and the target transmitter. The experiments were carried out at various frequencies between 6 and 15 MHz.

Ross found that site calibration was not feasible. While it was possible to measure bearing error as each of the above-mentioned quantities was varied in turn, the amount of information required for a complete calibration was too great to obtain in a reasonable period of time. This conclusion followed from three measured effects:

1. The observed errors were not predictable functions of the azimuthal position of the target-transmitter.

2. Calibration at one frequency gave no information about calibration at another. There were, for example, significant differences in observed errors when the frequency was changed by only two per cent.

3. There was a lesser, but noticeable dependence of bearing error on the distance between the target transmitter and the direction-finder. This dependence is less strong as the distance increases.

The erratic character of the bearing errors measured led Ross to hypothesize that they were random in character; i.e., "for any particular bearing and wavelength the error which might be observed could be regarded as the total effect of a large number of causes each contributing a small fraction to the total error, the causes of the errors being regarded as scattered at random over a considerable area all around the direction-finder." He further suggested that "in addition to the direct wave from the transmitter, a large number of reflected waves from many directions originate from countless suitable reflectors; e.g., trees, metal poles and pylons, buildings with metal frameworks, small hills, etc., scattered over a wide area surrounding the direction-finder."

Ross presented some experimental justification for his hypothesis; e.g., it is a good explanation of the very variable nature of the error with small changes in wavelength. He did not, however, attempt to express his ideas mathematically and to derive therefrom the observ-

able results. The modern statistical approach which follows is an application of the theory of rough-surface scattering to the D/F problem.

In subsequent sections of this chapter a statistical model of a site is developed based on the work of Beckmann[2] and Siddiqui[3] and a single parameter is suggested as a means of evaluating a site. The probability of errors in bearing of a specified magnitude depends both on this parameter and on the type of direction-finder used. In Appendix A the relation of this parameter to bearing uncertainty for an Adcock type direction-finder is presented. A similar relationship may be worked out for other types of D/F systems.

B. General Assumptions

Certain general assumptions are necessary in order to develop the analysis. Before stating these, however, the problem is defined more precisely by the following observations:

1. Ross examined the influence of three variables on bearing error. The first area considered in the analysis is the influence of only one of these variables, angle, on bearing error. The necessary assumptions in this case seem more reasonable (i.e., defensible) than in the case of the other two variables.

2. The emphasis is placed upon the relationships between the reradiated and the direct waves, without reference to any particular type of direction-finder. This is done in order to make the results as general as possible. The effect of the site on the spatial structure of the fields is independent

of the direction-finder, but the bearing errors resulting from site imperfections are different for different direction-finders.

3. The primary concern is with sites which are characterized by the presence of extended reradiators. Most sites are of this type.

The assumptions essential to the analysis may now be stated. These assumptions, in mathematical terms, are those employed in the theory of electromagnetic scattering from a rough surface, and those used in the theory of ionospheric propagation. Their interpretation in view of the present problem requires some words of justification. Each listed assumption is therefore followed by an explanation suggesting the reason why it may be applied.

1. The site is illuminated by a vertically polarized monochromatic plane wave.

   This assumption restricts the analysis to ground waves launched by a vertically polarized transmitting antenna placed on the surface of the earth. Strictly speaking, of course, there is always present in a ground wave a small horizontally polarized component, whose magnitude depends on the conductivity of the earth. A vertically polarized receiving antenna, however, will not respond to this component and, in effect, will behave as if the wave were vertically polarized. This is not to say that the methods to be employed are not applicable to other polarizations. In the conclusions it is suggested how this might be accomplished.

2. For any azimuthal position of the transmitting antenna, the field at the direction-finder is the resultant field of a direct wave from the transmitter and a number of scattered waves.

   The scattered waves refer to the fields radiated by the surface and volume currents induced by the direct wave on various obstacles present on the D/F site.

3. At the direction-finder the amplitude and phase (referred to the direct wave) of each of the scattered waves varies in a random manner as the angle of arrival of the direct wave changes

   The induced current distribution on an irregularly shaped obstacle, whose horizontal dimensions are large, has a complicated form. As the illumination angle of the direct wave changes, this current distribution changes also. Given an obstacle, it is a formidable job to calculate this distribution for a specific angle of arrival. It is virtually impossible to do so for all angles. Cramer[4] points out that in such a situation a probabilistic model may be more useful than a deterministic model. He states that the observable characteristics of a physical phenomenon may exhibit the fluctuations typical of random variables, even when the laws of the phenomenon are regarded as well known, provided that these laws are sufficiently complicated. He gives the following example:[5]

   "We do assume that it is possible to predict the annual number of eclipses (of the sun), and if the requisite tables are available, anybody can undertake to make such predictions.

Without the tables, however, it would be rather a formidable task to work out the necessary calculations, and if these difficulties should be considered insurmountable, prediction would still be practically impossible, and the fluctuations in the annual number of eclipses would seem comparable to the fluctuations in a sequence of games of chance."

It is convenient, then, to consider the amplitude and phase of the scattered wave, which are observable quantities produced by the induced current distribution on an obstacle, as random variables. It is difficult to say when such a model may not apply. It does not seem reasonable, for example, when the obstacle is a thin tower of known height. Then the amplitude and phase of the scattered waves appear to be more or less predictable functions of the angle of arrival. The question of the applicability of the model in this and other cases is dealt with more fully in subsequent sections of this work and particularly in the CONCLUSIONS (Chapter 5).

4. The number of scattered waves is sufficiently large.

   How many waves will be considered sufficient depends to a large extent on the probability density distributions of the amplitudes and phases of the scattered waves. In certain cases only one may be required. In most practical cases, no more than six[6] are required. Further explanation will be given in the next section.

These four assumptions are sufficient to derive the probability density distribution of the amplitude of the field at the direction-finder. This distribution, however, is a complicated expression,

depending on four parameters, which are not useful quantities for site evaluation. In order to derive practical results from the analysis, three more assumptions will be made. The first two have good justification. The last is less justifiable, but an indication of how it may be generalized, and therefore better justified, will be given.

5. Each of the scattered waves is statistically independent of the others.

   This assumption implies that the obstacle-to-obstacle interaction effects are small compared to the obstacle-to-direct wave interaction effect. In other words, the current induced on an obstacle A by the current induced on obstacle B is small compared to the current induced on obstacle A by the direct wave.

6. The amplitude and phase of each scattered wave are statistically independent random variables.

   From assumption 3 it can be argued that amplitude and phase may be considered to be independent. A change in the induced current distribution on an obstacle will not affect the relationship between them in an easily predictable way.

7. The phase of any one of the scattered waves is uniformly distributed between $-\pi$ and π.

   This assumption gives rise to a particularly useful result. A more general assumption would be that the probability density distribution of the phase is symmetrically distributed about zero. This case will be fully examined in the next section. It will be shown, however, that the difference

between the result of assumption 7, and the result of assuming a symmetric distribution is not, in general, significant for the actual range of parameters encountered.

C. Probability Distribution of Electric Field Amplitude

The vertically polarized field at the direction-finder is the sum of the vertically polarized components of the individual waves scattered by various obstacles, and the direct wave. If the scattered waves are represented by complex numbers $E_n e^{j\Phi_n}$ (suppressing the time factor $e^{j\omega t}$, as usual), where the values of Φ_n are referred to the direct wave, each individual wave will be represented by a vector in the complex plane. The resultant field will be given a vector sum in the complex plane (Figure 2-1). This sum is expressed mathematically

$$E\, e^{j\Phi} = E_d + \sum_{n=1}^{N} E_n e^{j\Phi_n} \qquad \text{(Eq. 2-1)}$$

where E_d is the amplitude of the direct wave and it is understood that the quantities E_n, Φ_n, the amplitude and phase of the nth scattered wave are random variables whose magnitude fluctuates as the azimuthal angle of arrival of the direct wave changes. Under the assumptions given in the preceding section, the probability density distribution of E is a Rice[7] distribution, given by

$$p(E) = \frac{2E}{\langle E_s^2 \rangle} \exp\left[- \frac{(E_d^2 + E^2)}{\langle E_s^2 \rangle} \right] I_o \left(\frac{2E_d}{\langle E_s^2 \rangle} E \right) \qquad \text{(Eq. 2-2)}$$

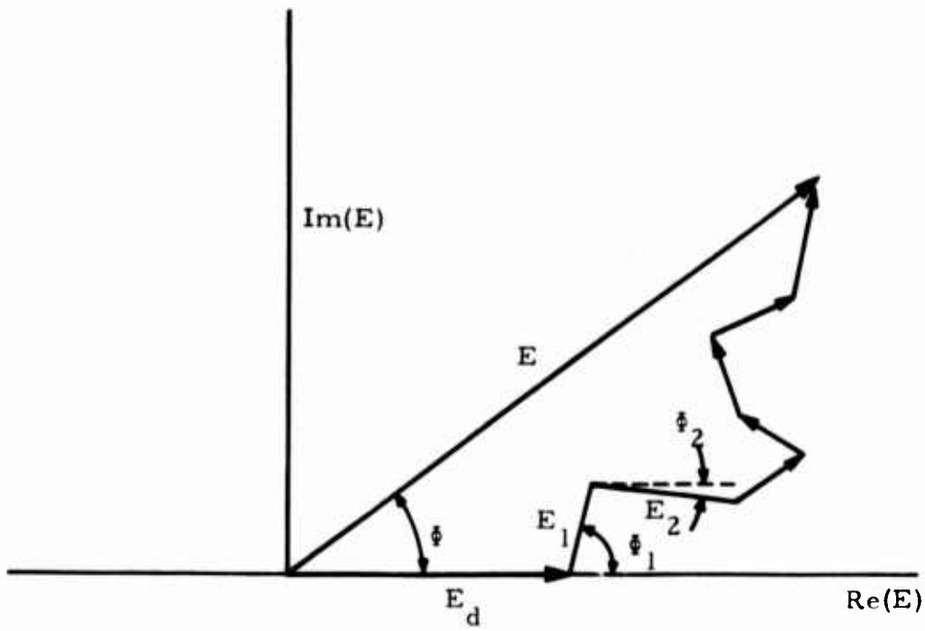

FIGURE 2-1 THE VECTOR SUM OF THE DIRECT WAVE PLUS THE SCATTERED WAVES

where $\langle E_s^2 \rangle$ is the sum of the mean square amplitudes of the scattered waves, averaged over all possible values of angle, i.e.:

$$\langle E_s^2 \rangle = \langle \left(\sum_{n=1}^{N} E_n e^{j\Phi_n} \right) \left(\sum_{n=1}^{N} E_n e^{-j\Phi_n} \right) \rangle = \sum_{n=1}^{N} \langle E_n^2 \rangle \qquad \text{(Eq. 2-3)}$$

(since $p(\Phi_n) = p(\Phi_m) = 1/2\pi$ for all n, m) and where I_o is the modified Bessel Function of the first kind and 0th order.

As was pointed out in the previous section, the comparatively simple form of the distribution is due primarily to assumption 7. Adopting the more general assumption that the $p(\Phi_n)$ are all symmetrical about $\Phi_n = 0$, Beckmann[8] has derived an expression for p(E). A summary of his derivation follows.

First, four quantities must be defined:

1) The average value of the real part of $E e^{j\Phi}$

$$\alpha = \langle E \cos \Phi \rangle = E_d + \langle \sum_{n=1}^{N} E_n \cos \Phi_n \rangle \qquad \text{(Eq. 2-4)}$$

2) The average value of the imaginary part of $E e^{j\Phi}$

$$\beta = \langle E \sin \Phi \rangle = \langle \sum_{n=1}^{N} E_n \sin \Phi_n \rangle \qquad \text{(Eq. 2-5)}$$

3) The variance of the real part of $E e^{j\Phi}$

$$s_1 = \langle (E \cos \Phi)^2 \rangle - \alpha^2 = \langle (\sum_{n=1}^{N} E_n \cos \Phi_n)^2 \rangle - \langle \sum_{n=1}^{N} E_n \cos \Phi_n \rangle^2$$

(Eq. 2-6)

4) the variance of the imaginary part of $E e^{j\Phi}$

$$s_2 = \langle (E \sin \Phi)^2 \rangle - \beta^2 = \langle (\sum_{n=1}^{N} E_n \sin \Phi_n)^2 \rangle - \langle \sum_{n=1}^{N} E_n \sin \Phi_n \rangle^2$$

(Eq. 2-7)

Now if N, the number of scattered waves is large enough and the distributions of $E_n \cos \Phi_n$ and $E_n \sin \Phi_n$ satisfy the conditions of the Central Limit Theorem, then $E \cos \Phi$ and $E \sin \Phi$ will be normally distributed with mean values α and β and variances s_1 and s_2 respectively. Moreover, if the distributions $p(\Phi_n)$ are symmetrical about zero as we have assumed, then the two quantities $E \cos \Phi$ and $E \sin \Phi$ will be uncorrelated. The proof of this proceeds as follows:

The covariance of these quantities is defined as

$$C = \langle (E \cos \Phi)(E \sin \Phi) \rangle - \alpha\beta$$

$$= \langle (E_d + \sum_{n=1}^{N} E_n \cos \Phi_n)(\sum_{n=1}^{N} E_n \sin \Phi_n) \rangle - \alpha\beta \qquad \text{(Eq. 2-8)}$$

But for $p(\Phi_n)$ symmetrical about zero

$$\beta = < \sum_{n=1}^{N} E_n \sin \Phi_n > = 0$$

hence

$$C = < \sum_{n=1}^{N} \sum_{m=1}^{N} E_n E_m \cos \Phi_n \sin \Phi_m >$$

If the identity is employed that

$$\cos \Phi_n \sin \Phi_m = \frac{1}{2} (\sin (\Phi_n + \Phi_m) - \sin (\Phi_n - \Phi_m))$$

it follows that

$$C = 0 \qquad \text{(Eq. 2-9)}$$

where the assumption that $\Phi_1, \ldots, \Phi_n$ are independent variables has been used.

Since E cos Φ and E sin Φ are each normally distributed and uncorrelated, they are statistically independent. Thus the two-dimensional distribution of E cos Φ and E sin Φ is the product of their individual distributions:

$$p(E \cos \Phi \; E \sin \Phi) = \frac{1}{2\pi \sqrt{s_1 s_2}} \exp \left[- \frac{(E \cos \Phi - \alpha^2)}{2s_1} - \frac{(E \sin \Phi)^2}{2s_2} \right]$$

(Eq. 2-10)

In order to determine p(E), the distribution function of the amplitude of the resultant, the variables in (2-10) must be changed from

(E cos Φ, E sin Φ) to (E, Φ). The Jacobian of this transformation is E, hence the distribution p(E) is given by

$$p(E) = \int_{-\pi}^{\pi} p(E, \Phi)\, d\Phi = E \int_{-\pi}^{\pi} p(E \cos \Phi,\ E \sin \Phi)\, d\Phi$$

$$= \frac{E}{\sqrt{s_1 s_2}} \int_{-\pi}^{\pi} \exp\left[- \frac{(E \cos \Phi - \alpha)^2}{2s_1} - \frac{(E \sin \Phi)^2}{2s_2} \right] d\Phi$$

(Eq. 2-11)

This integral is solved by Beckmann[9]. The final form is

$$p(E) = \frac{E}{\sqrt{s_1 s_2}} \exp\left[- \frac{\alpha^2}{2s_1} - \frac{(s_1 + s_2)}{4s_1 s_2} E^2 \right]$$

$$\times \sum_{m=0}^{\infty} (-1)^m \epsilon_m I_m \left(\frac{s_2 - s_1}{4s_1 s_2} \right) I_{2m} \left(\frac{\alpha E}{s_1} \right) \qquad \text{(Eq. 2-12)}$$

where I_m is the modified Bessel Function of order m and

$$\epsilon_m = 1 \qquad m = 0$$
$$= 2 \qquad m \neq 0 \qquad \text{(Eq. 2-13)}$$

If assumption 7 is introduced, (2-12) becomes a Rice distribution, for then

$$\alpha = E_d$$

$$s_1 = \frac{1}{2} \sum_{n=1}^{N} \langle E_n^2 \rangle = \frac{1}{2} \langle E_s^2 \rangle \qquad \text{(Eq. 2-14)}$$

$$s_2 = \frac{1}{2} \sum_{n=1}^{N} \langle E_n^2 \rangle = \frac{1}{2} \langle E_s^2 \rangle \left(= \frac{1}{2} \langle E_s^2 \rangle \right)$$

giving

$$p(E) = \frac{2E}{\langle E_s^2 \rangle} \exp - \left(\frac{(E_d^2 + E^2)}{\langle E_s^2 \rangle} \right) I_o \left(\frac{2E_d}{\langle E_s^2 \rangle} E \right) \qquad \text{(Eq. 2-15)}$$

the distribution stated at the beginning of this section.

Section B mentioned that for the range of parameters under consideration in the present problem, there is little difference between assuming that the $p(\Phi_n)$ are symmetrical about zero and assuming that the $p(\Phi_n) = 1/2\pi$ from $-\pi$ to π. It is expected that the $p(\Phi_n)$ will not be unusual (e.g., δ-function) distributions, so s_1 and s_2 are probably not greatly different from each other. In this case the dominant term in the summation of (2-12) will be the first, $I_o(\alpha E/s_1)$ since

$$I_m \left(\frac{s_1 - s_2}{4 s_1 s_2} E^2 \right)$$

is small for $m > 0$. The result is that (2-12) and (2-15) have approximately the same form regardless of which of the two assumptions are made.

An observation should be made on how large N must be to satisfy the conditions of the Central Limit Theorem. This depends on the density distributions of the quantities being summed. If $E_n \cos \Phi_n$ and $E_n \sin \Phi_n$ are distributed normally, E cos Φ and E sin Φ are normally distributed, then, for $N \geq 1$. If they are distributed uniformly, E cos Φ and E sin Φ are for all practical purposes distributed normally for $N \geq 4$. Even if the E_n were constant, with Φ_n a random variable uniformly distributed between $-\pi$ and π, then it has been shown that E cos Φ and E sin Φ are normally distributed for $N \geq 6$.[10]

An approximation of (2-15) useful for further work is now made. First, the expression is modified by carrying out the substitutions

$$r = \frac{E}{E_d} ; \qquad k^2 = \frac{\langle E_s^2 \rangle}{E_d^2} \qquad \text{(Eq. 2-16)}$$

This gives

$$p(r) = \frac{2r}{k^2} \exp\left[- \frac{(1 + r^2)}{k^2} \right] I_o\left(\frac{2r}{k^2}\right) \qquad \text{(Eq. 2-17)}$$

It is expected that the magnitude of the scattered waves will be small compared to the magnitude of the direct wave. Mathematically this means that $k^2 << 1$ and $r \approx 1$, so it is useful to find an approximation for (2-17) in this range. For large values of the argument the Bessel Function

$$I_o \frac{2r}{k^2} \approx \sqrt{\frac{k^2}{4\pi r}} \exp\left[\frac{2r}{k^2}\right] \qquad \text{(Eq. 2-18)}$$

Substituting (2-18) into (2-17),

$$p(r) \approx \frac{1}{\sqrt{\pi k^2}} \exp\left[- \frac{(r-1)^2}{k^2} \right] \qquad \text{(Eq. 2-19)}$$

is obtained. Therefore for small values of k^2 and $r \approx 1$, the distribution function is approximately normally distributed with a mean of 1 and a variance of $k^2/2$.

It is suggested that k^2 be used as the evaluation parameter for sites which meet the assumptions. Values of k^2 above an arbitrary criterion will indicate an intolerable level of scattered power present on the site. The utility of this parameter may be gauged from the discussion of narrow-aperture direction-finders given in Appendix A.

D. Summary

In this chapter the theory of rough-surface scattering is employed to develop an analytical model which will be as general as possible in its application to D/F sites. A hypothesis based on measurements performed on several sites is presented in Section A. In Section B, part of this hypothesis is quantized by proposing in mathematical terms, a number of general assumptions concerning the nature of the reradiated fields. In Section C the consequences of these assumptions are derived and a single parameter, which is the ratio of scattered power to direct power, to characterize D/F sites is suggested.

Chapter 3

SITE EVALUATION BY FREQUENCY VARIATION

A. Scattering Characteristics as a Function of Frequency

In the statistical model of rough-surface scattering (or ionospheric propagation) which has been applied to the problem of D/F site evaluation, an interpretation is given of the variation in the intensity of the total electric field at the direction-finder as the angle-of-arrival of the direct wave changes. The statistical approach to this problem, however, leads to an inference not discussed with relation to the rough-surface scattering problem, namely, that the fluctuations in the observed electric field intensity when the frequency of the direct wave is varied might possess the same statistical characteristics as when the angle-of-arrival is varied. This implication has not been drawn in the rough-surface scattering model or the ionospheric propagation model, since both are primarily concerned with time or angle varying signal fluctuations at a fixed frequency.

Clearly, two questions are being posed:

1. Is the electric field intensity at the direction-finder a random function of both angle-of-arrival and frequency?
2. Does the probability distribution which describes the variation-with-angle case also describe the variation-with-frequency case?

Should the answer to both questions be in the affirmative, then an important result follows; i.e., that the suggested site evaluation parameter, k^2, can be determined by examining the fluctuations of the

received intensity as the frequency of the direct wave is swept over some arbitrary bandwidth, the angle-of-arrival being fixed.

The questions above are addressed in this chapter in two ways. First of all, in this section, a discussion is given of the reasonableness of the assumptions of Chapter 2, as they apply to the scattering behaviour of complex obstacles as a function of frequency. Secondly, in the next section, the answers to these questions are given for several arrays of hemispherical bosses on a conducting ground plane.

Assumptions 1, 2, and 4 of Chapter 2 require no explanation for this case of variable frequency; the others do.

1. The site is illuminated by a vertically polarized monochromatic plane wave.

2. For any transmitter frequency, the field at the direction-finder is the resultant field of a direct wave and a number of scattered waves.

3. At the direction-finder the amplitude and phase (referred to the direct wave) of each of the scattered waves varies in a random manner as the frequency of the direct wave changes.

The same justification is given as in Chapter 2. If an obstacle is sufficiently large with respect to the longest wavelength used, then the current distribution on the obstacle changes in a complicated fashion as the frequency of the direct wave changes. According to Cramer, it is quite reasonable to consider the amplitude and phase of the field produced by this complicated current distribution as random variables dependent on frequency.

4. The number of scattered waves is sufficiently large.

5. Each of the scattered waves is statistically independent of the others.

If the obstacle-to-obstacle distance is large enough with respect to the longest wavelength used, the effects of multiple scattering may be neglected, or, in other words, the induced current on one obstacle has negligible effect on the induced current on another obstacle. It is reasonable to assume the scattered waves are independent under this condition.

6. The amplitude and phase of each scattered wave are statistically independent random variables over frequency.

   For complex obstacles the amplitude and phase of each scattered wave are not predictably related when frequency is varied. From Cramer's point of view, therefore, if it is convenient to assume them independent of each other, one may do so; the assumption does not contradict any observable behaviour.

7. The phase of any one of the scattered waves is uniformly distributed between $-\pi$ and π.

   This is again the least defensible assumption. As before, it can be generalized. In any case, it is reasonable to expect the phase of a wave reradiated from an obstacle to fluctuate over a period as the frequency changes, as long as the range of frequencies is large enough.

Now at any frequency, the scattered waves may be represented by complex numbers $E_n e^{j\Phi_n}$ where Φ_n is the phase referred to the direct wave. The sum of the direct wave plus the scattered waves is expressed, as before,

$$Ee^{j\Phi} = E_d + \sum_{n=1}^{N} E_n e^{j\Phi_n} \qquad \text{(Eq. 3-1)}$$

where E_d is the amplitude of the direct wave and E_n Φ_n, the amplitude and phase of the nth scattered wave are random variables whose magnitude fluctuates as the frequency of the direct wave changes. Under the assumptions given above, the random fluctuations of E as frequency changes are described by the Rice distribution:

$$p(E) = \frac{2E}{\langle E_s^2 \rangle_\omega} \exp\left(-\frac{(E_d^2 + E^2)}{\langle E_s^2 \rangle_\omega}\right) I_o\left(\frac{2E_d}{\langle E_s^2 \rangle_\omega} E\right) \qquad \text{(Eq. 3-2)}$$

where $\langle E_s^2 \rangle_\omega$ is the sum of the mean square amplitudes of the scattered waves, averaged over frequency; i.e.,

$$\langle E_s^2 \rangle_\omega = \sum_{n=1}^{N} \langle E_n^2 \rangle_\omega \qquad \text{(Eq. 3-3)}$$

If the substitutions

$$r = \frac{E}{E_d} \quad ; \quad k_\omega^2 = \frac{\langle E_s^2 \rangle_\omega}{E_d^2} \qquad \text{(Eq. 3-4)}$$

are made, then

$$p(r) = \frac{2r}{k_\omega^2} \exp\left(-\frac{(1+r^2)}{k_\omega^2}\right) I_o\left(\frac{2r}{k_\omega^2}\right) \qquad \text{(Eq. 3-5)}$$

The assumptions lead to the same type of distribution as that given in Chapter 2, with the difference that the decribing parameter k_ω^2 of (3-5) is not necessarily the same as the k^2 of (2-16). Referring to the k^2 of (2-16) as k^2(angle) and the k_ω^2 of (3-5) as k^2(frequency), the inference made at the beginning of this section is that

$$k^2(\text{angle}) = k^2(\text{frequency}) \qquad \text{(Eq. 3-6)}$$

Or, in other words, the two-dimensional variation of r (with angle and frequency) can be described by the same distribution.

For complex obstacles it is a formidable job to investigate analytically the conditions under which the inference might be true. If it can be shown, however, that the inference is applicable to obstacles of simple shape, then it may be applied with more confidence to complex obstacles. In the next section its applicability to a randomly distributed array of perfectly conducting hemispherical bosses on a perfectly conducting ground plane is examined in detail.

B. Scattering from Hemispherical Bosses on a Ground Plane

As was shown by Beckmann[1], scattering from a perfectly conducting hemispherical boss on a ground plane is equivalent to the scattering from a sphere of the direct wave and its image in the plane. Accordingly, the specific case to be examined is a planar array of randomly distributed perfectly conducting spheres of different radii. A plane wave, whose wave normal is parallel to the plane of the array, and whose electric field vector is perpendicular to the plane of the array, impinges upon it. The situation is illustrated in Figure 3-1.

If the spheres are placed sufficiently far apart so that the effects of multiple scattering can be neglected, the total scattered electric field at some point (P in 3-7) within the array is the sum of the scattered fields from each of the spheres considered individually, with a suitable adjustment in phase. Referring to the figure, the scattered field at point P of the ith sphere of radius a_i located at ρ_i, ψ_i, with respect to the x - y coordinate system is denoted

$$\tilde{E}_i(\theta_i, \rho_i, a_i)$$

where θ_i is the smaller angle between the wave normal and the radius vector from P to the center of the sphere. If ψ is the angle between the wave normal and the x-axis, then

$$\begin{aligned} \theta_i &= |\pi + (\psi - \psi_i)| \quad \text{if} \quad \psi < \psi_i \\ &= |\pi - (\psi - \psi_i)| \quad \text{if} \quad \psi > \psi_i \end{aligned} \qquad \text{(Eq. 3-7)}$$

(θ_i is restricted to the range 0 - π for computational purposes.)

1850D

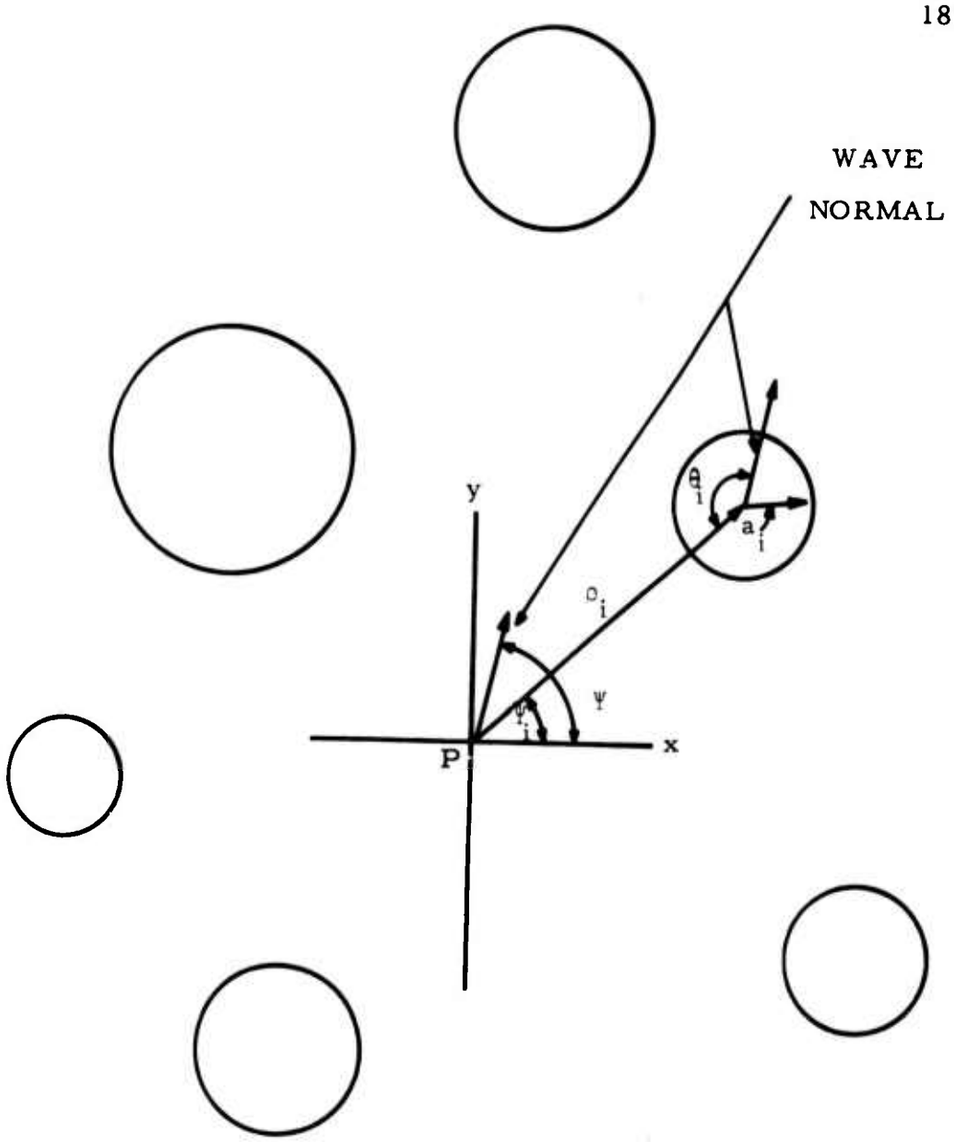

FIGURE 3-1 A Z-POLARIZED PLANE WAVE OF UNIT AMPLITUDE INCIDENT ON A PLANAR ARRAY OF PERFECTLY CONDUCTING SPHERES. ($\vec{E}$ POINTS OUT OF THE PAGE)

The total scattered field at P is thus given by

$$\tilde{E}_t = \sum_{i=1}^{N} \exp\left[-jk\rho_i \cos(\psi - \psi_i)\right] \tilde{E}_i(\theta_i, \rho_i, a_i) \qquad \text{(Eq. 3-8)}$$

where N is the total number of spheres, and $k = 2\pi/\lambda$ is the wave number of free space.

An expression for $\tilde{E}_i(\theta_i, \rho_i, a_i)$ has been given by several [2, 3] investigators. If the magnitude of the incident field is unity, then

$$\tilde{E}_i = -\frac{1}{k\rho_i} \sum_{n=1}^{\infty} \left[c_n \hat{H}_n^{(2)}(k\rho_i) \sin\theta_i \cdot \frac{d P_n^1(\cos\theta_i)}{d(\cos\theta_i)} - jb_n \frac{d}{d(k\rho_i)} \hat{H}_n^{(2)}(k\rho_i) \cdot \frac{P_n^1(\cos\theta_i)}{\sin\theta_i} \right] \qquad \text{(Eq. 3-9)}$$

where

$$c_n = -\frac{j^{-n}(2n+1)}{n(n+1)} \cdot \frac{\hat{J}_n(ka_i)}{\hat{H}_n^{(2)}(ka_i)}$$

$$b_n = -\frac{j^{-n}(2n+1)}{n(n+1)} \cdot \frac{\frac{d}{d(ka_i)} \hat{J}_n(ka_i)}{\frac{d}{d(ka_i)} \hat{H}_n^{(2)}(ka_i)}$$

$\hat{J}_n(x), \hat{H}_n^{(2)}(x)$ are spherical Bessel Functions of order n

$P_n^1(\cos\theta)$ are Legendre Functions of the first kind of order n.

A computer program was written to calculate $\tilde{E}_i$. As a check on the program, the normalized bistatic scattering cross sections of a single sphere were computed for 40 values of ka_i equispaced from $ka_i = .65$ to $ka_i = 6.5$. The bistatic scattering cross section σ_ρ is defined as

$$\sigma_\rho(\theta_i) = \lim_{\rho_i \to \infty} 4\pi \rho_i^2 \mid E_i(\theta_i) \mid^2$$

It is the ratio of the total power reradiated by a fictitious isotropic scatterer (that maintains the same field in all directions as that maintained by the sphere in a specified direction) to the real magnitude of the Poynting vector of the incident wave at the sphere.

A sample result of the calculations is given in Figure 3-2. The values of $ka_i = 1.7$, and 2.3 are those for which the value of the back scattering cross section ($\sigma(180^\circ)$) is a maximum or a minimum when plotted as a function of ka_i. The curves calculated for all maximum and minimum values of $\sigma(180^\circ)$ are the same as those given by King and Wu.[4] Since the bistatic scattering cross section is symmetric in θ_i, it is presented only for $\theta_i = 0$ to 180°.

The values of ka_i for which the bistatic scattering cross sections were calculated lie in the "resonance" region of the sphere, characterized by significant fluctuations in the amplitude and phase of the scattered field as the angle of arrival and the frequency of the direct wave changes. Although the behaviour of the scattered wave in this region may not completely satisfy the assumptions made in Chapters 2-B and 3-A, the resonance region is the one likely to give the best results in a statistical analysis. Accordingly, all computations were carried out in this range of ka_i.

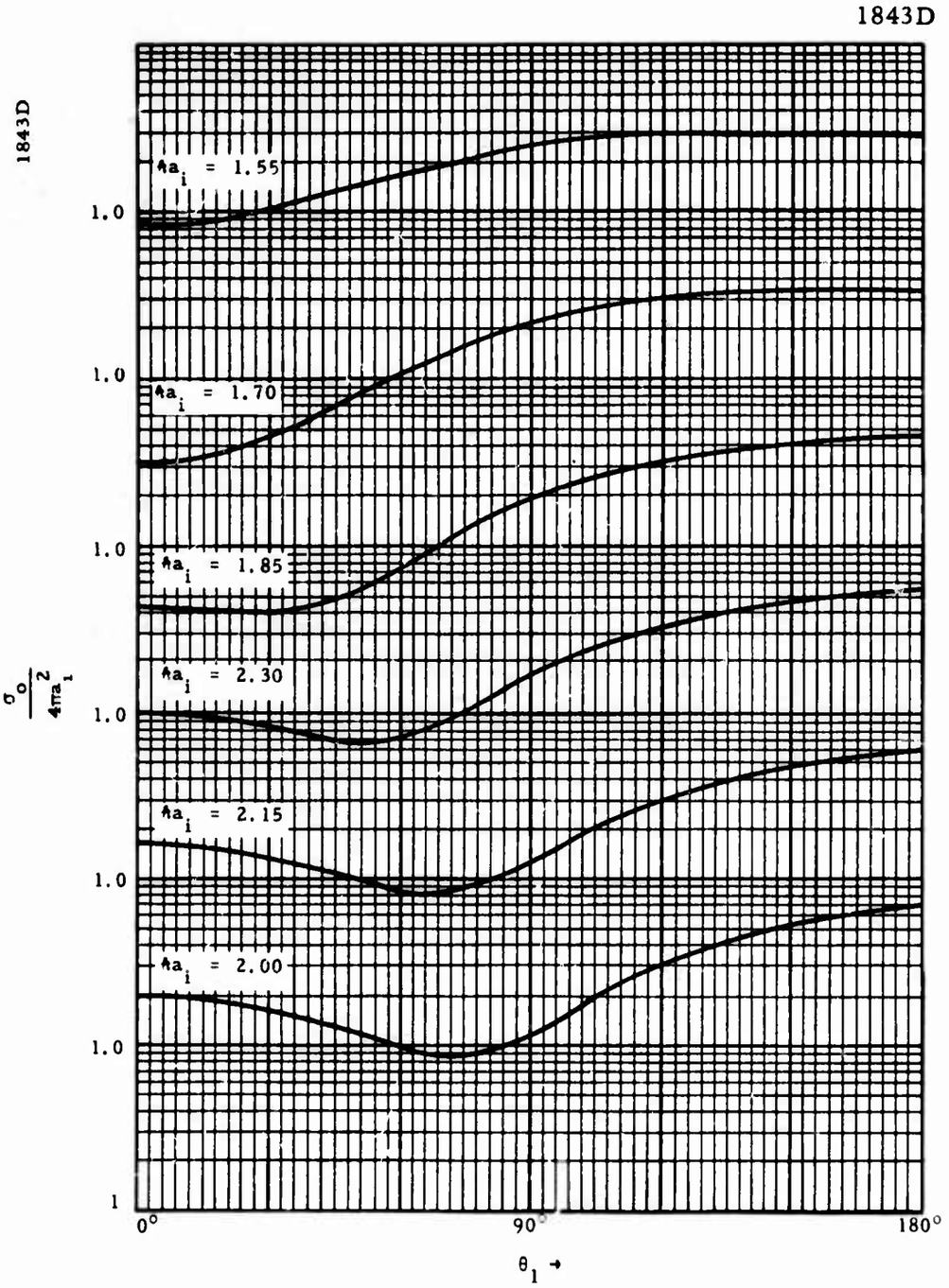

FIGURE 3-2 NORMALIZED BISTATIC SCATTERING CROSS SECTIONS OF A PERFECTLY CONDUCTING SPHERE IN A PLANE-WAVE FIELD

In Figures 3-4, 3-6, 3-8, 3-10, 3-12 and 3-14, are given plots of the total (direct plus scattered) electric field amplitude as the angle of arrival (constant frequency) and the frequency (constant angle of arrival) of the direct wave changes. The plots are given for each of the six configurations of spheres sketched in Figures 3-3, 3-5, 3-7, 3-9, 3-11 and 3-13. The configurations were chosen to examine the variations as (1) the number of spheres, and (2) the average distance of the spheres from the observation point, were varied. The plots for constant frequency were carried out at the geometric mean value of θ over the band ($\pi/2 - 2\tau$) over which the plots for constant angle of arrival were made. The plots for constant angle of arrival were carried out for $\psi = 0$.

The average value of the computed field and the variance σ^2 of all the observations are computed for each case and presented in the figures. From the values of these two quantities, it appears that the average value of the amplitudes for changing angle and frequency are more nearly unity, and the variances for the two cases are more nearly equal, for a large number of spheres at four or more wavelengths' average distance from the observation point (Figures 3-12 and 3-14). Note particularly the inverse-square dependence of σ^2 on distance for eight spheres; this is what the statistical analysis predicts, since σ^2 would then be half the average scattered power at the observation point.

The method employed to determine whether the case of many spheres, four or more wavelengths distant, can be interpreted statistically is described in detail in Appendix B. By means of this method the probability that the fluctuations in amplitude are described by the hypothesized distribution may be calculated. In the first column of Table 3-1

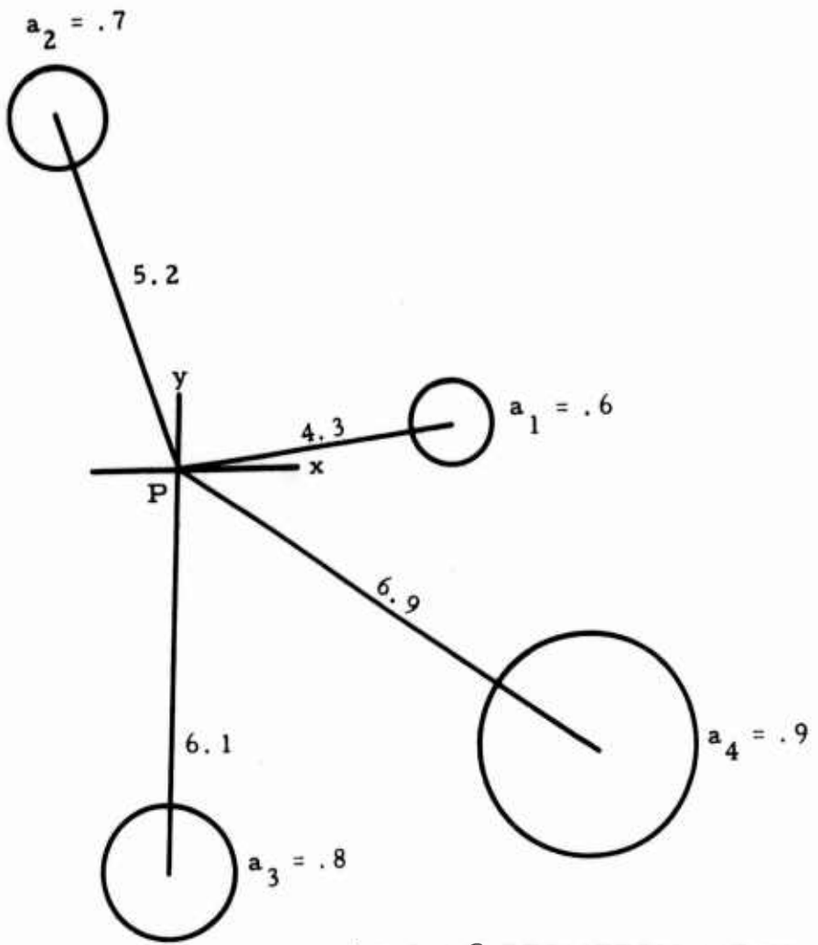

FIGURE 3-3 CONFIGURATION OF FOUR SPHERES ARRANGED ABOUT OBSERVATION POINT (SMALLEST MEAN DISTANCE)

1847D

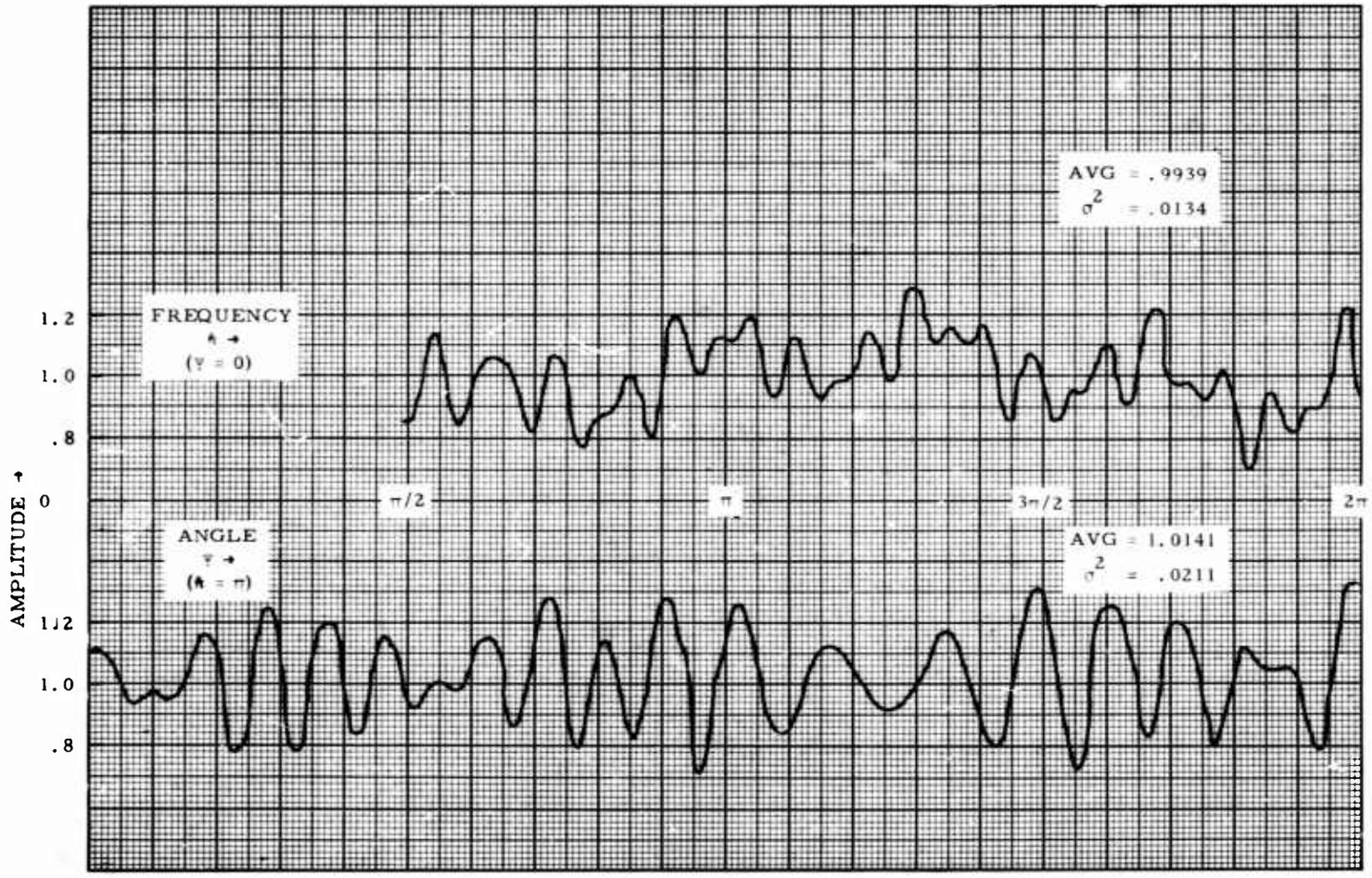

FIGURE 3-4 TOTAL (DIRECT PLUS SCATTERED) ELECTRIC FIELD AMPLITUDE (FOUR SPHERES)

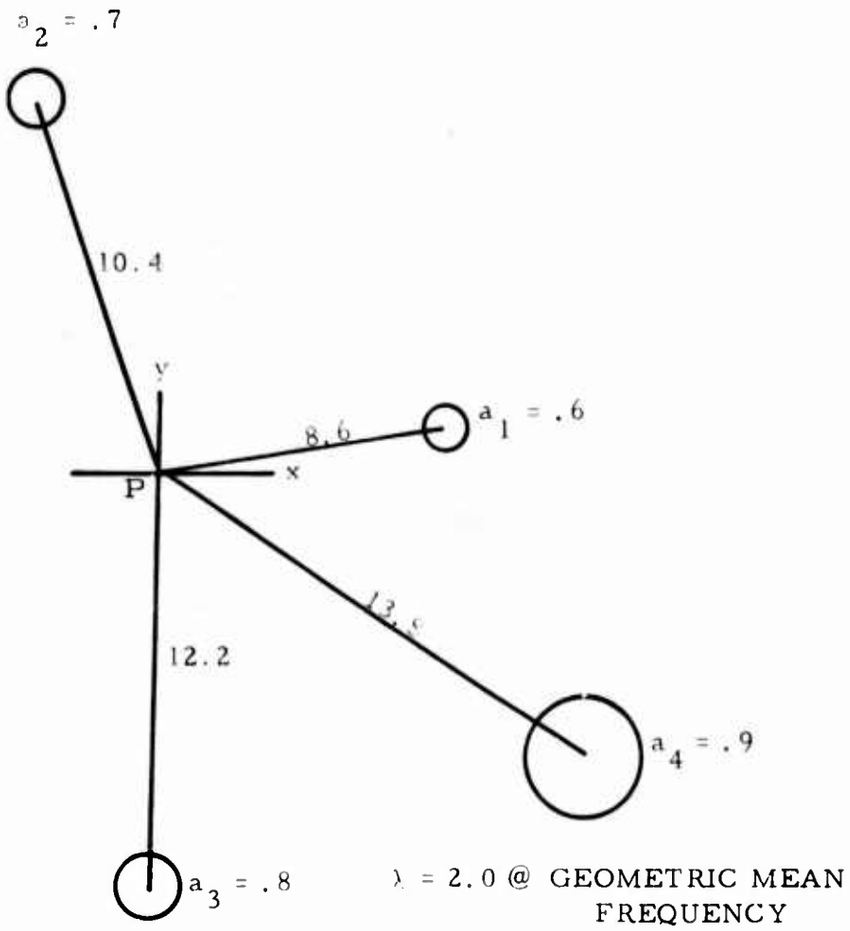

FIGURE 3-5 CONFIGURATION OF FOUR SPHERES ARRANGED ABOUT OBSERVATION POINT (INTERMEDIATE MEAN DISTANCE)

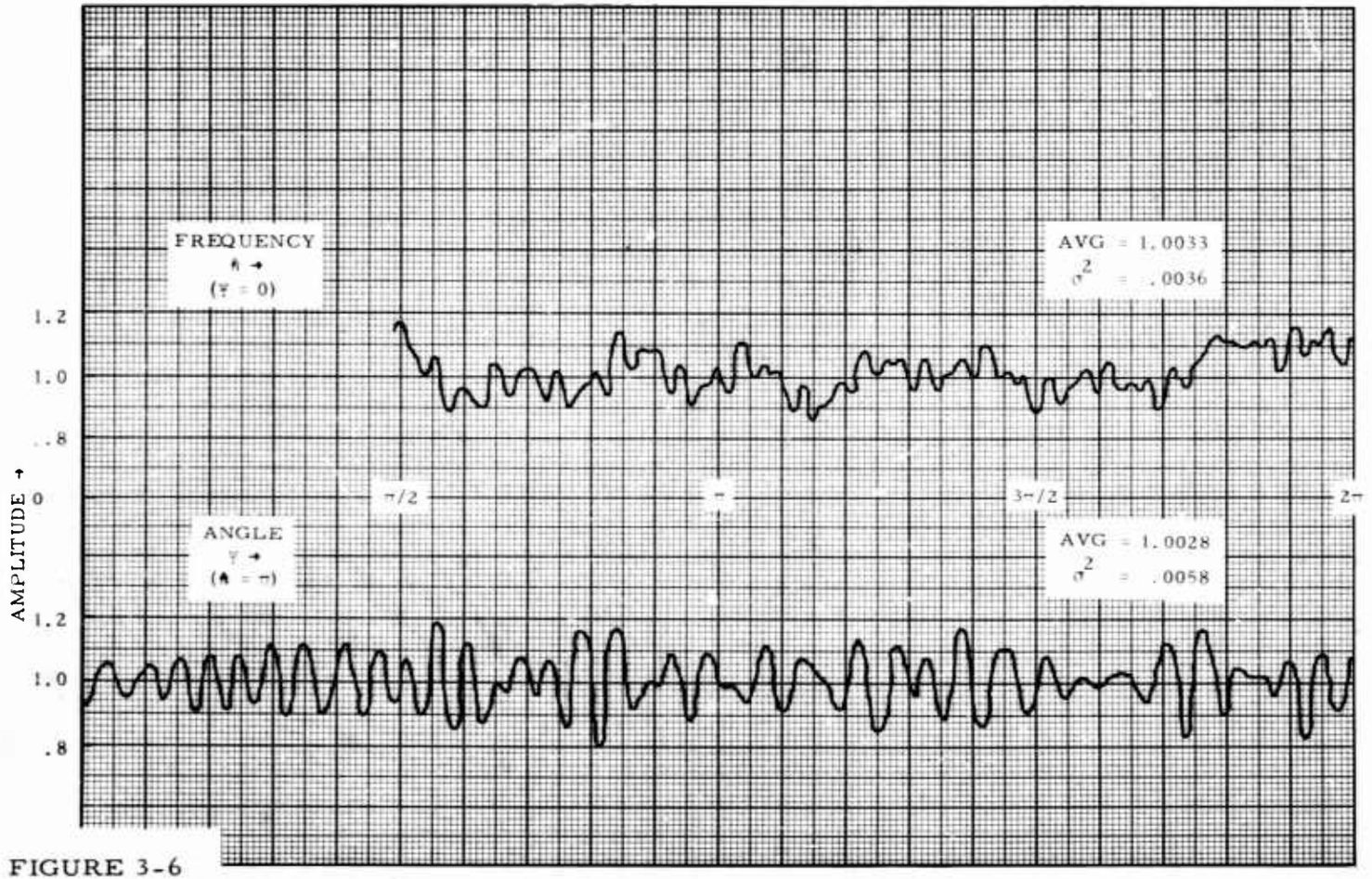

FIGURE 3-6

TOTAL (DIRECT PLUS SCATTERED) ELECTRIC FIELD AMPLITUDE (FOUR SPHERES)

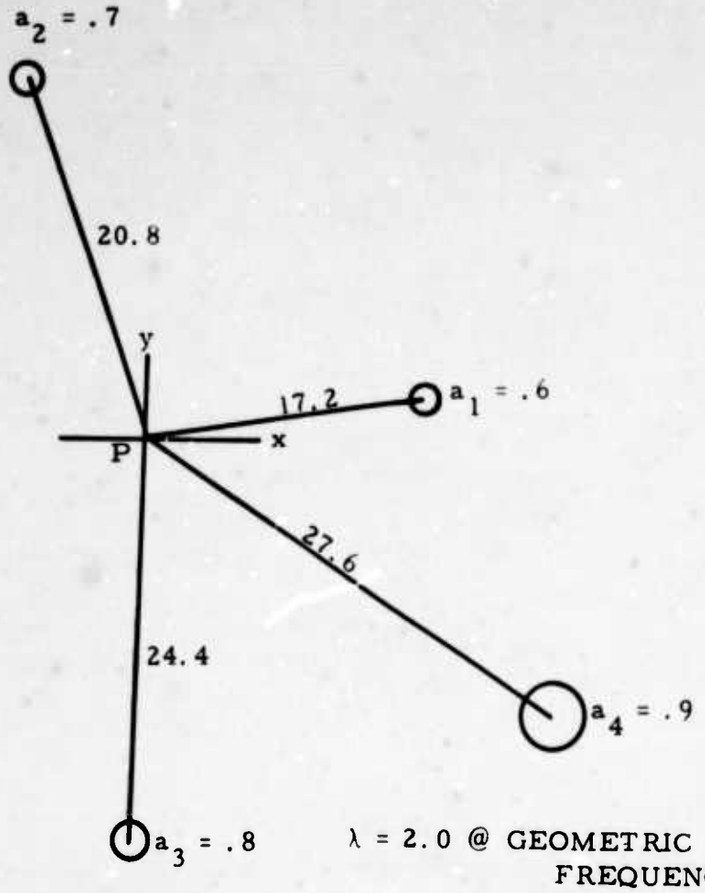

FIGURE 3-7 CONFIGURATION OF FOUR SPHERES ARRANGED ABOUT OBSERVATION POINT (LARGEST MEAN DISTANCE)

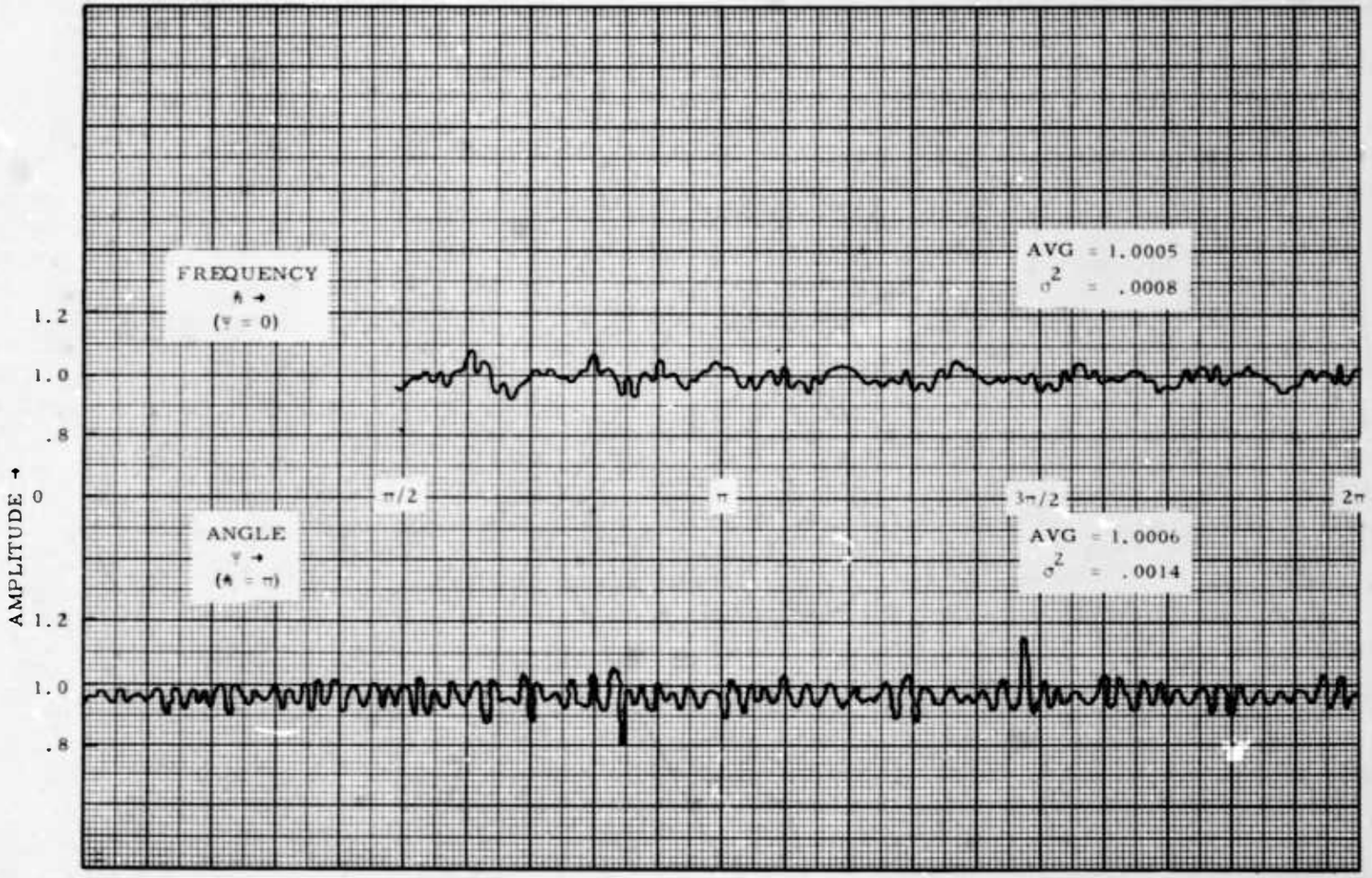

FIGURE 3-8 TOTAL (DIRECT PLUS SCATTERED) ELECTRIC FIELD AMPLITUDE (FOUR SPHERES)

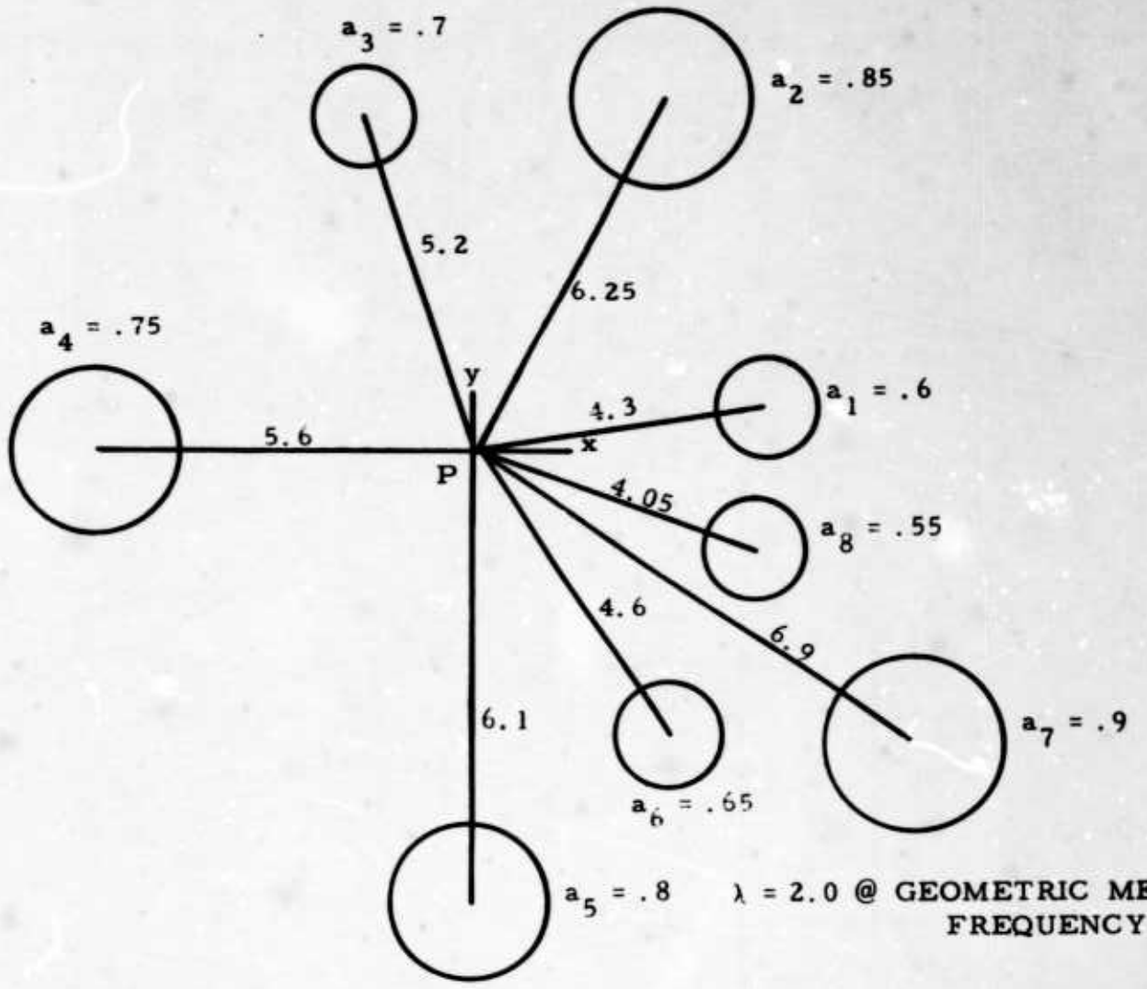

FIGURE 3-9 CONFIGURATION OF EIGHT SPHERES ARRANGED ABOUT OBSERVATION POINT (SMALLEST MEAN DISTANCE)

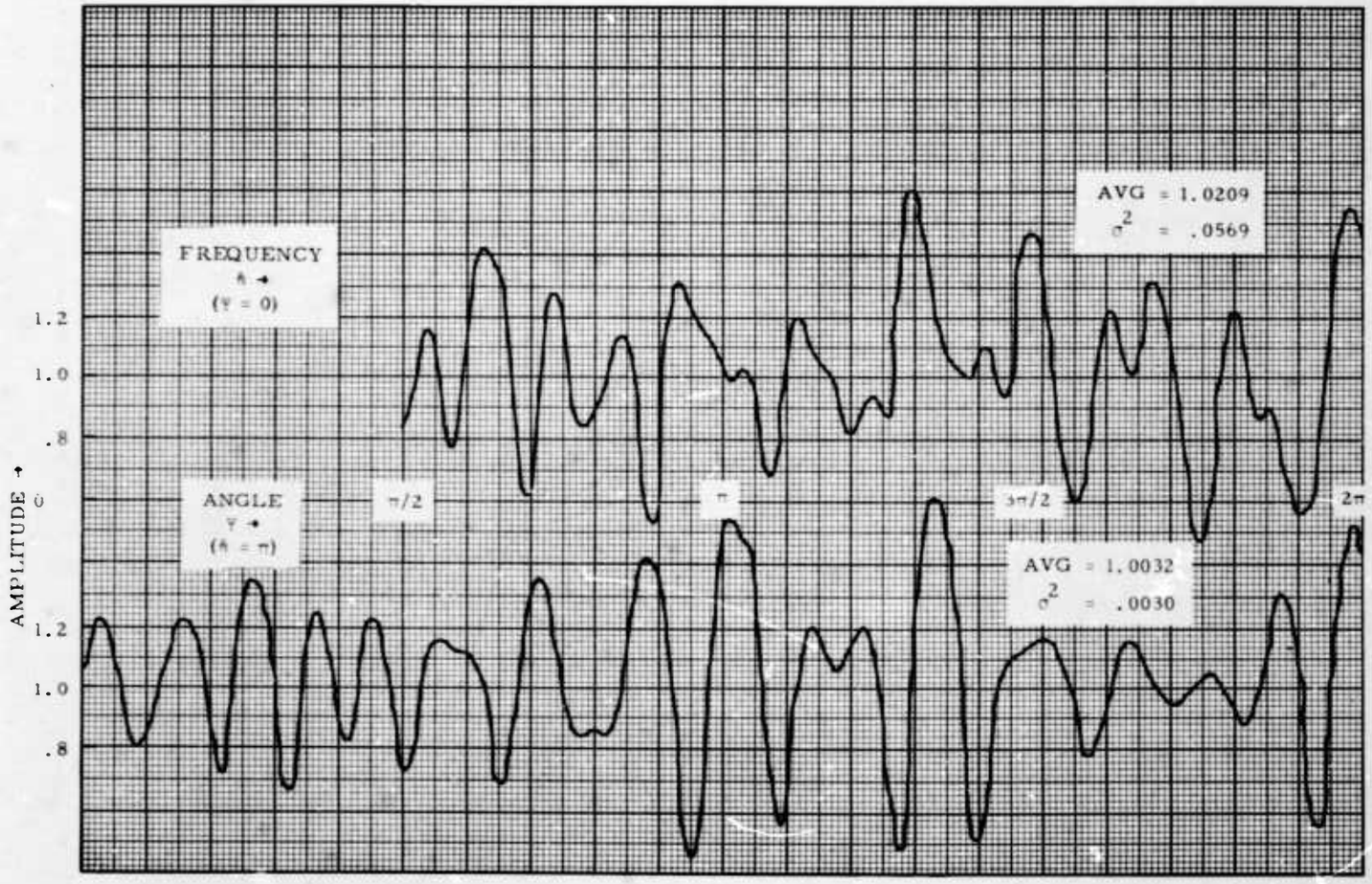

FIGURE 3-10 TOTAL (DIRECT PLUS SCATTERED) ELECTRIC FIELD AMPLITUDE (EIGHT SPHERES)

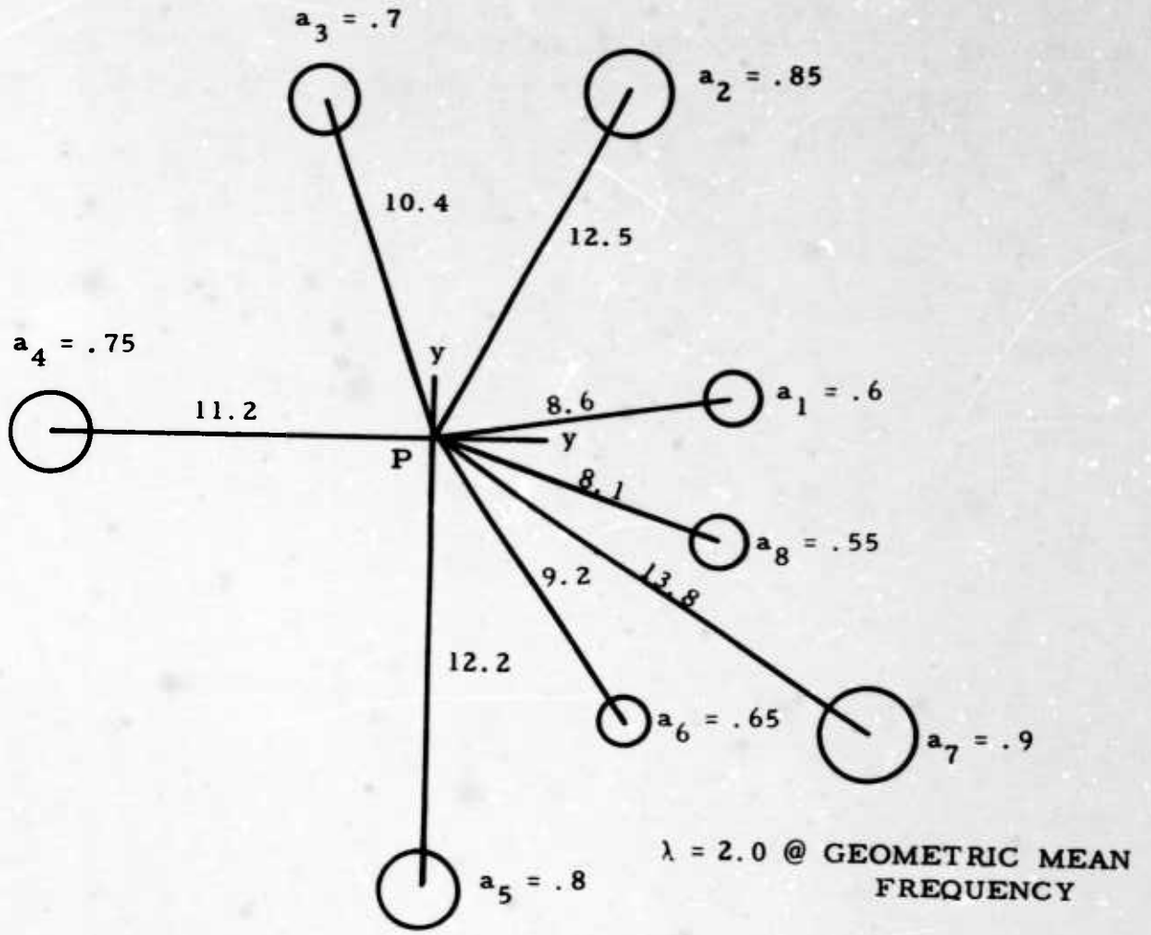

FIGURE 3-11 CONFIGURATION OF EIGHT SPHERES ARRANGED ABOUT OBSERVATION POINT (INTERMEDIATE MEAN DISTANCE)

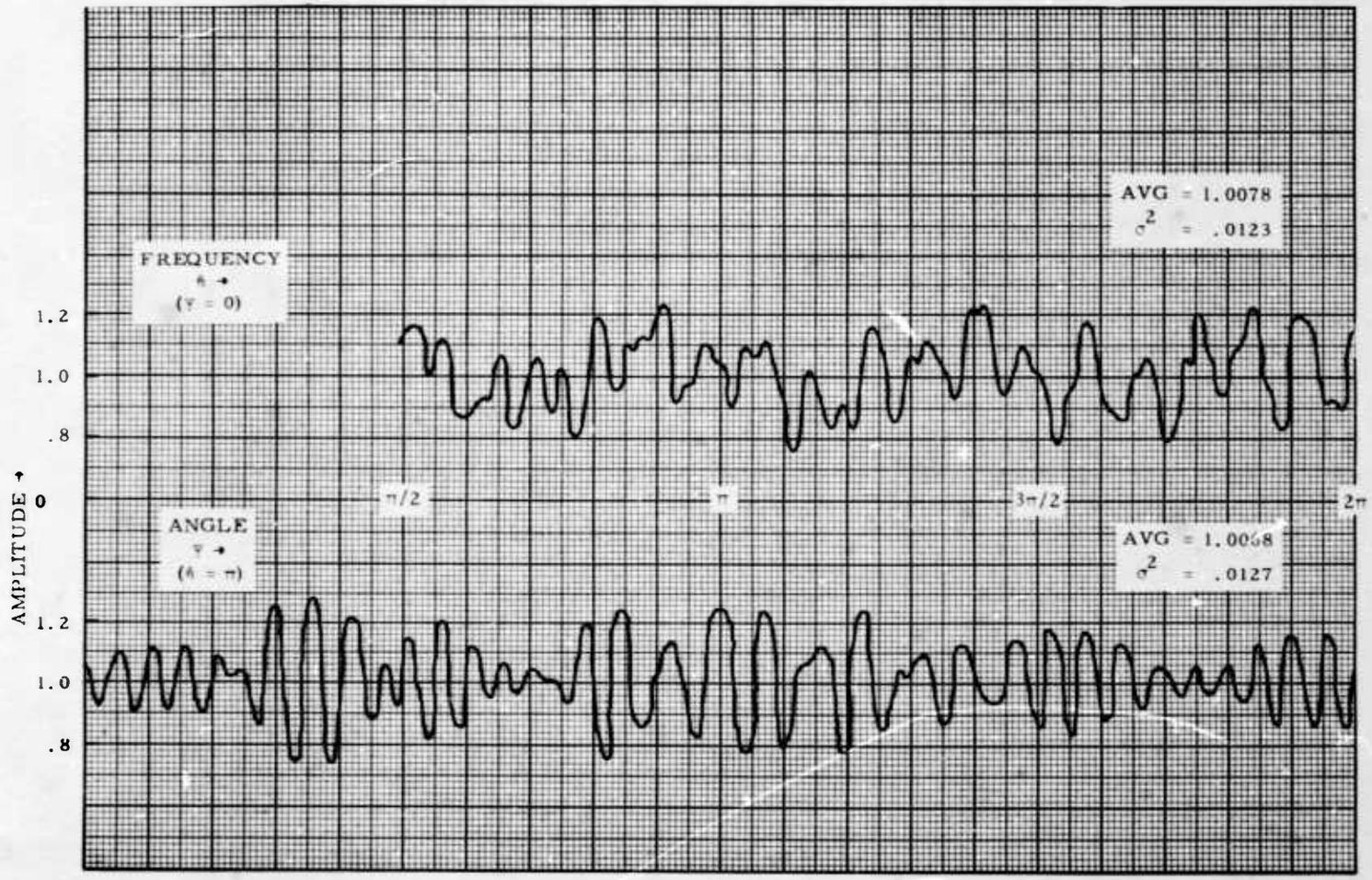

FIGURE 3-12 TOTAL (DIRECT PLUS SCATTERED) ELECTRIC FIELD AMPLITUDE (EIGHT SPHERES)

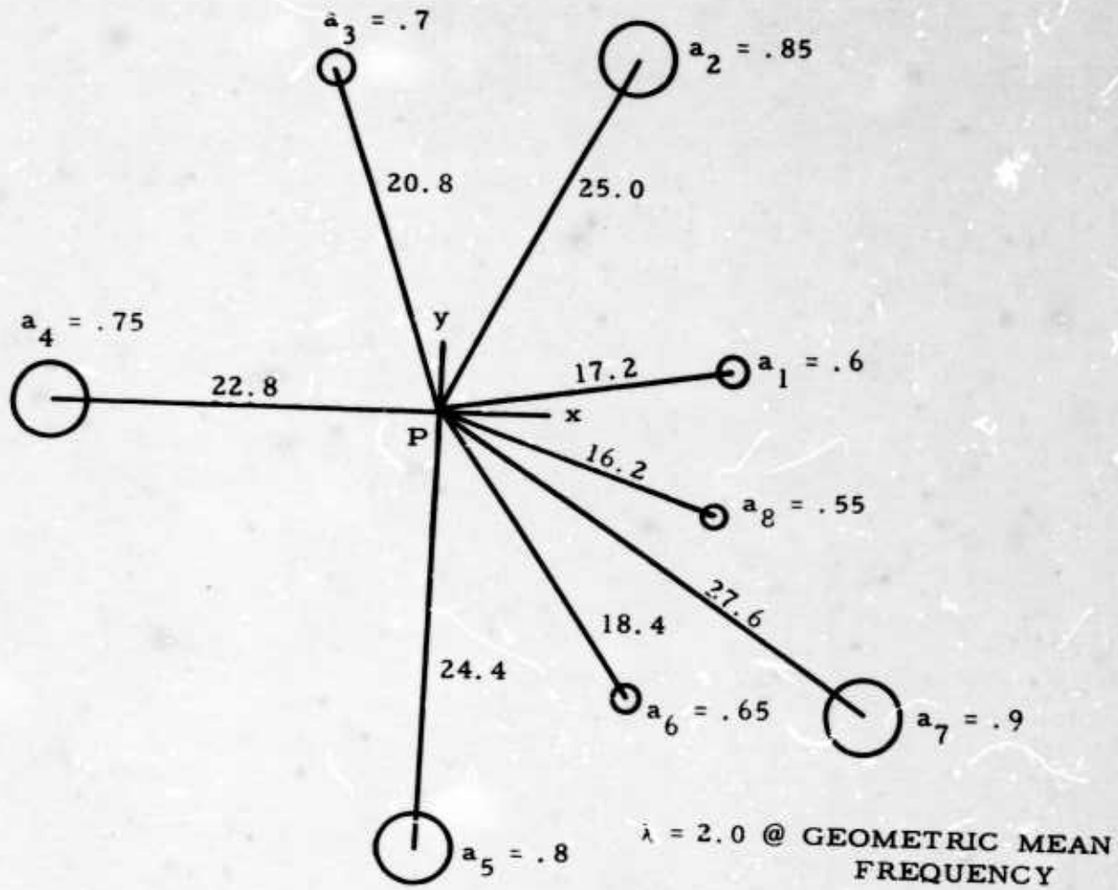

FIGURE 3-13 CONFIGURATION OF EIGHT SPHERES ARRANGED ABOUT OBSERVATION POINT (LARGEST MEAN DISTANCE)

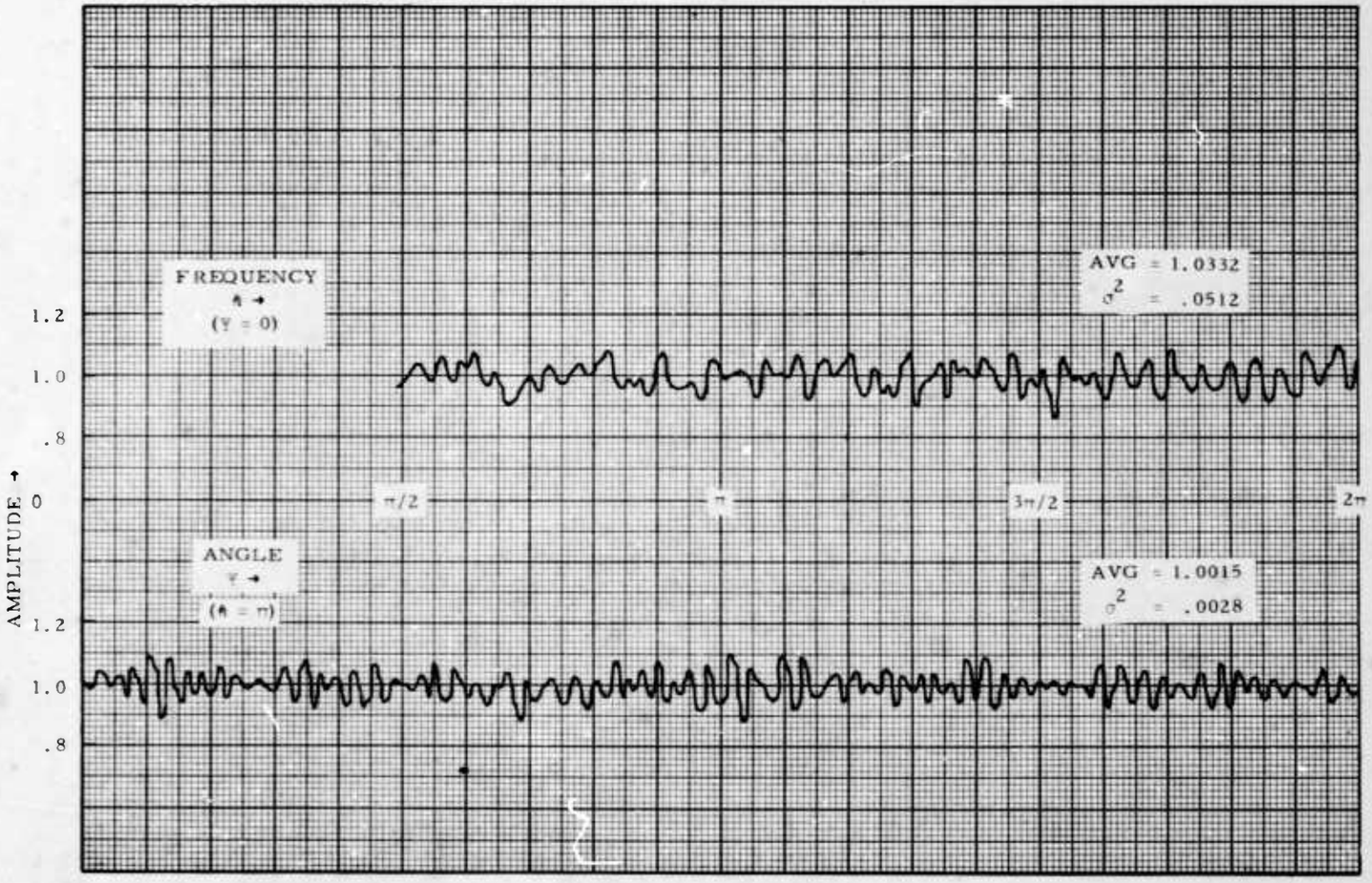

FIGURE 3-14 TOTAL (DIRECT PLUS SCATTERED) ELECTRIC FIELD AMPLITUDE (EIGHT SPHERES)

k^2(angle)		χ^2 probability	k^2(frequency)		χ^2 probability
.0230		>30%	.0180		>50%
.0256		>20%	.0232		>20%
.0198		>10%	.0182		>50%
.0242		>30%	.0184		>50%
.0154		> 5%	.0236		>30%
.0204		>20%	.0248		>50%
.0262		>30%	.0242		>50%
.0236		>50%	.0268		>50%
.0244		> 5%	.0588		>10%
.0210	Increasing	>30%	.0172	Increasing	>10%
.0216	Frequency	> 5%	.0230	Angle	>50%
.0244	↓	>50%	.0374	↓	>50%
.0192		>20%	.0378		>70%
.0240		>10%	.0284		>50%
.0210		>70%	.0280		>50%
.0252		>50%	.0268		>20%
.0256		>20%	.0320		>70%
.0204		> 5%	.0298		>50%
.0262		>20%	.0332		>50%
.0278		>20%	.0390		> 5%
.0212		>50%	.0360		>50%
.0324		> 5%	.0328		>50%
.0342		>50%	.0294		>30%
.0340		>10%	.0176		>50%
.0406		>50%	.0332		>50%
.0218		>50%	.0290		>20%
.0246		>50%	.0288		>70%
.0222		>30%	.0254		>50%
.0372		>50%	.0204		>50%
.0268		>70%	.0272		>50%
.0376		>10%	.0244		>30%
.0322		>50%	.0172		>10%
.0290		>70%	.0142		>70%
.0308		>30%	.0224		>70%
.0328		>50%	.0156		>50%
.0306		>50%	.0210		>50%

Avg. k^2 (angle) = .0262	Avg. k^2 (frequency) = .0258
Std. dev. k^2 (angle) = .0058	Std. dev. k^2 (frequency) = .0076

TABLE 3-1

k^2 (ANGLE) AND k^2 (FREQUENCY) FOR

36 VALUES OF FREQUENCY AND ANGLE RESPECTIVELY

are given 36 values of k^2(angle) calculated at 36 equispaced values of θ from $\theta = \frac{\pi}{2}$ to $\theta = \pi$. In the second column are given the probabilities that the independent samples over angle have the hypothesized distribution, as measured by χ^2. In the third column are given 36 values of k^2(frequency), measured at 36 equispaced values of ψ from $\psi = 0$ to $\psi = 2\pi$. In the fourth column are given the probabilities that the independent samples over frequency have the hypothesized distribution, as measured by χ^2. The calculations pertaining to the configuration of eight spheres given in Figure 3-14 are presented in a similar fashion in Table 3-2.

Several comments can be made about these tables. First of all, as indicated by the values of χ^2 probability, the data are in good agreement with the hypothesized distribution. The agreement is uniformly good for the various values of k^2(frequency), and appears to improve somewhat with increasing frequency for the various values of k^2(angle) for the smaller average distance. Secondly, that the agreement between the average values of the two k^2 should be so close for each table is not too surprising, but that the variation in the values of the two k^2 should be comparatively small certainly is. The largest and smallest values of k^2(angle) in Table 3-1 are .0406 and .0154, and of k^2(frequency) are .0588 and .0142. The largest and smallest values of k^2(angle) in Table 3-2 are .0104 and .0030 and of k^2(frequency) are .0116 and .0032. This indicates that a single measurement at one value of frequency or angle is likely to be less than a factor of two incorrect as an estimate of k^2(angle) or k^2(frequency) respectively (see the discussion given in Appendix C). Thirdly, the average values of k^2 exhibit a strong inverse square dependence on distance, as predicted. The difference between the computations of Table 3-1 and

k^2 (angle)	χ^2 probability	k^2 (frequency)	χ^2 probability
.0050	>50%	.0042	>70%
.0070	>20%	.0068	>50%
.0054	>70%	.0052	>70%
.0030	>30%	.0070	>30%
.0046	>50%	.0050	>50%
.0062	>50%	.0038	>70%
.0042	>10%	.0064	>70%
.0044	>70%	.0084	>30%
.0038	Increasing >30%	.0072	Increasing >70%
.0070	Frequency >70%	.0090	Angle >50%
.0050	↓ >50%	.0106	↓ >50%
.0048	>50%	.0052	>90%
.0060	>50%	.0066	>70%
.0068	>70%	.0016	>90%
.0056	>30%	.0082	>50%
.0074	>50%	.0066	>50%
.0070	>50%	.0040	>30%
.0044	>70%	.0042	>50%
.0076	>30%	.0056	>50%
.0068	>30%	.0090	>70%
.0052	>20%	.0082	>70%
.0054	>70%	.0060	>70%
.0060	>50%	.0056	>30%
.0082	>50%	.0058	>70%
.0092	>90%	.0050	>50%
.0084	>10%	.0102	>90%
.0040	>50%	.0074	>70%
.0066	>70%	.0072	>70%
.0050	>90%	.0064	>50%
.0082	>50%	.0054	>50%
.0062	>50%	.0058	>70%
.0104	>70%	.0044	>90%
.0056	>50%	.0032	>30%
.0088	>90%	.0044	>70%
.0086	>50%	.0052	>70%
.0098	>50%	.0062	>50%

Avg. k^2 (angle) = .0063	Avg. k^2 (frequency) = .0064
Std. dev. k^2 (angle) = .0018	Std. dev. k^2 (frequency) = .0019

TABLE 3-2

k^2 (ANGLE) AND k^2 (FREQUENCY) FOR

36 VALUES OF FREQUENCY AND ANGLE RESPECTIVELY

Table 3-2 is that the distance from each of the spheres to the observation point has been doubled, and the average values of k^2 are observed to drop by a factor of four.

Since the agreement between k^2(angle) and k^2(frequency) is good for a frequency spread of two octaves, it seems reasonable to inquire what bandwidth is necessary to obtain good agreement. To this end, the bandwidth was reduced to one octave and k^2(frequency) was measured in each of the two cases given above. Table 3-3 presents the value of k^2(frequency) for 18 equispaced values of ψ for each case. The average values of k^2(frequency) are seen to be in good agreement with those of Tables 3-1 and 3-2. Reducing the bandwidth necessary to calculate k^2(frequency) even further did not appear practical, since the number of independent sample points available rapidly diminishes.

The resonance region was chosen as the frequency range of most interest, but the statistical model proved so successful in this range that it appeared worthwhile to investigate the scattering behaviour of the spheres above and below this region. Accordingly, brief calculations were made of the relationship between k^2(angle) and k^2(frequency) for eight spheres for values of $\psi < \pi/2$ and $> 2\pi$. It was found that the two k^2 were approximately equal for $\psi \geq \pi/4$, but k^2(angle) started to become significantly less than k^2(frequency) below this value of ψ. It was found that k^2(angle) began to grow appreciably larger than k^2(frequency) for values of $\psi \geq 3\pi$. In the case of $\psi \geq \pi/4$ it appears that the frequency is too low for large fluctuations in amplitude to occur as the angle-of-arrival is varied. In the case of $\psi \geq 3\pi$, the large forward-scattering behaviour of the spheres caused great changes in amplitude to occur whenever a sphere was directly

Eight Spheres Near Observation Point		Eight Spheres Far From Observation Point
k^2 (frequency) one octave		k^2 (frequency) one octave
.0278		.0060
.0156		.0052
.0212		.0072
.0184		.0044
.0120		.0100
.0372	Increasing	.0056
.0454	Angle	.0094
.0318	↓	.0058
.0304		.0068
.0250		.0048
.0282		.0104
.0256		.0080
.0364		.0060
.0290		.0066
.0244		.0048
.0258		.0056
.0224		.0088
.0212		.0054
Avg. k^2 (frequency) = .0265		Avg. k^2 (frequency) = .0067
Std. dev. k^2 (frequency) = .0074		Std. dev. k^2 (frequency) = .0018

TABLE 3-3

k^2 (ANGLE) AND k^2 (FREQUENCY) FOR

18 VALUES OF FREQUENCY AND ANGLE RESPECTIVELY

between the direct wave source and the observation point ($\psi_i = \psi - \pi$). Unless the cut in angle taken to determine k^2(frequency) also coincides with one of these angles, the fluctuations in amplitude with frequency are small compared to the large forward-scattering component.

Finally, both k^2(angle) and k^2(frequency) were computed for each of 10 configurations of spheres. The values are given in Table 3-4. Since the preceding computation has indicated that a one-octave average is sufficient to provide a good estimate of k^2(frequency), the computations were performed for one octave only. The values given in the table are averages of 18 samples of k^2(angle) and 18 samples of k^2(frequency). Configurations 1 through 6 are various arrangements of eight spheres, all of which differ from the two previously examined. In configurations 1, 3, and 5 the closest sphere is four wavelengths distant from the observation point at the lowest frequency at which computations were made. In configurations 2, 4, and 6 the closest sphere is eight wavelengths distant from the observation point. Configurations 7 through 10 are arrangements of 16 spheres. In configurations 7 and 9 the closest sphere is four wavelengths distant. In configurations 8 and 10 the closest sphere is eight wavelengths distant. The values of k^2(angle) and k^2(frequency) for each of the eight-sphere configurations are higher than the configurations previously considered, because in the previous configurations the larger spheres were placed further away from the observation point than the smaller spheres.

The values given in Table 3-4 strongly bear out the hypothesis that the two k^2 are equal for arrays of many objects. That k^2 represents the mean scattered power at the observation point is also strongly

Configuration No.	k^2 (angle)	k^2 (frequency)
1	.0283	.0288
2	.0068	.0067
3	.0271	.0278
4	.0065	.0065
5	.0294	.0292
6	.0072	.0071
7	.0537	.0541
8	.0127	.0130
9	.0552	.0560
10	.0135	.0137

TABLE 3-4

AVERAGE k^2 (ANGLE) AND k^2 (FREQUENCY) FOR EACH OF 10 CONFIGURATIONS OF SPHERES

borne out by the table, as for each configuration k^2 is seen to decline by approximately a factor of four when the mean distance from the spheres to the observation point is doubled. Another indication that this is the case is the fact that the value of k^2 approximately doubles when the number of spheres is doubled.

Calculation of electromagnetic scattering from arrays of many spheres have therefore shown that a statistical model can successfully represent the observed effects. In addition, the values of k^2(angle) and k^2(frequency) are equal for a large number of spheres. The value of k^2(frequency) at one angle or of k^2(angle) at one frequency is a good (within a factor of two) estimate of the many-angle average or many-frequency average of these quantities. Finally, for the configurations considered, a one-octave measurement of k^2(frequency) is sufficient.

C. Summary

This chapter enlarges the scope of the analytical model of a D/F site by suggesting and then investigating a new concept, namely, that the characteristics of a site might be determined by averaging over frequency rather than angle-of-arrival. In Section A the reasonableness of the statistical assumptions applied to this case is discussed. In Section B the concept is found to be true for arrays of hemispherical bosses on a conducting ground plane.

BLANK PAGE

Chapter 4

EXPERIMENTAL PROCEDURE

A. Experimental Model

Before describing the experimental procedure in detail, a brief introduction is given: The purpose of the measurement is, basically, to answer two questions for cases which cannot be done theoretically. Does the analytical model fit a variety of sites, both for varying angle of arrival and for varying frequency? Under what conditions are k^2 (angle) and k^2 (frequency) approximately equal? In order to answer these questions, some means must be found to measure the amount of fluctuation of the electric field magnitude at the center of an obstacle-strewn D/F site as (1) a plane wave of constant magnitude and frequency impinges on the site at various angles of arrival or (2) a plane wave of constant magnitude and angle of arrival but variable frequency impinges on the site. The experimental procedure followed in the first case is, in essence, to move a target transmitter of constant frequency about an omnidirectional (in azimuth) receiving antenna on a circle of constant radius centered on the receiving antenna. In the second case, the target transmitter is fixed in azimuth and the frequency of transmission is swept over some arbitrary band. In each case, the observed fluctuations in received signal level are proportional to the fluctuations in the electric field magnitude at the receiving antenna. These measured fluctuations are then analyzed in a specific way to answer the questions posed earlier.

Checking the theoretical conclusions in the 1 - 30 MHz range, with a large variety of sites, presents many practical difficulties. Not only is a sufficiently large variety of sites unavailable in the Syracuse area, but obstacles of the requisite size and number are not readily transportable. In addition, the variation in received signal level with angle of arrival is not easily investigated, if the radius of the circle along which the target transmitter must move is large. The problems involved in keeping to a precise circular path two miles, say, in diameter are obvious.

In order to simplify the experiment as much as possible the work was carried out at microwave frequencies. The same type of scattering phenomena observable in the HF band will, with a suitable reduction in the size of the scatterers, appear in the microwave region. Also, if the electrical parameters of the media used in the experiment are judiciously chosen to match those of the full size media in the HF band, the magnitude of the scattered waves relative to the directly transmitted wave is the same order of magnitude in both cases. Specifically, if the complex relative dielectric constant of the material chosen to represent the earth at microwave frequencies is in the range $5 \leq \epsilon_r' \leq 30$, $3 \leq \epsilon_r'' \leq 30$, which is the range of the complex relative dielectric constant of the earth at HF, then the material is suitable for an approximate simulation of the earth. (It should be noted here that this statement is equivalent to saying that the conductivity of the earth by a factor equal to the ratio of operating frequencies). A new type of carbon-loaded dielectric foam manufactured by the Emerson

and Cuming Company under the trade name of Eccosorb LS-26 has, at microwave frequencies, a complex relative dielectric constant of 5 + j12, so it meets this requirement.

Figure 4-1 is a diagram of the experimental apparatus and Figure 4-2 is a photograph of it. It consists of an 8' x 12' x 1/2" plane of plywood on which is placed a 3/4" thick layer of LS-26. Two feet from one end of the plywood sheet is a $\lambda/4$ (at 5 GHz) monopole, used as the transmitting antenna. The monopole is constructed of a brass sleeve fitted over the stub end of a type N panel mount (Figure 4-3). At the other end of the plywood sheet a hole 4' in diameter has been cut. A circular disk of 3/4" thick pressboard slightly less than 4' in diameter is centered in the hole and rotates freely within it on eight aluminum rollers equispaced around the periphery of the disk. At the center of the pressboard disk is another $\lambda/4$ monopole, used as the receiving antenna. The pressboard is also covered with a 3/4" thick layer of LS-26. The receiving antenna is thus placed on a rotatable "site" approximately 20λ (at 5 GHz) in diameter. The transmitting antenna is fixed, but rotating the site around the receiving antenna is equivalent to holding the site fixed and moving the transmitting antenna around it, as long as the effect of only those objects less than 10 wavelengths distant from the direction-finder is of interest.

During the measurement procedure various obstacles are placed on the "site." They consist of either various pieces of LS-26 cut to resemble hills, ridges, etc., or groups of thin vertical conductors to represent trees, poles, etc., or metal frameworks to represent buildings, storage facilities, etc. The fluctuations in received signal

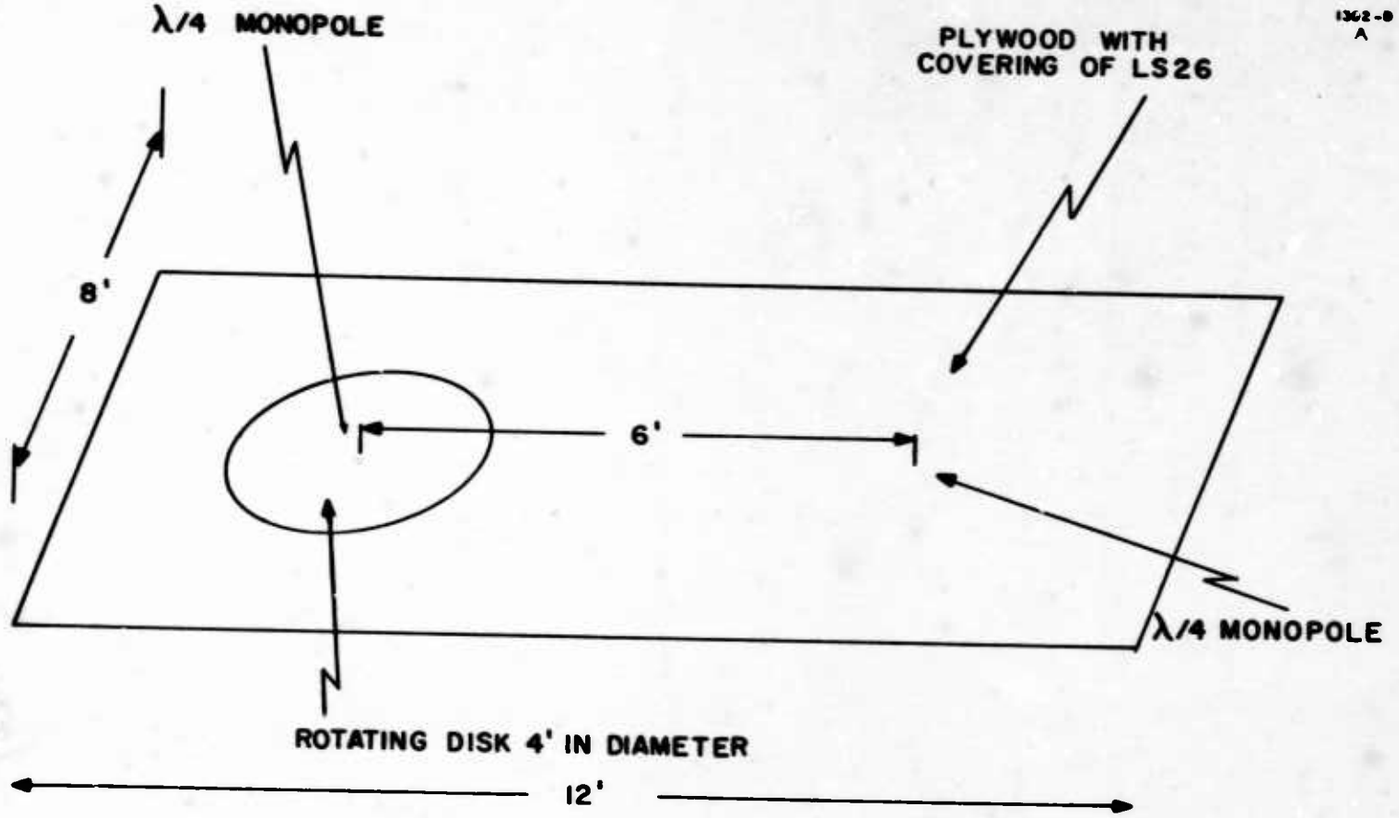

FIGURE 4-1 DIAGRAM OF EXPERIMENTAL APPARATUS

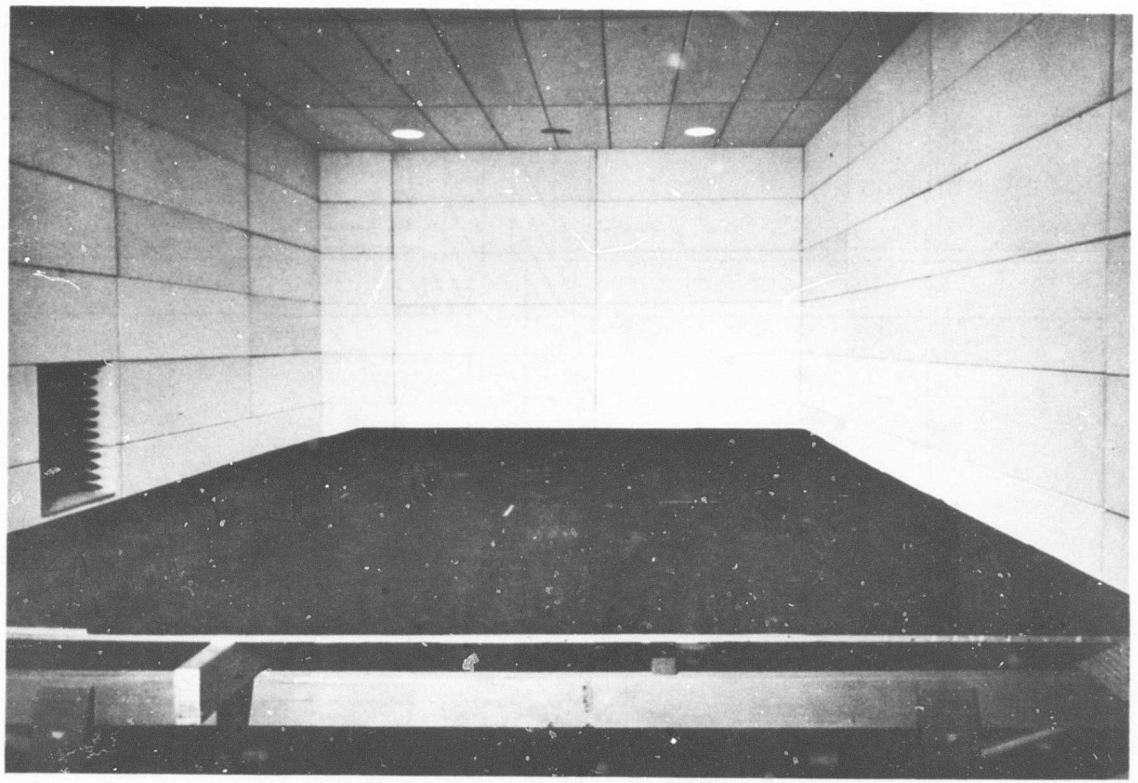

FIGURE 4-2 PHOTOGRAPH OF EXPERIMENTAL APPARATUS

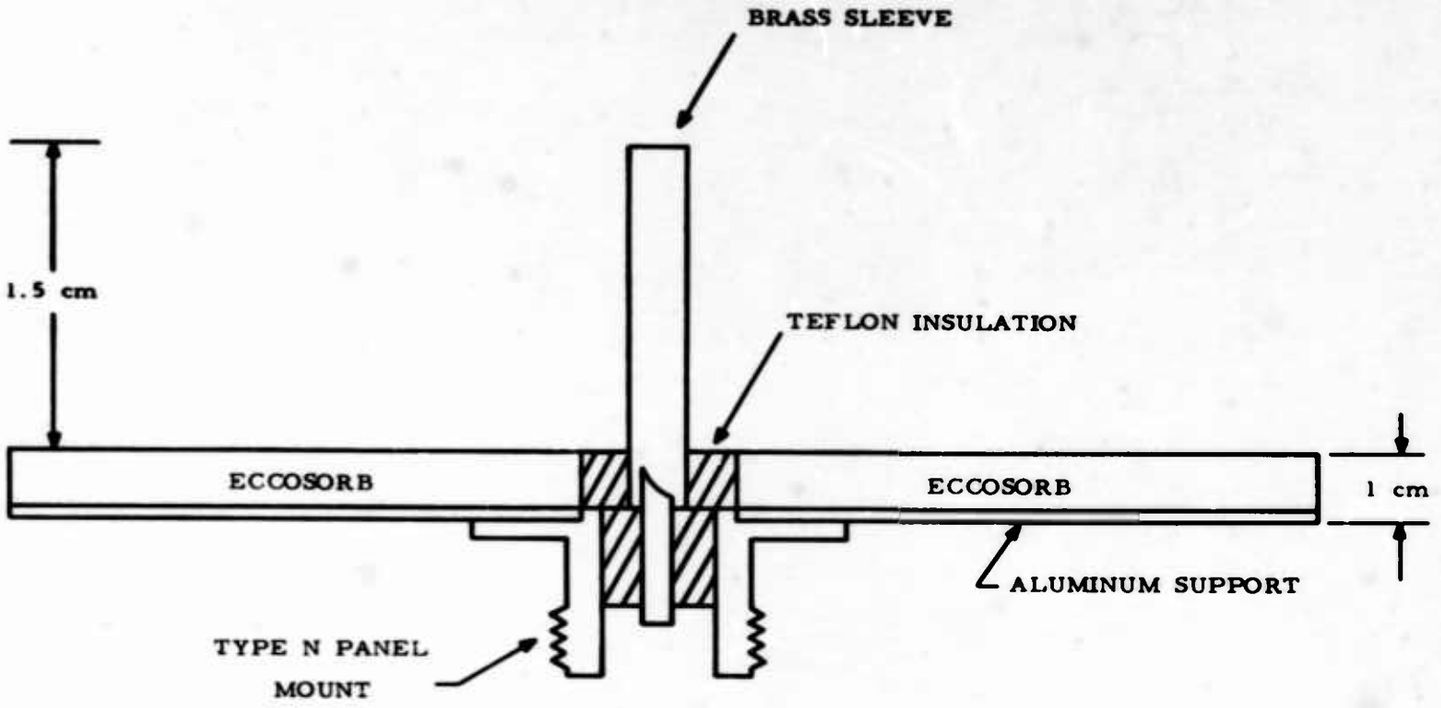

FIGURE 4-3 DETAIL OF ANTENNAS

level are observed as a function of the angular position of the pressboard disk and then of the frequency of transmission for many different configurations of these obstacles.

The plywood plane rests on saw-horses four feet above the floor of the anechoic chamber in which the entire assembly is placed. The anechoic chamber functions adequately above 2 GHz. The pressboard disk is rotated by a Scientific-Atlanta azimuth positioner, which is controlled by a servomechanism drive, and synchronized with a polar recorder.

A block diagram of the transmitting-receiving system is given in Figure 4-4. The transmitting system consists of a sweep oscillator which drives a microwave amplifier. The oscillator is square-wave modulated at 1 kHz. The amplifier will deliver up to 500 mW of power to the $\lambda/4$ antenna. The transmitting system is placed beneath the plywood plane to minimize interference with the measurements.

The receiving system employs a tunnel diode detector, the audio output of which is fed into the bolometer amplifier of the polar recorder. The tunnel diode detector is employed instead of a conventional crystal detector because the received signal level is on the order of -35 dBm. This level is approximately equal to the tangential sensitivity of a conventional detector. The tangential sensitivity of a tunnel diode detector, on the other hand, is approximately -55 dBm.

The data collection system functions in the following manner: The AC output of the bolometer amplifier is fed into a high input impedance full-wave rectifier. The DC output of the rectifier is sampled by a

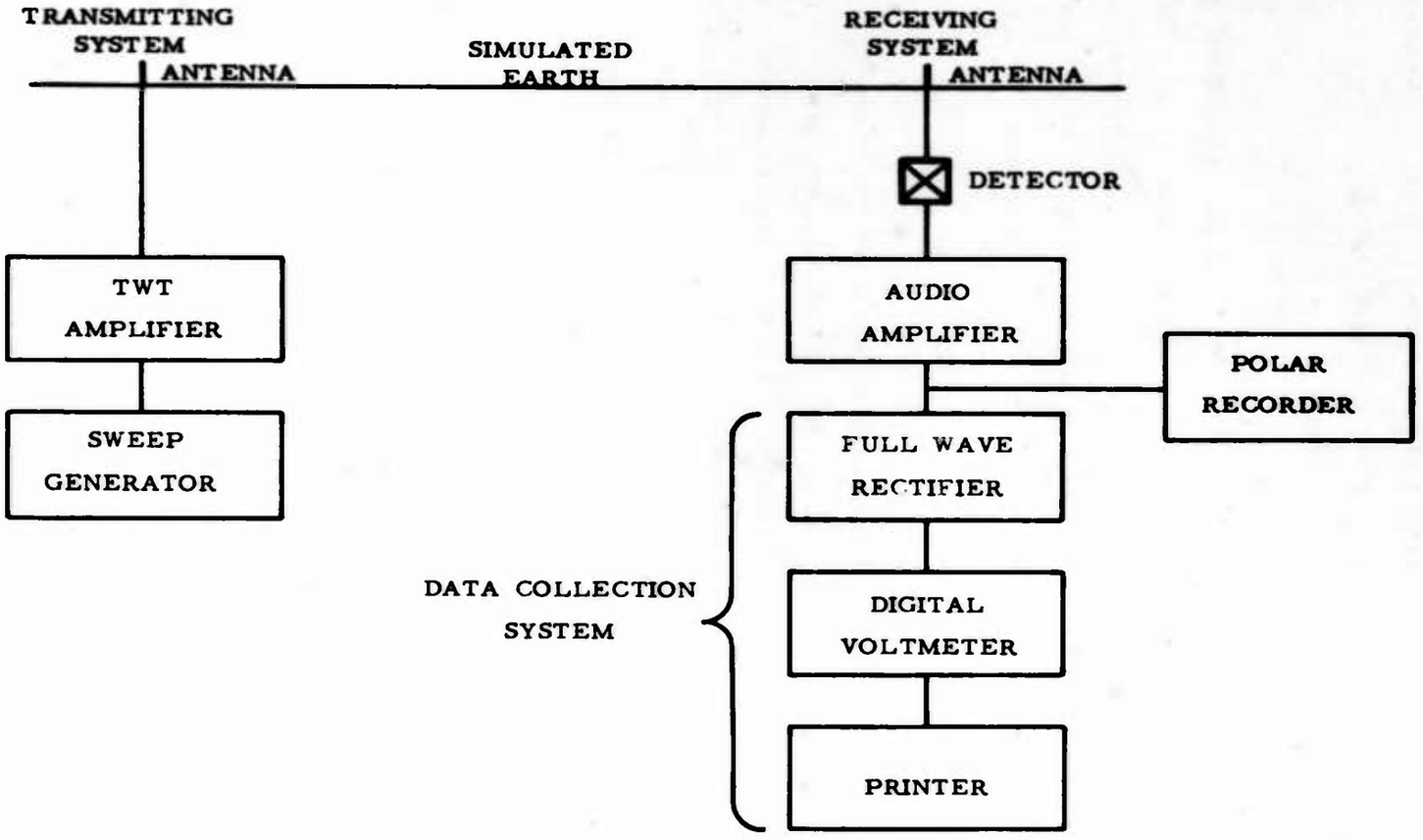

FIGURE 4-4 BLOCK DIAGRAM OF TRANSMITTING-RECEIVING SYSTEM

digital voltmeter. The digitized output of the voltmeter is fed into a printer. The sampling rate of the voltmeter is synchronized with the rotation rate of the polar recorder to provide approximately one sample per degree of angle. When the variations with respect to frequency are investigated, the positioner is disconnected from the pressboard disk, and the rotation rate of the polar recorder is synchronized with the sweep rate of the oscillation. In this case, the angular variable, θ, is directly proportional to frequency. The sampling rate of the voltmeter is then adjusted to provide approximately one sample every 10 MHz of frequency.

The experimental apparatus supplies outputs in each of two forms. The polar recorder graphs (linearly) received power versus angle and versus frequency. The digital sampling system in effect samples these graphs and provides a printed list of these samples. Since only relative magnitudes are of importance, no absolute calibration of the system is necessary. The plotted graphs are of interest only as a pictorial indication of the amount of variation observed. Several of these are exhibited in Section C of this chapter. All of the analysis is done on the digital samples which are transferred to punched cards and analyzed by computer.

B. Adjustment of Data

A preliminary look at the data indicated that it would have to be adjusted before analysis. It was found that the magnitude of the direct wave was not independent of angle or frequency. This was determined from measurements made without any obstacles present on the rotating

disk. The variation with angle was first thought due to mechanical problems with the rotatable site, but when these were overcome, some variation persisted. This variation is ascribed to inhomogeneity in the Eccosorb LS-26.

The manufacturer states that reasonable tolerances, within a 2' x 2' sheet of the material, are $\epsilon_r' = 5 \pm 2$, $\epsilon_r'' = 12 \pm 5$. Differences of this order of magnitude are sufficient to explain the 0.5 - 1 dB variation in the observed magnitude of the direct wave. The variation with frequency is a result of several factors:

1. The antennas are $\lambda/4$ long at the mean frequency of the band. The sensitivity of the transmitting-receiving system therefore varies with frequency.
2. The Eccosorb is dispersive. Its dielectric constant varies slowly with frequency.
3. The output of the sweeper-amplifier combination varies slightly over the band, regardless of how well leveled the sweeper is.

Fortunately, however, the variation is slow compared to the rapid fluctuations of the scattered wave magnitude E_s. This suggests that a moving average be computed and the ratio of the amplitude of the total (direct plus scattered) signal to the amplitude of the moving average signal be used as the variable r. (Note that this procedure is necessary in the full-scale case as well, since it is expected that the amplitude of the direct wave will be similarly dependent on the path attenuation and the type of transmitting-receiving system used.) The moving average is calculated in order to remove deterministic quantities from the data. (See Appendix C)

Figure 4-5 shows a moving average computed over 45° (dotted line) and the actual measurement with obstacles present (solid line). Figure 4-6 shows a moving average computed over 400 MHz (dotted line) and the measurements with obstacles present (solid line). The averaging intervals, 45° and 400 MHz, respectively, were chosen as those which most accurately reproduced the case with obstacles absent (Figure 4-7 for angle and Figure 4-8 for frequency). It was decided to compute this moving average rather than remeasure the obstacle-free case each time because this is what one would do in an actual, full-scale, investigation (the obstacle-free case being unavailable). In the figures, the ordinate is the measured amplitude of the received voltage normalized to its average value. This is done to remove the effect of gain settings on the presented amplitudes.

The independent sample points were determined according to the procedure given in Appendix B. The correlation between pairs of points was calculated and the interval between samples was chosen as that which gave zero correlation. The independent sampling points were then analyzed according to the modified χ^2 minimum method.

C. Experimental Results

The obstacles introduced onto the site were of several types:

1. Pieces of Eccosorb LS-26 cut to resemble hills, ridges, etc.
2. Metal frameworks in the shape of buildings or storage facilities.
3. Clusters of vertical conductors to represent groups of trees.
4. Long horizontal conductors to represent fences, telephone wires, etc.

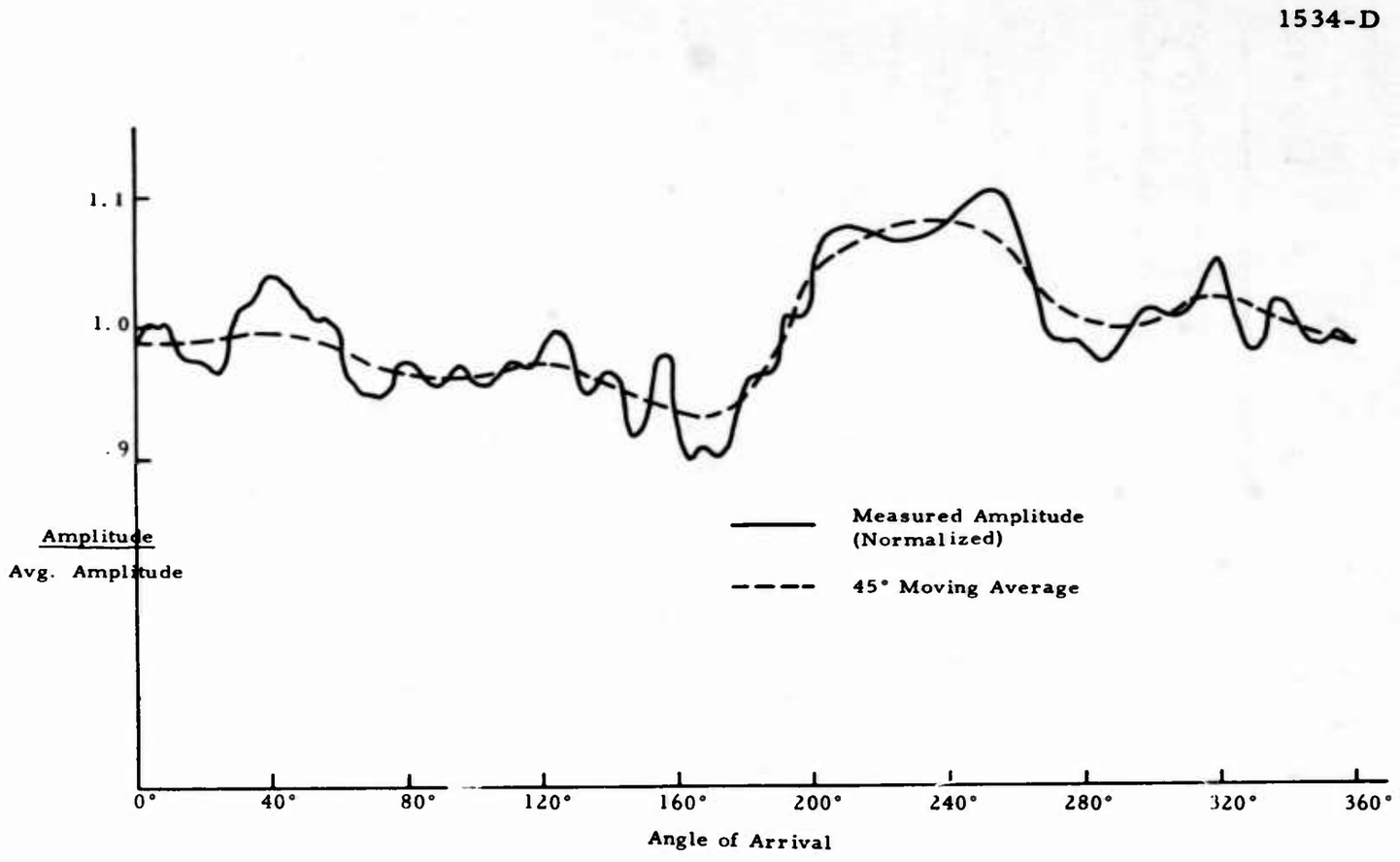

FIGURE 4-5

MEASURED AMPLITUDE AND MOVING AVERAGE AMPLITUDE FOR VARYING ANGLE CASE

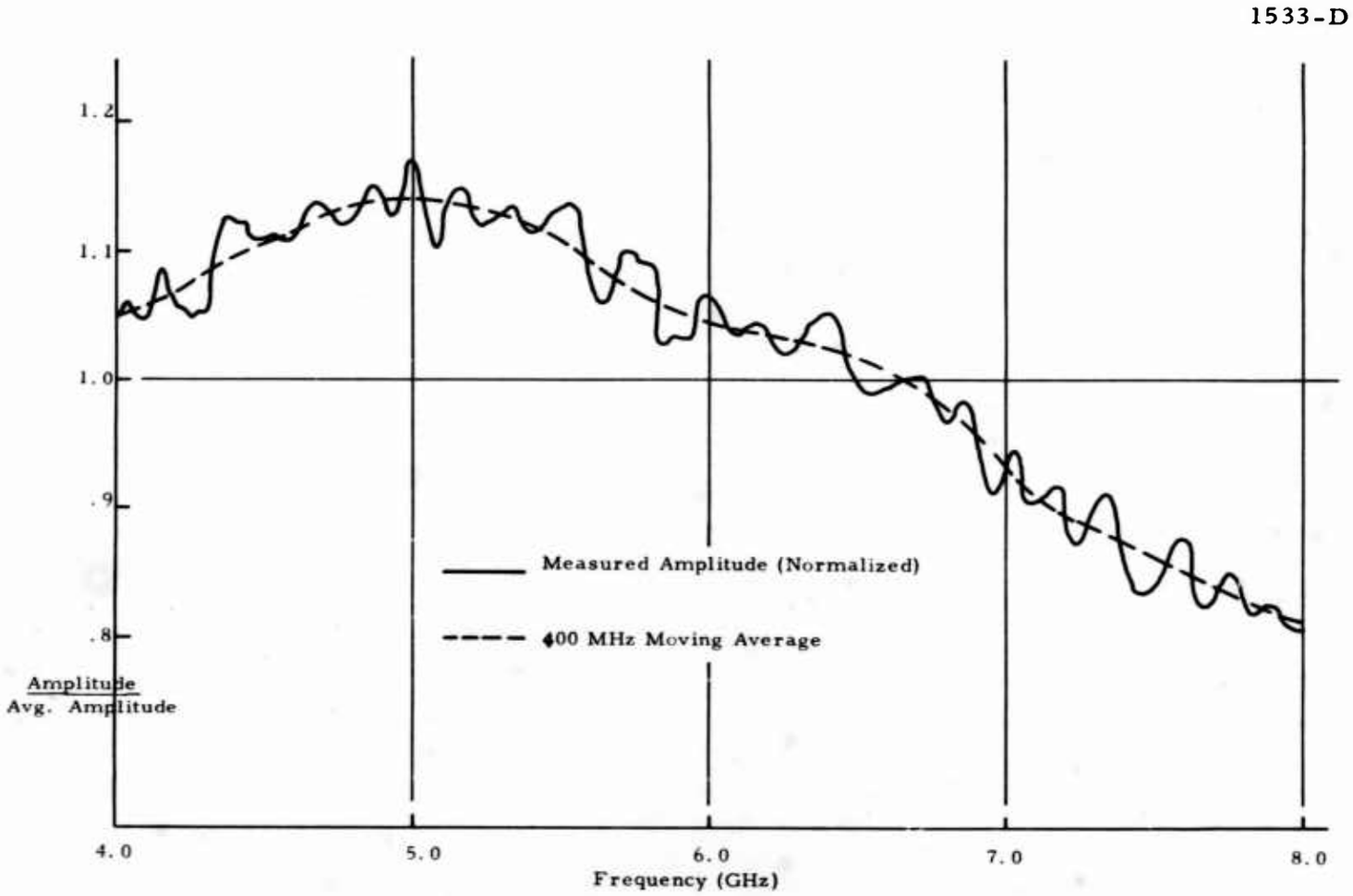

FIGURE 4-6

MEASURED AMPLITUDE AND MOVING AVERAGE AMPLITUDE FOR VARYING FREQUENCY CASE

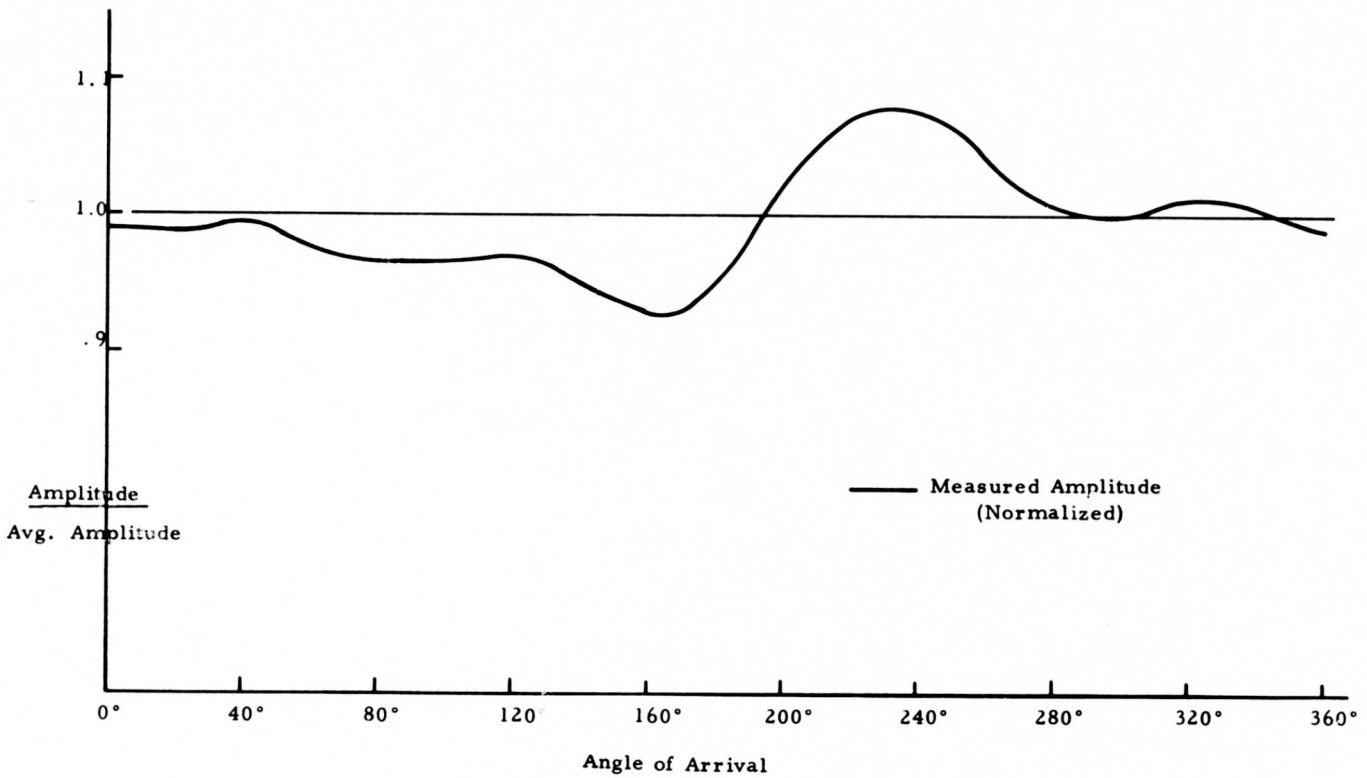

FIGURE 4-7 MEASURED AMPLITUDE FOR VARYING ANGLE CASE – NO OBSTACLES

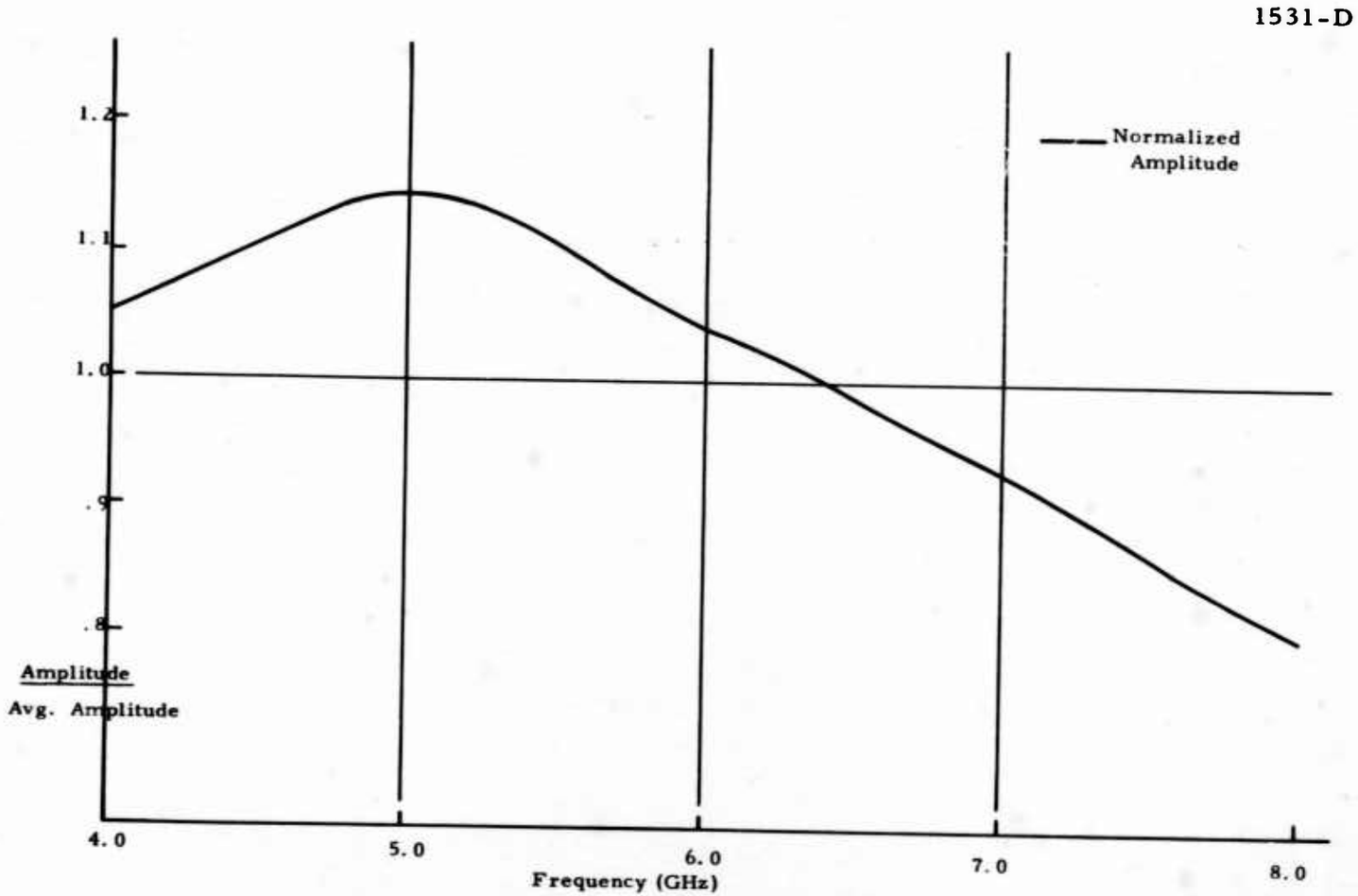

FIGURE 4-8 MEASURED AMPLITUDE FOR VARYING FREQUENCY CASE – NO OBSTACLES

It should be emphasized that it is not important that the correspondence between the microwave obstacles, and what they are chosen to represent, be exact. The microwave experiment stands by itself; the analysis given in Chapter 2 may be applied to it regardless of whether or not it is a precise representation of the HF problem. The microwave obstacles, however, have been chosen to be similar to naturally occurring obstacles in the HF band in order to support the application of the statistical theory to HF. It is certainly reasonable to propose that if the statistical analysis is successful in the microwave region it will also be successful at HF when applied to obstacles of similar dimensions (with respect to a wavelength) and similar electrical characteristics.

The measurements for the varying angle case were performed at 5 GHz. The measurements for the varying frequency case were performed over an octave band from 8 GHz to 4 GHz. This frequency range was initially chosen because it is the range over which the sweeper operates. Other measurements were performed with an increased range (down to 2 GHz and up to 12 GHz), but, for the obstacle configurations considered, the value of k^2 (frequency) increased very slowly as the bandwidth was increased.

Twenty-four different configurations were examined. Figures 4-9, 4-10, 4-11 and 4-12 are the polar plots of received signal power versus angle of arrival for each configuration. Figures 4-13, 4-14, 4-15 and 4-16 are the polar plots of received signal power versus frequency for each configuration. There are six configurations per figure. Each plot is linear, with the radius proportional to received power.

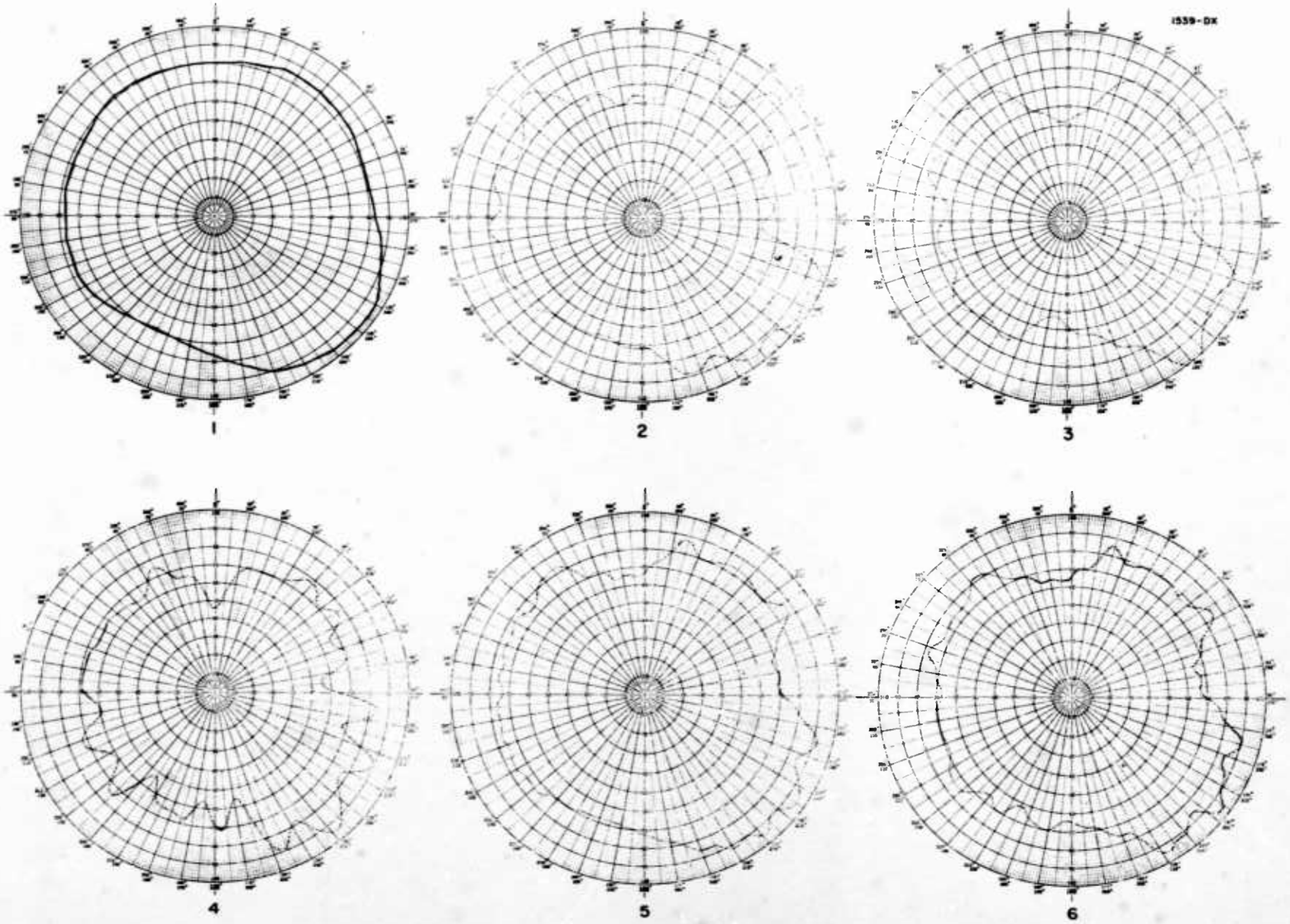

FIGURE 4-9 POLAR PLOTS OF RECEIVED SIGNAL POWER VS ANGLE OF ARRIVAL FOR VARIOUS OBSTACLE CONFIGURATIONS

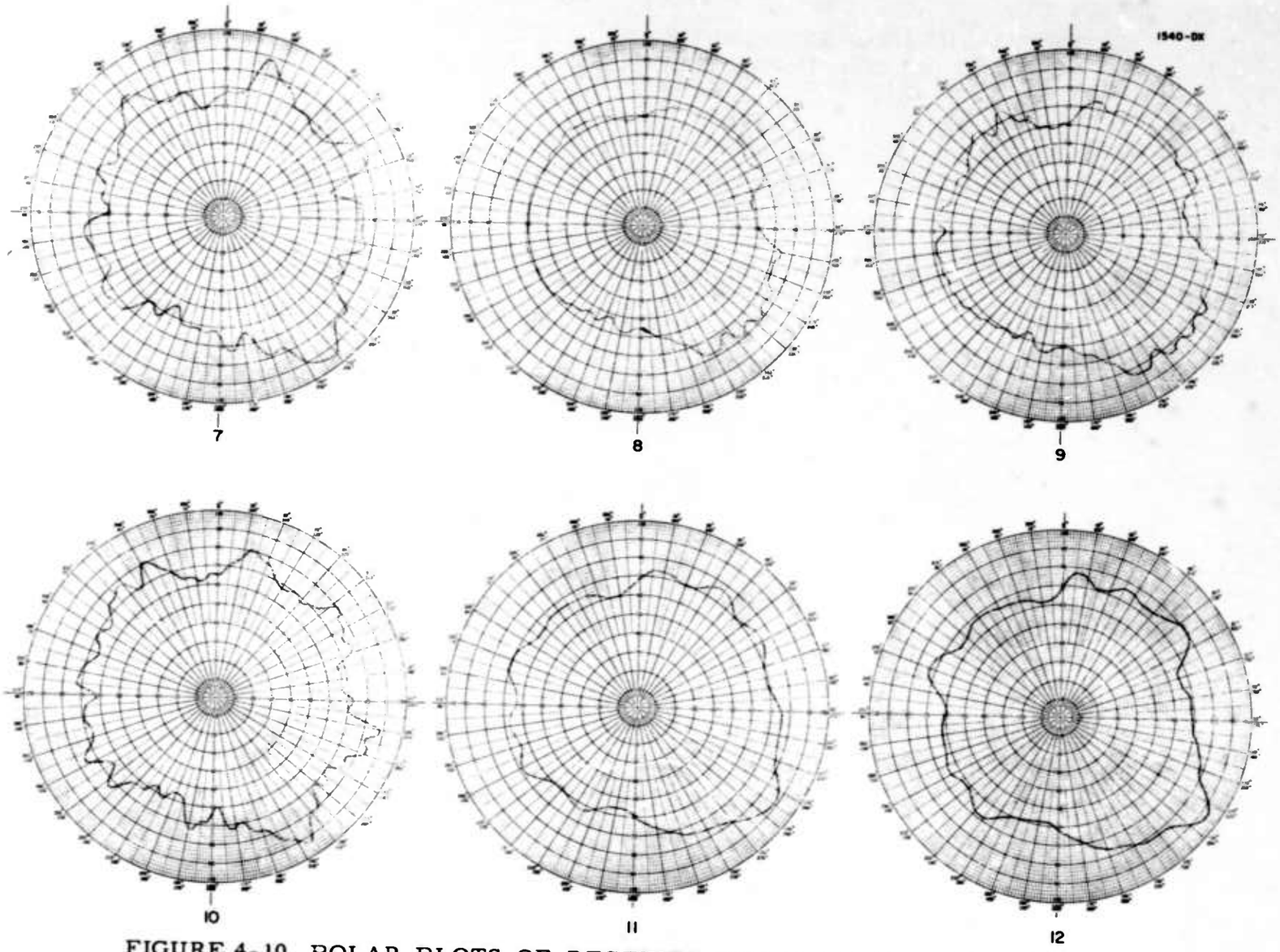

FIGURE 4-10 POLAR PLOTS OF RECEIVED SIGNAL POWER VS ANGLE OF ARRIVAL FOR VARIOUS OBSTACLE CONFIGURATIONS

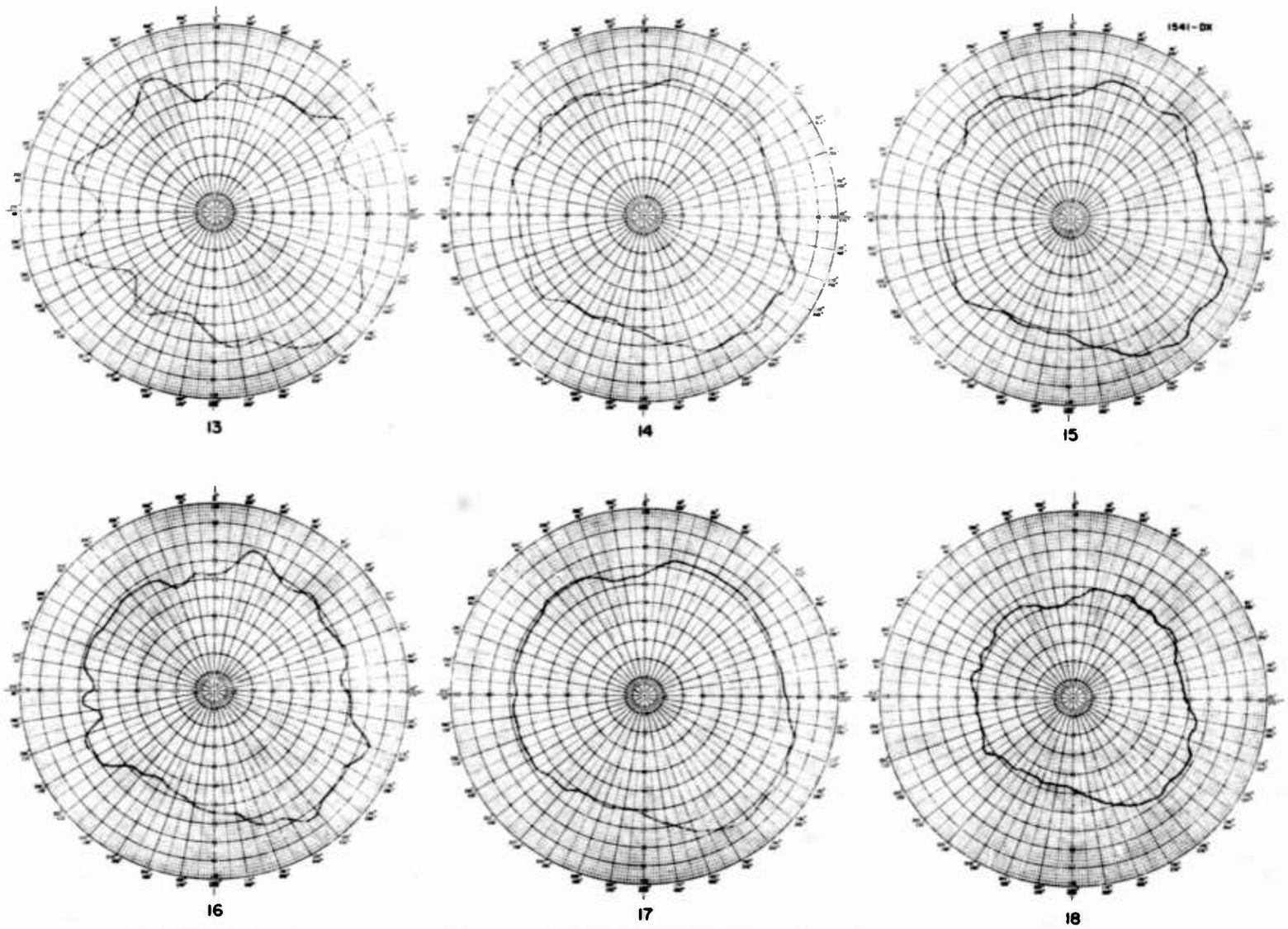

FIGURE 4-11 POLAR PLOTS OF RECEIVED SIGNAL POWER VS ANGLE OF ARRIVAL FOR VARIOUS OBSTACLE CONFIGURATIONS

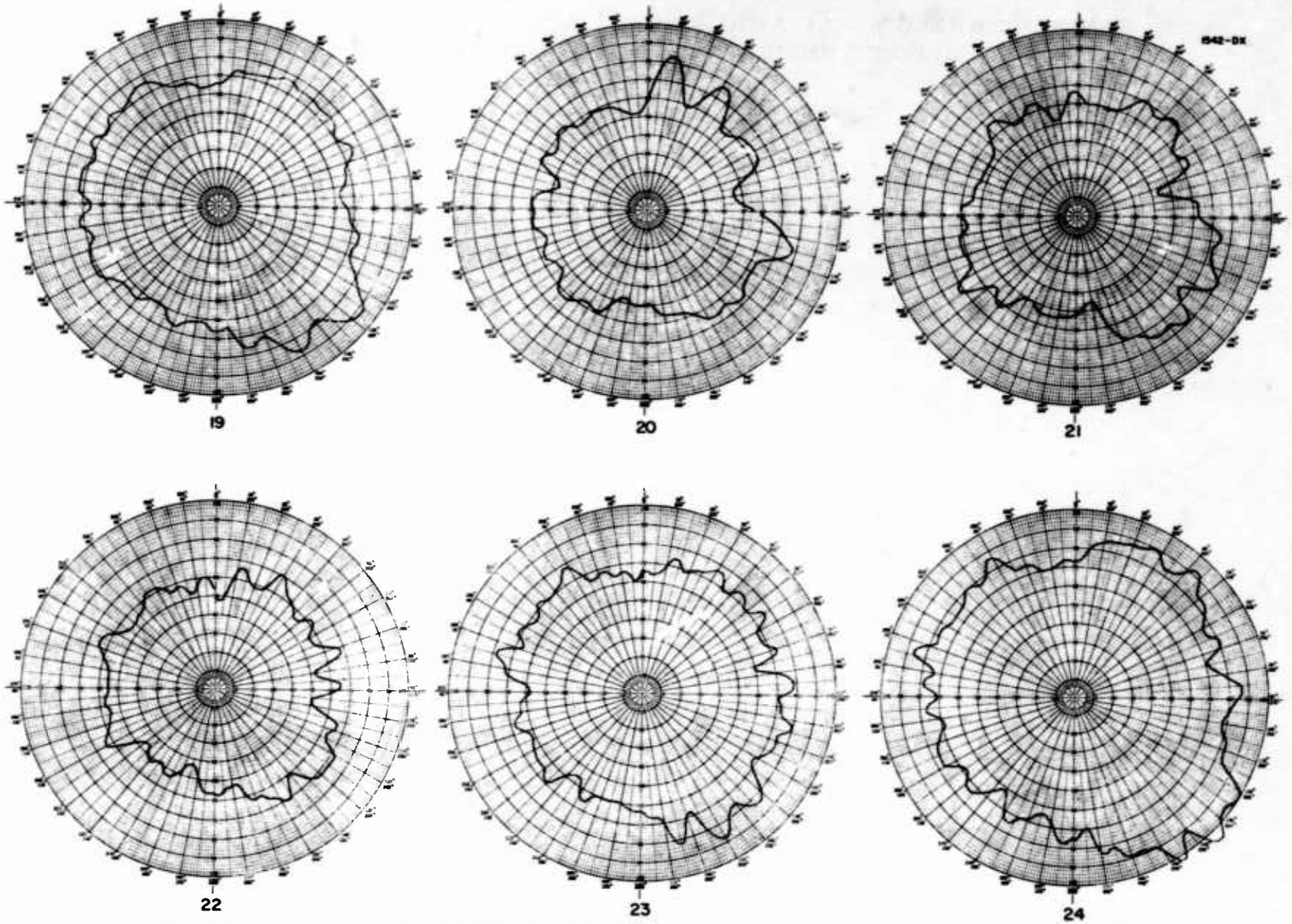

FIGURE 4-12 POLAR PLOTS OF RECEIVED SIGNAL POWER VS ANGLE OF ARRIVAL FOR VARIOUS OBSTACLE CONFIGURATIONS

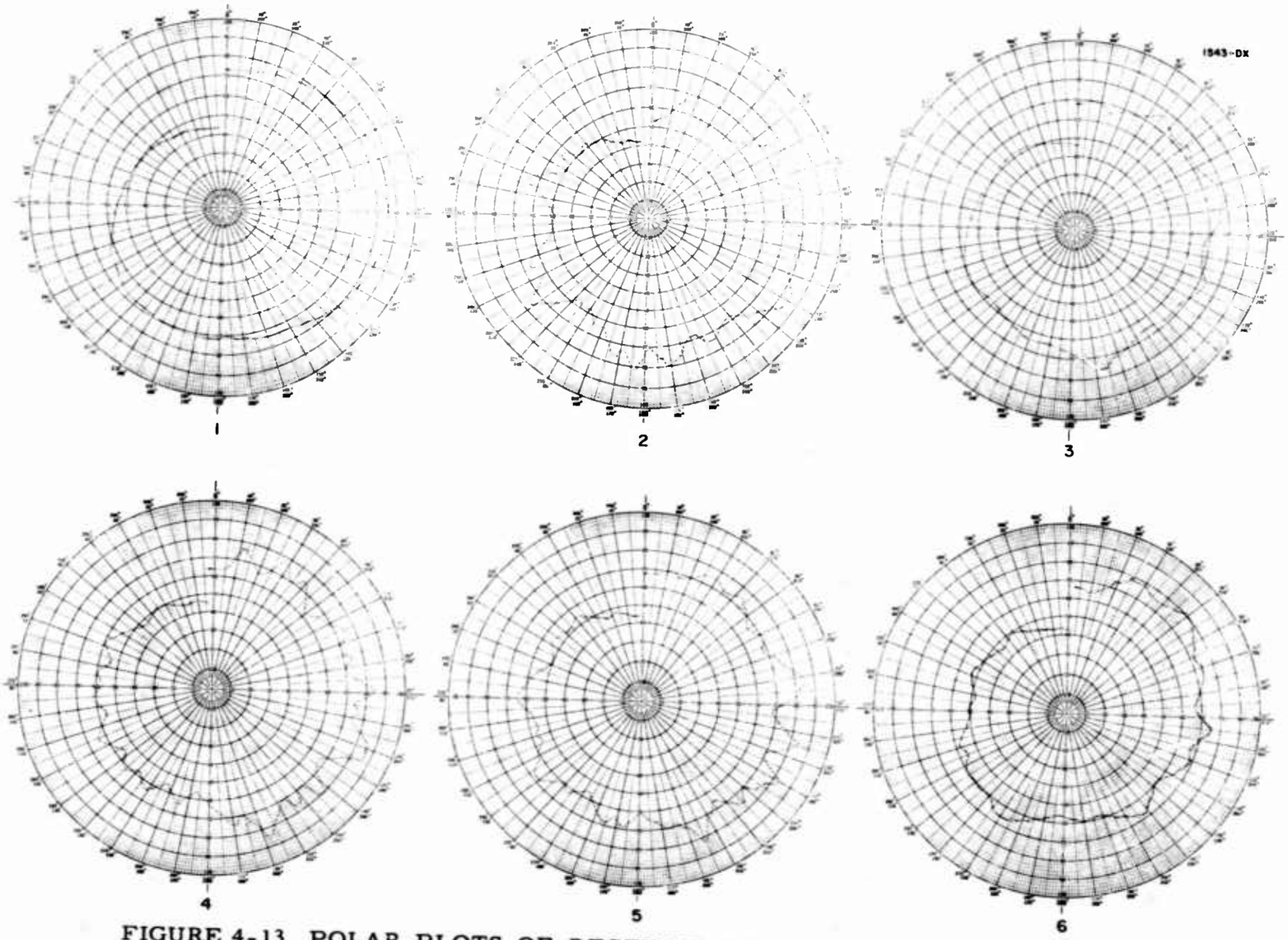

FIGURE 4-13 POLAR PLOTS OF RECEIVED SIGNAL POWER VS FREQUENCY FOR VARIOUS OBSTACLE CONFIGURATIONS

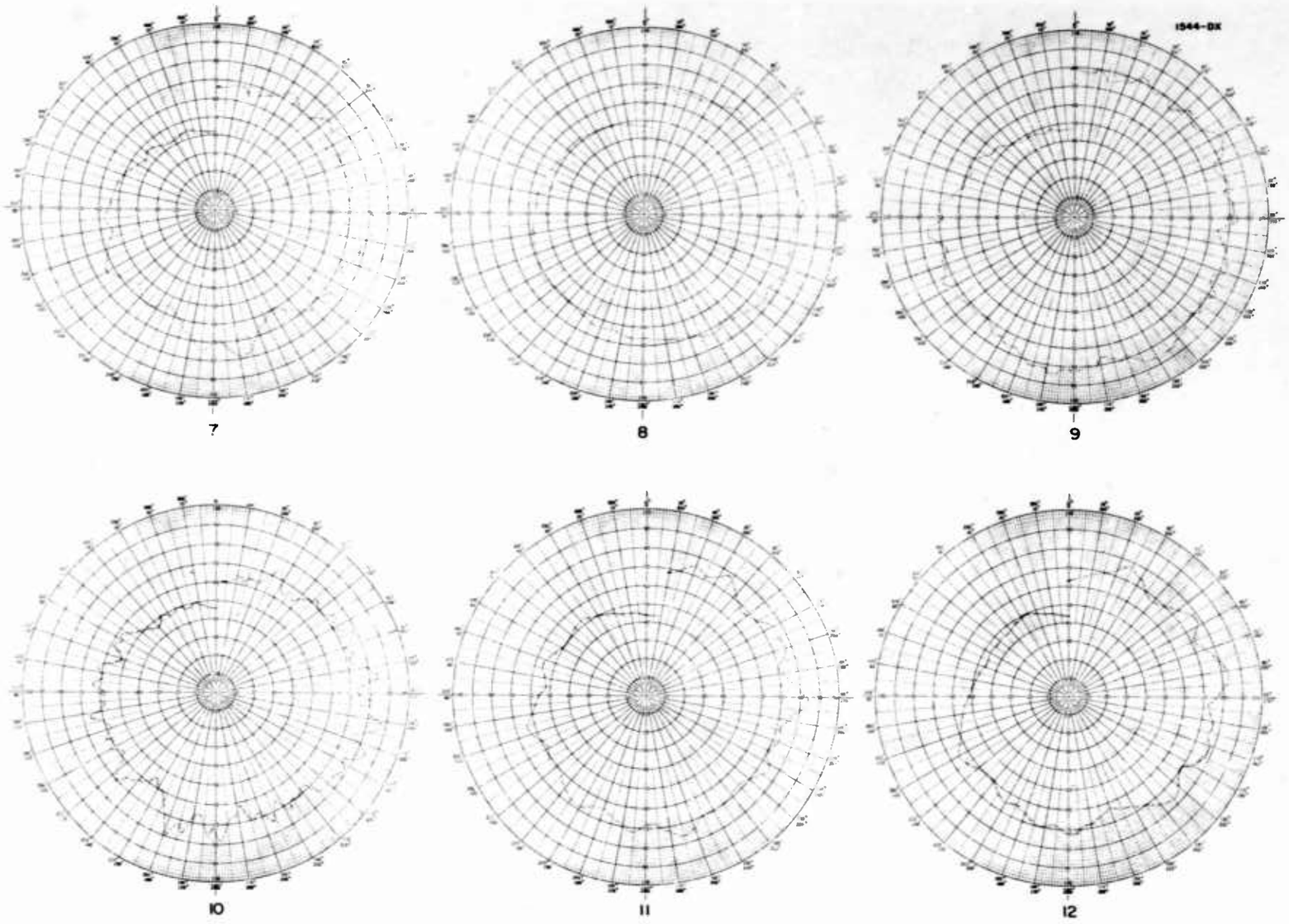

FIGURE 4-14 POLAR PLOTS OF RECEIVED SIGNAL POWER VS FREQUENCY FOR VARIOUS OBSTACLE CONFIGURATIONS

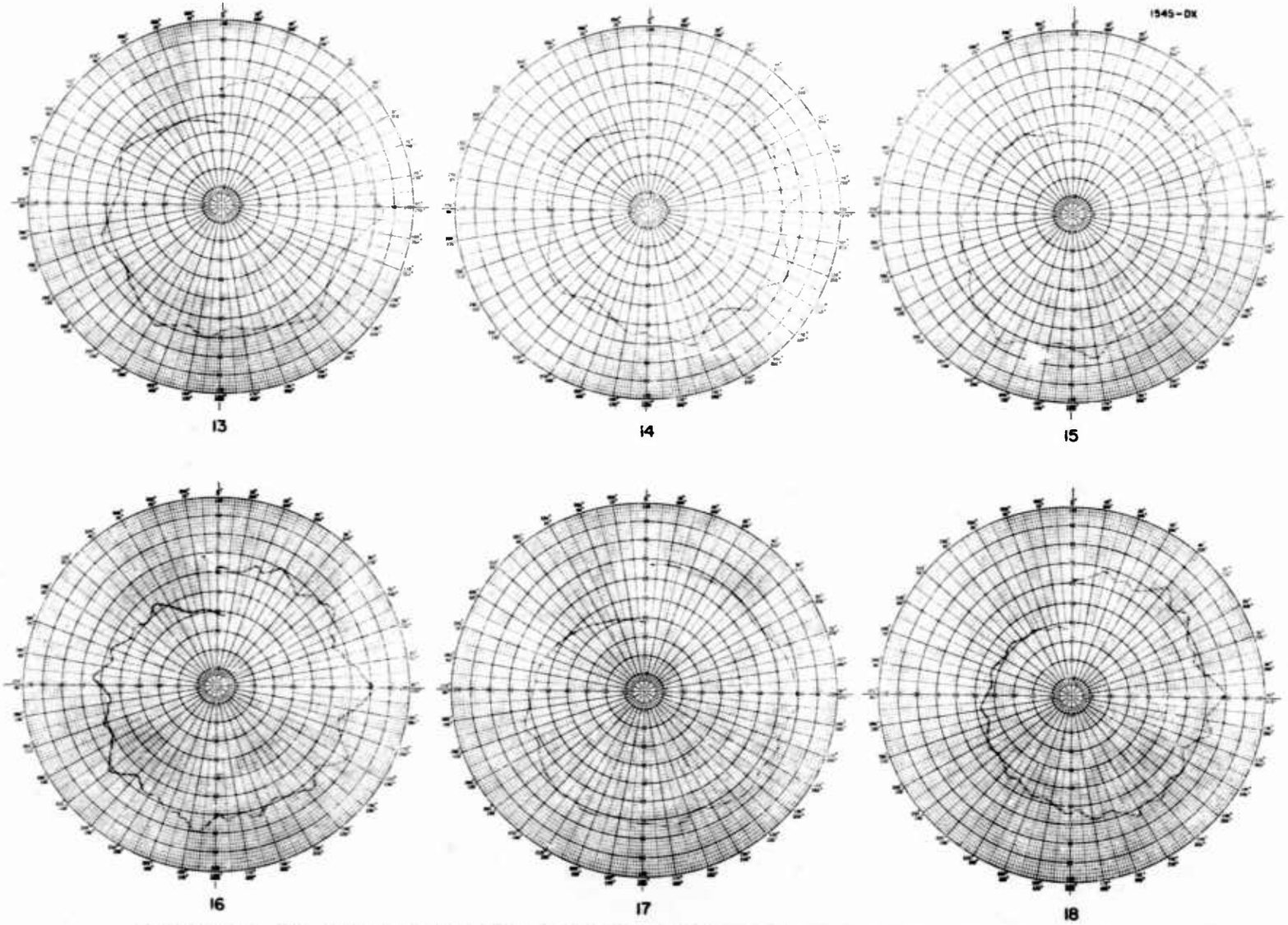

FIGURE 4-15 POLAR PLOTS OF RECEIVED SIGNAL POWER VS FREQUENCY FOR VARIOUS OBSTACLE CONFIGURATIONS

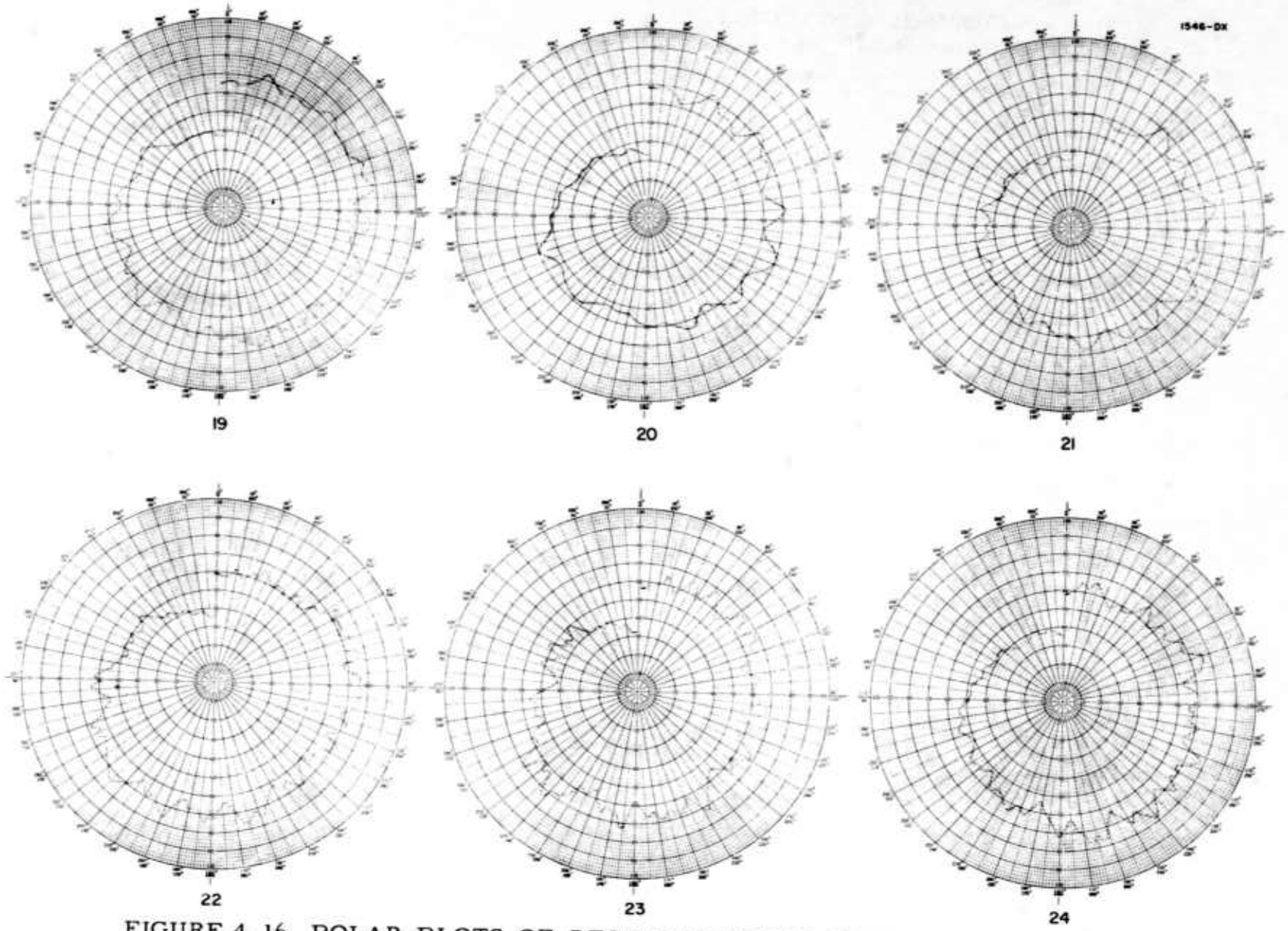

FIGURE 4-16 POLAR PLOTS OF RECEIVED SIGNAL POWER VS FREQUENCY FOR VARIOUS OBSTACLE CONFIGURATIONS

Table 4-1 summarizes the results of the measurements, after the adjustments described in Chapter 2-B are performed. Column 1 gives the number of the obstacle configuration presented. Column 2 is the value of k^2 for the case of varying angle. Column 3 states the probability, as measured by χ^2, that the data has the hypothesized distribution, for the varying angle case. Column 4 is the value of k^2 for the case of varying frequency. Column 5 is the probability, as measured by χ^2, that the data has the hypothesized distribution, for the varying frequency case. Column 6 is the ratio of k^2 for the varying angle case to k^2 for the varying frequency case. Column 7 is the value of k^2 (angle) for various cases normalized to the value of k^2 (angle) for the first case measured with obstacles present. Column 8 is the value of k^2 (frequency) for various cases normalized to the value of k^2 (frequency) for the first case measured with obstacles present.

A description of each obstacle configuration, which appears in the plots, and the table, follows. A few representative sketches are given in Figures 4-17 and 4-18. For the sake of convenience, they are referred to according to what they are meant to represent at HF instead of what they are (e.g., "hill" instead of "piece of Eccosorb"). The configurations were chosen so that the effect of three quantities on the value of k^2 could be determined: 1) the number of obstacles present; 2) the distance from the direction-finder to the obstacles; 3) the type of obstacles. In the listing, the wavelength λ refers to the wavelength at 5 GHz.

1. No obstacles present.

2. Two irregularly shaped hills, approximately $\lambda/4$ high and $\lambda/2$ - λ long, placed $>2\lambda$ away from the receiving antenna.

Configuration Number	ANGLE		FREQUENCY		k^2 (angle) / k^2 (frequency)	k^2 (angle) / k^2 (angle, case 2)	k^2 (frequency) / k^2 (angle, case 2)
	k^2	χ^2 prob.	k^2	χ^2 prob.			
1	.000155	>50%	.000021	>80%	7.4		
2	.002606	>20%	.000932	>30%	2.8	1.00	1.00
3	.002135	>70%	.000553	>50%	3.9	.82	.59
4	.003695	>50%	.002437	>20%	1.5	1.42	2.62
5	.001020	>50%	.000344	>50%	3.0	.38	.37
6	.001374	> 5%	.000529	>50%	2.6	.53	.57
7	.002242	>20%	.001170	>50%	1.9	.86	1.25
8	.000728	>70%	.000283	> 5%	2.6	.28	.32
9	.001138	>10%	.000437	>80%	2.6	.44	.47
10	.002369	>10%	.000931	>10%	2.5	.91	1.00
11	.000842	>90%	.000240	>30%	3.5	.32	.26
12	.001655	>50%	.000421	>50%	3.9	.63	.45
13	.002930	>70%	.000733	>50%	4.0	1.17	.79
14	.000419	>50%	.000140	>50%	3.0	.16	.15
15	.000567	>50%	.000157	>80%	3.6	.22	.17
16	.001197	>30%	.000446	>50%	2.8	.46	.48
17	.000219	>50%	.000069	>20%	3.2	.08	.07
18	.000337	>50%	.000152	>50%	2.2	.13	.16
19	.000918	>50%	.000530	>80%	1.7	.35	.57
20	.004171	>50%	.001589	>50%	2.7	1.47	1.70
21	.002763	>30%	.001777	>30%	1.6	1.06	1.90
22	.003093	>50%	.002052	>30%	1.6	1.18	2.20
23	.001693	>50%	.001449	>50%	1.2	.65	1.50
24	.001312	>50%	.000912	>50%	1.4	.50	.98

TABLE 4-1

k^2 (ANGLE) AND k^2 (FREQUENCY) FOR VARIOUS OBSTACLE CONFIGURATIONS

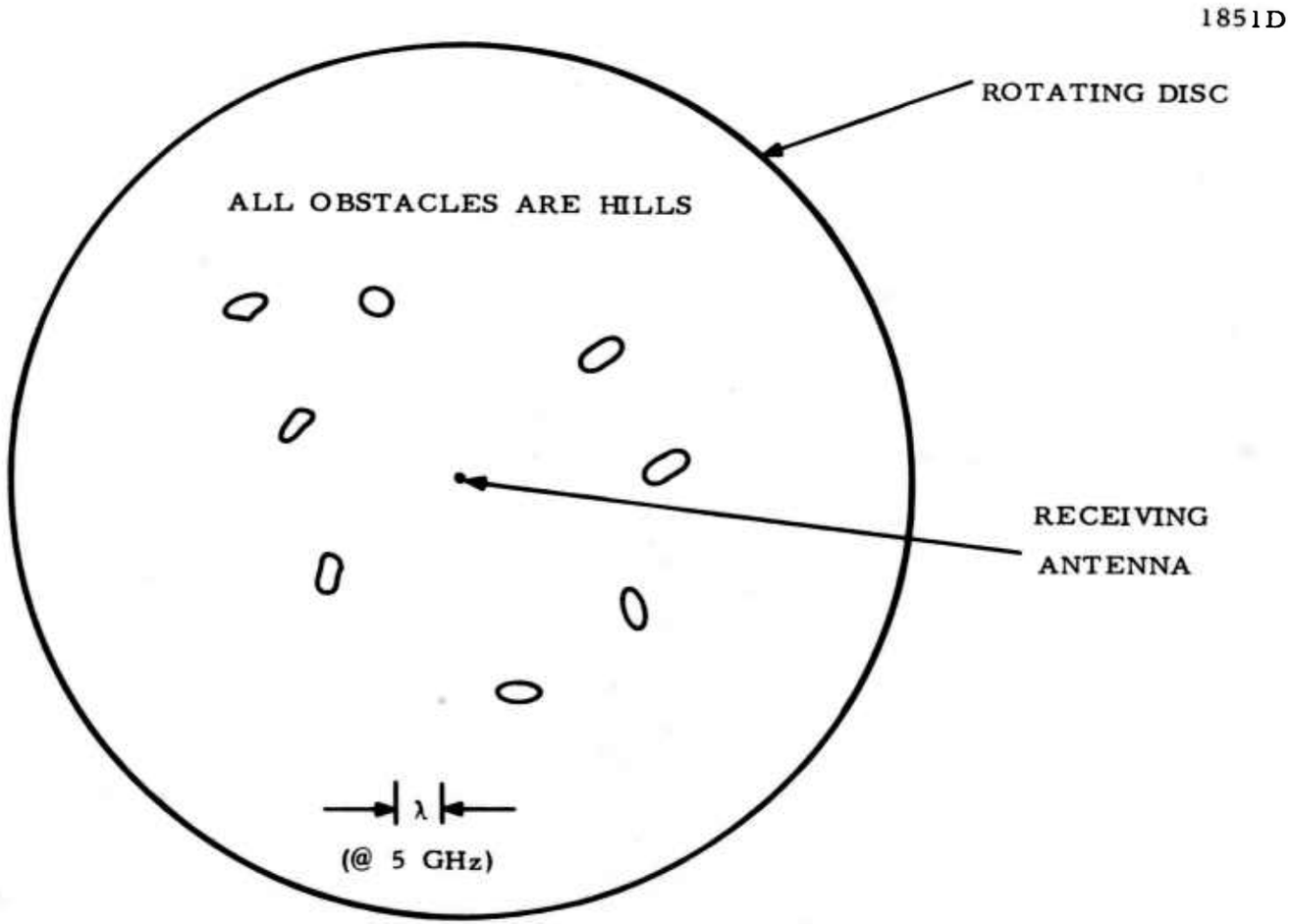

FIGURE 4-17 OBSTACLE ARRANGEMENT IN CASE 7

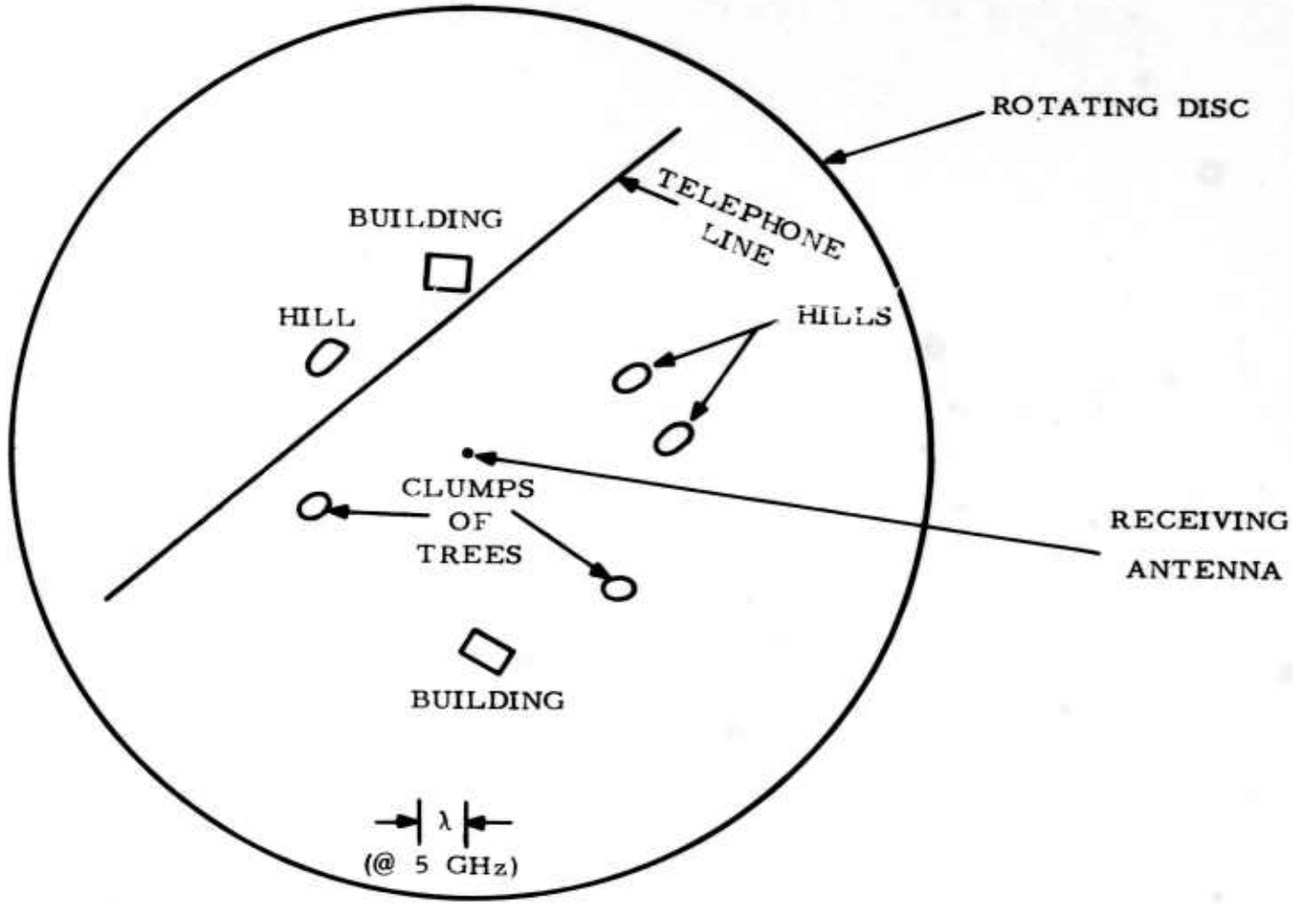

FIGURE 4-18 OBSTACLE ARRANGEMENT IN CASE 16

3. Four irregularly shaped hills, of the same general characteristics, placed >2λ away from the receiving antenna.

4. Eight irregularly shaped hills, of the same general characteristics, placed >2λ away from the receiving antenna.

5. Two of the same obstacles, placed >4λ away from the receiving antenna.

6. Four of the same obstacles, placed >4λ away from the receiving antenna.

7. Eight of the same obstacles, placed >4λ away from the receiving antenna.

8. Two of the same obstacles, placed >6λ away from the receiving antenna.

9. Four of the same obstacles, placed >6λ away from the receiving antenna.

10. Eight of the same obstacles, placed >6λ away from the receiving antenna.

11. A clump of trees <λ/4 high and ~λ long, and a building <λ/4 high and ~λ long, placed >2λ from the receiving antenna.

12. A telephone line ~λ/4 high, and a hill <λ/4 high and ~λ long added to the obstacles in 11 and placed >2λ from the receiving antenna.

13. Two clumps of trees, two buildings, three hills, and a telephone line, all with the same characteristics as in 11 and 12, and all placed >2λ from the receiving antenna.

14. The same obstacles as in 11, placed >4λ from the receiving antenna.

15. The same obstacles as in 12, placed >4λ from the receiving antenna.

16. The same obstacles as in 13, placed >4λ from the receiving antenna.

17. The same obstacles as in 11, placed >6λ from the receiving antenna.

18. The same obstacles as in 12, placed >6λ from the receiving antenna.

19. The same obstacles as in 13, placed >6λ from the receiving antenna.

20. Twenty obstacles, of various sizes and shapes, all <λ/4 high and between λ/4 and 2λ long, and placed >2λ from the receiving antenna.

21. The same 20 obstacles, placed >4λ from the receiving antenna.

22. As in 21, the obstacles rearranged.

23. The same 20 obstacles, placed >6λ from the receiving antenna.

24. As in 23, the obstacles rearranged.

The results in Table 4-1 call for some comment. A list of observations on the data is given, with some explanations of the observed effects.

1. Using the 5 per cent criterion for χ^2, all the configurations given in the table fall within the hypothesized distribution. Surprisingly, even situations with only two obstacles have a high probability of being in this class, indicating that $E_n \cos \Phi_n$ and $E_n \sin \Phi_n$ $(n = 1, 2)$ are sometimes close to a normal distribution. Since most of the probabilities given in the table are significantly greater than the minimum necessary, the analytical model appears to explain successfully the measured fluctuations in received power.

2. The value of k^2 (angle) and k^2 (frequency) increases as the number of obstacles increases. This is what is expected, since each additional obstacle is another source of scattered power.

3. The value of k^2, for both cases, decreases as the obstacle-free radius around the receiving antenna increases. The value of k^2 is approximately inversely proportional to the distance from the obstacles to the receiving antenna. The relationship between k^2 and this distance is difficult to establish, however, since in moving the obstacles outward from the receiving antenna, their relative orientation cannot be maintained easily. Thus another variable, whose influence is not known, is unavoidably introduced.

4. The value of k^2 (angle) is greater than k^2 (frequency) for all configurations considered. As previously noted, k^2 (frequency) appears to converge very slowly to k^2 (angle) as the bandwidth of the sweep increases.

5. The agreement between k^2 (angle) and k^2 (frequency) improves as the number of obstacles increases, becoming very good for a large number of obstacles. This may result from the fact that the number of independent samples of the data, and, correspondingly, the accuracy in the estimate of k^2, increases, as the number of obstacles increases, for both the varying angle and the varying frequency case. The number of independent samples is roughly dependent on the rapidity of the fluctuations in the received power. These fluctuations are much more rapid as the number of obstacles increases.

6. The agreement between k^2 (angle) and k^2 (frequency) improves as the obstacle-free radius around the receiving antenna increases. This is traceable to the same sources as 5, above, since the rapidity of the fluctuations in the received power increases as the distance to the obstacles increases and hence more independent samples of the data are available.

From these observations, either k^2 (angle) or k^2 (frequency) appear to satisfy the requirements that one would intuitively expect a "site goodness" parameter to meet. If increasing k^2 is taken to mean that a site is less suitable for direction-finding, then the expected cases exhibit this behavior, namely:

1. The closer the obstacles are, the more inaccuracy is introduced into the D/F measurement. k^2 increases as the obstacles are moved closer.

2. The more obstacles there are, the more the accuracy of the D/F system is impaired. k^2 increases as the number of obstacles increases.

3. The larger the obstacles are, the more error they introduce. k^2 increases as the obstacle size increases.

Since k^2 (frequency) exhibits the same trends as k^2 (angle), as columns 7 and 8 of Table 4-1 show, it is just as useful a parameter as k^2 (angle) even though there is a discrepancy between it and k^2 (angle) for finite bandwidths. In fact, it is probably unnecessary to increase the bandwidth in practical situations, since various sites may still be compared with each other on the basis of a "standard bandwidth" k^2 (frequency). The following section will elaborate on how site comparisons on this basis might be accomplished.

D. Summary

The experimental measurements carried out to verify the validity of the analytical model are presented in this Chapter. In Section A is given a description of the experimental apparatus, the transmitting-receiving system, and the automated data collection system. The experiments were carried out at microwave frequencies for reasons of convenience, but because of the electrical parameters chosen, the observed scattering effects are similar to those expected in the HF band. A necessary adjustment of the data is presented in Section B. In Section C the experimental results are given. The value of k^2 (angle) and k^2 (frequency) is calculated for each configuration of obstacles tested and the probability that such a configuration is described

by the analytical model is given. In addition several observations are made concerning the nature of k^2 (angle) and k^2 (frequency) and their usefulness as measures of site suitability.

Chapter 5

CONCLUSIONS AND RECOMMENDATIONS

A. Conclusions

The commonly accepted method of D/F site evaluation[1] is to move a target transmitter of fixed frequency on a circular path of large (with respect to a wavelength) radius centered on the direction-finder. If the maximum variation of the received signal as a function of the angular position of the target transmitter is greater than some arbitrary criterion, the site is rejected for direction-finding. Since it is usually desired to use the direction-finder over a frequency band, this test is repeated for a number of frequencies within the band.

It is possible to represent in a three-dimensional plot the electric field amplitude at the direction-finder as a function of the angular position and the frequency of the target transmitter. The amplitude is the z-coordinate of a surface whose x and y coordinates are angle and frequency respectively. The method described above gives the value of z along several lines of constant y. The surface could therefore be completely described if a sufficient number of these lines were chosen. Similarly the surface could be completely described if the value of z were given along a sufficient number of lines of constant x. In other words, the evaluation method described in the first paragraph can be carried out equivalently by placing the target transmitter at a number of points on the chosen circular path and varying the frequency over the band of interest, a seemingly trivial observation. In practice, however, this latter measurement is easier to perform.

The difficulty involved in the former measurement lies in keeping the radius of the circle constant for large radii. This is necessary to insure that the observed perturbations in the received signal arise not from variations in the transmitter-receiver distance, but only from the fluctuations in the amplitudes and phases of the scattered waves brought about by the changing angle of arrival of the direct wave. In the latter case, the changes in the absolute magnitude of the direct wave caused by variations in the transmitter-receiver distance do not affect the result. The quantity of interest is the maximum fluctuation from the average signal magnitude over the band, where it is assumed that allowance is made for the slowly-varying-with-frequency-sensitivity of the transmitting-receiving system.

The above observation is true of any site. The question of most interest to the engineer, though, is how many points on the approximate circular path must be used to evaluate the site. There is no single answer to this question applicable to all sites. In the body of this work, however, it is shown that for a certain class of sites very few, perhaps only one or two, points are necessary. In general these sites are characterized by the presence of several "resonant" obstacles; i.e., obstacles whose dimensions are on the order of a wavelength in magnitude in the frequency band of interest.

For this type of site a one-parameter probability distribution can be derived for the electric field amplitude at the direction finder as either (A) the angle of arrival or (B) the frequency of the direct wave is varied. The computations described in Chapter 3 and the experimental work given in Chapter 4 indicate that the parameter of case (A) is

approximately the same as the parameter of case (B) when several resonant obstacles are present. In addition, the results of Chapters 3 and 4 strongly suggest that only a small number of target transmitter positions are necessary to provide sufficient data to calculate this parameter when the technique of frequency variation is employed. This parameter, k^2, which is the ratio of the mean square power in the scattered waves to the power in the direct wave, is proposed as a figure of merit for sites having the characteristic mentioned above.

The computational work has also given indications of when a small number of transmitter positions may not be sufficient to evaluate a site. Above the resonance region, for example, extended obstacles are more directional reradiators than in the resonance region. An estimate of k^2 by frequency variation in this range is therefore critically dependent on the transmitter's angular position. Below the resonance region the magnitude of the fluctuations in the scattered power as the angular position of the transmitter is changed is overestimated by a k^2 measured through the resonance region.

The question of how many obstacles must be present for a rapid determination of k^2 by frequency variation has been left unanswered. The computational and experimental work has indicated that the answer to this question depends greatly on the types of obstacles involved; i.e., their shape, conductivity, etc. A single obstacle with a complex geometrical form may satisfy the requirements as well as many obstacles with simple geometrical shapes.

Finally, the experimental confirmation is somewhat limited. Although in the computational work it was indicated that the k^2 estimated by frequency variation would be different from the k^2 estimated by angle-of-arrival variation for obstacles large with respect to a wavelength, an extensive investigation of this effect was not undertaken in the experimental work. Thus it is difficult to define precisely the obstacle size beyond which k^2 may not be determined by a small number of measurements. For the range of obstacle sizes used in the experimental work, however, the k^2 estimated by frequency variation at a single transmitter position is very close to that determined by angle-of-arrival variation at the geometric mean frequency of the band.

From the table given in Chapter 4 it can be seen that if all the k^2(angle) are normalized to one value of k^2(angle) and similarly all the k^2(frequency) are so normalized (columns 7 and 8), then each normalized k^2(angle) is within a factor of two of each normalized k^2 (frequency) for all configurations except number 23. Indications are strong therefore that k^2(frequency) = k^2(angle) except for a bandwidth-dependent multiplicative factor.

B. Recommendations

Several recommendations for futher work in this area have evolved from the investigations reported here. A list of them follows:

1. The investigation was concerned with the use of the statistical methods employed in the analysis of rough-surface scattering to provide a rational basis of D/F site selection. No attempt has so far been made to suggest a means of correcting for the

errors introduced by the scatterers. The previous work mentioned in the introduction outlines a means of correcting for the presence of one point scatterer. The method given in Appendix D is a more general method to correct for the errors introduced by several point scatterers, but, as can be seen from the complexity of the mathematics, this solution becomes quite cumbersome for more than three scatterers. In addition, it places severe requirements on the antenna pattern of the receiving antenna. Accordingly, it is recommended that further work be carried out to provide simpler means of correcting for the presence of a number of scatterers during the D/F procedure.

2. The fluctuations in received signal level versus varying elevational angle of arrival could be examined theoretically and experimentally. The assumptions made in Chapter 2 may apply to this case as well.

3. Further analytical investigation of the surface and volume current distributions on and in a complex obstacle is suggested. Although such an investigation must necessarily be approximate, it would serve to cast further light on what conditions must be met in order that k^2(angle) be the same as k^2(frequency) for a single obstacle.

4. Full scale experimental work is suggested, preferably in a geographic area where a good site is readily available. The change in the value of k^2 as complex obstacles are added to the site may then be observed.

5. The problem of siting a hydrophone array on the bottom of the ocean is analogous to that of siting a radio direction-finder. Random scattering of sound waves from various solid obstacles and eddies disrupt the performance of such an array. The statistical analysis could be restated in acoustical terms and applied to this problem as well.

6. The angle-frequency relationship noted in this work may have an analogy in a time-frequency relationship in ionospheric propagation. Perhaps the statistical characteristics of the ionosphere can be determined by frequency variation also.

C. Summary

The general conclusions arrived at from the study and some recommendations for further work are presented in this chapter. In Section A the applicability of the statistical methods is discussed and a simplification of the standard method of site evaluation is suggested. In Section B further work in this area, both analytical and experimental is recommended.

Appendix A

Narrow aperture direction-finding systems typically function by using figure 8 or cardioid antenna patterns to directly null out the signal received from a distant transmitter. The depth of the null determines how accurately the measurement can be made, as illustrated in Figure A-1. The uncertainty of the measurement increases as the depth decreases. The null depth is affected by phase and amplitude imbalances in the antenna structure, a low signal-to-noise ratio of the receiver, polarization error, and other failures of the system to perform according to its theoretical capacity. It is also affected by external noise and multipath propagation caused by site nonuniformities.

The parameter k^2 is the average power contained in the resultant of the scattered waves to the power contained in the direct wave and may be directly related to the depth of the null. For example, for two vertical electric dipoles spaced a distance d apart, and connected 180° out of phase with each other, the voltage response in the azimuthal plane to the direct wave is given by

$$V_o = AE_o \sin \left(\frac{\pi d}{\lambda} \sin \theta_o \right) \qquad \text{(Eq. A-1)}$$

where A is the voltage response of the system to a unit field and θ_o is the angle of arrival of the direct wave. The voltage response to the scattered waves is given by:

$$V_s = A \sum_{n=1}^{N} E_n e^{j\Phi_n} \sin \left(\frac{\pi d}{\lambda} \sin \theta_n \right) \qquad \text{(Eq. A-2)}$$

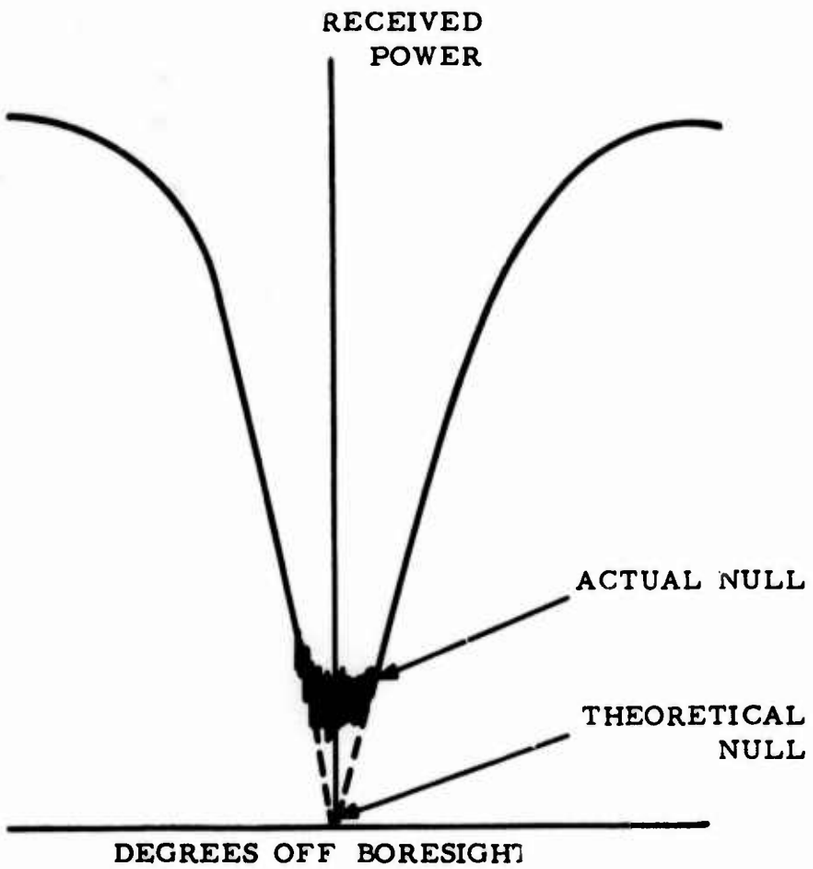

FIGURE A-1 D/F ACCURACY VERSUS NULL DEPTH FOR A SMALL-APERTURE DIRECTION-FINDER

FIGURE A-1 D/F ACCURACY VERSUS NULL DEPTH FOR A SMALL-APERTURE DIRECTION-FINDER

where θ_n is the angle of arrival of the nth scattered wave. The power received from the scattered waves averaged over all angles of arrival of the direct wave is:

$$P_s = \frac{\langle V_s^2 \rangle}{Z} = \frac{A^2}{Z} \left\langle \sum_{n=1}^{N} \sum_{m=1}^{N} E_n E_m e^{j(\Phi_n - \Phi_m)} \sin\left(\frac{\pi d}{\lambda} \sin\theta_n\right) \right.$$

$$\left. \cdot \sin\left(\frac{\pi d}{\lambda} \sin\theta_m\right) \right\rangle \qquad \text{(Eq. A-3)}$$

where Z is the input impedance to the receiver. Assume $E_1, \ldots, E_n$, $\Phi_1, \ldots, \Phi_n$ are independent random variables, as before, and, in addition, that θ_n is a random variable independent from E_n and Φ_n and uniformly distributed from 0 to 2π. Then (A-3) becomes:

$$P_s = \frac{A^2}{Z} \sum_{n=1}^{N} \langle E_n^2 \rangle \left\langle \sin^2\left(\frac{\pi d}{\lambda} \sin\theta_n\right) \right\rangle \qquad \text{(Eq. A-4)}$$

Now

$$\left\langle \sin^2\left(\frac{\pi d}{\lambda} \sin\theta_n\right) \right\rangle = \frac{1}{2\pi} \int_0^{2\pi} \sin^2\left(\frac{\pi d}{\lambda} \sin\theta_n\right) d\theta_n$$

$$= \frac{1}{2}\left(1 - J_o\left(\frac{2\pi d}{\lambda}\right)\right) \quad \text{for all } \theta_n \qquad \text{(Eq. A-5)}$$

so we can write

$$\langle P_s \rangle = \frac{A^2}{Z} \langle E_s^2 \rangle \cdot \frac{1}{2}\left(1 - J_o\left(\frac{2\pi d}{\lambda}\right)\right) \qquad \text{(Eq. A-6)}$$

If the power contained in the direct wave is much greater than the power contained in all the scattered waves, $k^2 < .01$ say, then the maximum power received by the antenna (at $\theta_o = \pi/2$) is primarily that of the direct wave; i.e.,

$$P_{T_{max}} = P_D + P_s \approx P_D \Big|_{\theta_o = \frac{\pi}{2}} = \frac{A^2}{Z} E_D^2 \sin^2 \left(\frac{\pi d}{\lambda}\right) \qquad \text{(Eq. A-7)}$$

where P_T = total received power.

The minimum power received by the antenna (at $\theta_o = 0$) is a random variable whose average value is given by (A-6). So the average value of the ratio of maximum power to minimum power, or the null depth, is given by

$$\left\langle \frac{P_{T_{max}}}{P_{T_{min}}} \right\rangle = \frac{P_D}{\langle P_s \rangle} = \frac{E_D^2}{\langle E_s^2 \rangle} \cdot \frac{2 \sin^2 \left(\frac{\pi d}{\lambda}\right)}{\left(1 - J_o \left(\frac{2\pi d}{\lambda}\right)\right)} \qquad \text{(Eq. A-8)}$$

The expression $(\sin^2 x/2)/(1 - J_o(x))$ is not a very sensitive function of x and ≈ 1 for $x < \pi$ (if we take the first two terms of the expansion for J_o).

Hence we can write

$$\left\langle \frac{P_{T_{max}}}{P_{T_{min}}} \right\rangle \approx \frac{2}{k^2} \qquad \text{for } \frac{d}{\lambda} < \frac{1}{2} \qquad \text{(Eq. A-9)}$$

That this is a reasonable result can be seen by noticing that $\sin^2 (\frac{\pi d}{\lambda} \sin \theta_n) \approx (\frac{\pi d}{\lambda})^2 \sin^2 \theta_n$ for $\pi d/\lambda$ small. The average value of $\sin^2 \theta_n$ over a period is 1/2. So a uniform angular distribution of scatterers would give at the output of the two-element antenna about one-half the power output from an isotropic antenna of the same sensitivity.

Expression (A-9) gives the null depth of the two-element antenna as a function of k^2. The accuracy of D/F measurement can be simply related to the null depth by examining the pattern of the direction-finder (e.g., Figure A-1). Therefore, it is reasonable to suggest k^2 as a one-parameter criterion to employ in judging the suitability of a site for direction finding. Its usefulness may be appreciated by noting that Equation A-9 is independent of the aperture of the antenna, for apertures less than one-half wavelength. This implies that the choice of aperture for narrow aperture antennas is not determined by the accuracy requirements of the system. Problems of sensitivity and antenna balance are then the primary considerations in the aperture size chosen. The parameter k^2 essentially sets a limit to the accuracy obtainable from a narrow aperture antenna on a given site.

BLANK PAGE

Appendix B

The statistical test employed to verify that the observed amplitude has the hypothesized distribution specifies that statistically independent observations be used. Hence, both the computer data and the measured data must be processed to provide independent points. It will be recalled that for small values of k^2 the Rice distribution is very closely approximated by a Gaussian distribution. Initial calculations showed that the computed and measured values of k^2 would be less than .05, so if the data are distributed according to the hypothesized density function, then they are almost Gaussian distributed, with a mean of 1 and a variance of $k^2/2$. Now let r_a be a sample data point and r_b, another sample a fixed interval (in angle or frequency) distant from r_a. Further, let r_a and r_b range over the total number of sample points. (The number of possible pairs (r_a, r_b) is the total number of points divided by the interval between them.) Then the correlation coefficient of r_a and r_b is

$$\rho_{ab} = \langle (r_a - 1)(r_b - 1) \rangle \qquad \text{(Eq. B-1)}$$

where the brackets ($\langle\ \rangle$) denote an average taken over all possible sample points (in angle or frequency). When $\rho_{ab} = 0$, r_a and r_b are uncorrelated. Assuming r_a and r_b are each Gaussian random variables, then r_a and r_b are statistically independent for intervals where $\rho_{ab} = 0$. Statistically independent samples of the measured quantity r will be given by r_{i+n}, i = 1, . . . , N-n, where N is the total number of samples and n is the smallest number for which

$$\langle (r_i - 1)(r_{i+n} - 1) \rangle \approx 0$$

In practice, the computer program processing the data computes ρ_{ab} for $n = 0, 1, 2, \ldots$ and stops where ρ_{ab} changes sign. This interval is then used to choose the proper sample points for analysis.

Determining whether the sample points obtained are Rice distributed is the next problem. The technique to be employed is the <u>modified χ^2 minimum method</u> described by Cramer[1] and applied by Siddiqui[2] to radio propagation problems. This method involves setting up a test of the hypothesis that the data is Rice distributed. The test essentially states that if the hypothesis is true, then it is virtually impossible that a sample set of data points would be distributed very differently from a Rice distribution. The method proceeds as follows:

1. A maximum likelihood estimator for k^2 must be found. Let $r_1, r_2, \ldots, r_M$ be M independent observations of the variable r. Since the hypothesized distribution is approximated, for small values of k^2 and r near unity, by

$$p(r) = \frac{1}{\sqrt{\pi k^2}} \exp -\left(\frac{(r - 1)^2}{k^2}\right) \qquad \text{(Eq. B-2)}$$

the likelihood function associated with the density distribution p(r) is

$$L(r_1, r_2, \ldots, r_M; k^2) = \prod_{i=1}^{M} p(r_i) \qquad \text{(Eq. B-3)}$$

$$= \left(\frac{1}{\sqrt{\pi k^2}}\right)^M \exp\left(-\frac{1}{k^2} \sum_{i=1}^{M} (r_i - 1)^2\right)$$

A maximum likelihood estimator for k^2 is then given by a non-constant (i.e., dependent on $r_1, \ldots, r_M$) solution of

$$\frac{d}{d(k^2)} \log L(r_i, \ldots, r_M; k^2) = 0 \qquad \text{(Eq. B-4)}$$

From (B-3)

$$\frac{d \log L}{d(k^2)} = -\frac{M}{2}\left(\frac{1}{k^2}\right) + \left(\frac{1}{k^2}\right)^2 \left(\sum_{i=1}^{M} (r_i - 1)^2\right) \qquad \text{(Eq. B-5)}$$

From (B-5) therefore

$$k^2 = \frac{2}{M} \sum_{i=1}^{M} (r_i - 1)^2 \qquad \text{(Eq. B-6)}$$

which is twice the variance of the observations. This is what one would expect, since the approximating distribution (B-2) is Gaussian with a variance $k^2/2$.

2. The distribution of the measured data is compared with the distribution predicted by (B-2) with k^2 given by (B-6). An integer m, is chosen, not too small (at least 5) such that M/m is greater than 5, preferably greater than 10. Numbers x_1, $x_2, \ldots, x_{m-1}$ are determined such that

$$P_r(r < x_i) = \int_0^{x_i} p(r)\, dr = \frac{i}{m} \qquad i = 1, \ldots, m-1$$

(Eq. B-7)

The range $(0, \infty)$ of r is then divided into m nonoverlapping intervals $I_1 = (0, x_1), I_2 = (x_1, x_2), \ldots, I_m = (x_{m-1}, \infty)$, such that the expected number of observations in each interval is M/m. Let the actual number of observations falling in these intervals be $f_1, \ldots, f_m$. Then

$$\chi_o^2 = \sum_{i=1}^{m} \frac{\left(f_i - \frac{M}{m}\right)^2}{\frac{M}{m}} = \frac{m}{M}\left(\sum_{i=1}^{m} f_i^2\right) - M \qquad \text{(Eq. B-8)}$$

is approximately a χ^2 variate with m-2 degrees of freedom. A critical probability level α (= .05 or .01, say) is assigned and χ_α^2 is defined to be the number such that

$$P_r(\chi^2 \geq \chi_\alpha^2) = \alpha \qquad \text{(Eq. B-9)}$$

If the observed value $\chi_o^2 < \chi_\alpha^2$ the hypothesis that (B-2) is the density distribution function for r is accepted. If $\chi_o^2 > \chi_\alpha^2$ the hypothesis is rejected. In the present work, the number, M, of independent observations ranged between 35 and 70, so m was chosen to be equal to 6. The calculation of the x_i explicitly from (B-7) is quite difficult, but Norton[3] has derived an approximation for small values of k. Since r is approximately normally distributed for small values of k, it is appropriate to attempt a Taylor series expansion of the integral (B-7) in powers of k. Such an expansion provides an explicit expression for the quantities x_i associated with $P_r(r < x_i) = i/m$.

$$x_i \approx 1 + \frac{k y_{oi}}{\sqrt{2}} + \frac{k^2}{4} - \frac{k^3 y_{oi}}{8\sqrt{2}} \qquad \text{(Eq. B-10)}$$

Here y_{oi} is the value of the argument of the normal probability function (i.e., the limiting case as $k \to 0$) for the case

$$P_r(r < y_{oi}) = \frac{1}{\sqrt{2\pi}} \int_{-\infty}^{y_{oi}} \exp\left(-\frac{x^2}{2}\right) dx = \frac{i}{m} \qquad \text{(Eq. B-11)}$$

For example, $y_{o1} = -.9672$ for $P_r(r < y_{o1}) = 1/6 = .1667$; $y_{o3} = 0$ for $P_r(r < y_{o3}) = 3/6 = .5000$; $y_{o4} = .4350$ for $P_r(r < y_{o4}) = 4/6 = .6667$.

An example of this procedure follows. Thirty-six statistically independent samples of r are

.993	.943	.946	.944
.963	.972	1.017	.958
1.038	1.043	1.039	.995
.989	1.019	.974	.999
1.005	1.021	1.022	1.029
1.016	1.003	1.061	.967
1.043	1.025	.980	1.002
.983	.948	..979	1.012
.964	1.001	1.007	1.055

From these samples

$$k^2 = .0021$$

The resulting class intervals and the observed frequencies are

Class Intervals	Frequencies
0 - .969	8
.969 - .986	5
.986 - 1.000	4
1.000 - 1.014	6
1.014 - 1.031	7
1.031 - ∞	6

The expected frequency in each interval is 6. So we have

$$\chi_o^2 = \frac{6}{36}\left(\sum_{i=1}^{6} f_i^2\right) - 36 = 1.667$$

If we choose $\alpha = .05$, for four degrees of freedom the critical value of χ_α^2 is 9.488. Hence, the data are consistent with the hypothesized distribution. In fact, the probability that such a sample, as measured by χ^2, comes from the hypothesized distribution is more than 70 per cent.

Appendix C

The fact that a single measurement of k^2(frequency) at one angle is a good (within a factor of two) estimate of the average value of these quantities appears to have some relationship to the familiar concept of ergodicity. Briefly, an ensemble of time series is ergodic when two conditions hold: 1) the ensemble is stationary in the strict sense; 2) no strictly stationary subset of the ensemble has measure other than 0 or 1. For ergodic ensembles, the following theorem is true; the average value of any function of the random variable is the same whether the average is taken over the entire ensemble or over time for a particular member of the ensemble. Typically, in communication problems, very few, usually only one, members of the ensemble are available for analysis, so the "ergodic hypothesis" is made that the time series being analyzed is a member of an ergodic ensemble. Thus the time series available is considered to be representative of the entire ensemble and its characteristics are then the same as those of the other members.

In the calculations made in Chapter 3B, all the numbers of the ensemble are available. In other words, the variation of amplitude with frequency can be calculated for as many different angles-of-arrival as desired. Hence, the probability distribution of amplitude across the ensemble can be determined for various values of frequency. By analogy with the time-series case, if it is the same for all frequencies, the ensemble is stationary in the strict sense and the "ergodic theorem" states that a single member of the ensemble is typical of all other members. The average value of any function of the amplitude may be determined by averaging over frequency for a single angle-of-arrival.

The fact that k^2(frequency) for a single angle-of-arrival is a very good estimate of the average k^2(frequency) over all angles of arrival indicates that the conclusion of the ergodic theorem holds for these ensembles. The conditions of the theorem, however, are not true for all. For example, in the two configurations examined most closely (Tables 3-1 and 3-2), the distribution using the value of k^2(angle) averaged over the ensemble for all frequencies described the data (within the 5 per cent criterion for ψ^2 probability) for more than 95 per cent of the separate frequencies for which the calculations were made. The fact that this distribution did not hold 100 per cent of the time indicates that it is highly probable, but by no means certain, that the ergodic theorem can be used as a justification for using a single member of the ensemble as representative of all.

Appendix D

The material presented in this Appendix is a previous alternate approach to direction-finding in the presence of reradiators at the site. The method suggested is a means of resolving two or more components of a multipath field with a broad-beamed antenna. The method, as proposed, has two significant weaknesses:

1. In order to resolve several adjacent sources highly accurate knowledge is required of the single-source antenna pattern and the measured multiple-source antenna pattern.

2. All reflectors are assumed small with respect to a wavelength; i.e., they are assumed to be point sources of reradiation.

The second weakness in this approach led to the statistical procedure described in the body of this work.

The problem under consideration is to determine the angular position of each of several sources (i.e., the target transmitter and various reflectors, the transmitter position is fixed) when all are radiating sine waves of the same frequency but of different amplitudes and phases. The configuration to be investigated is shown in Figure D-1.

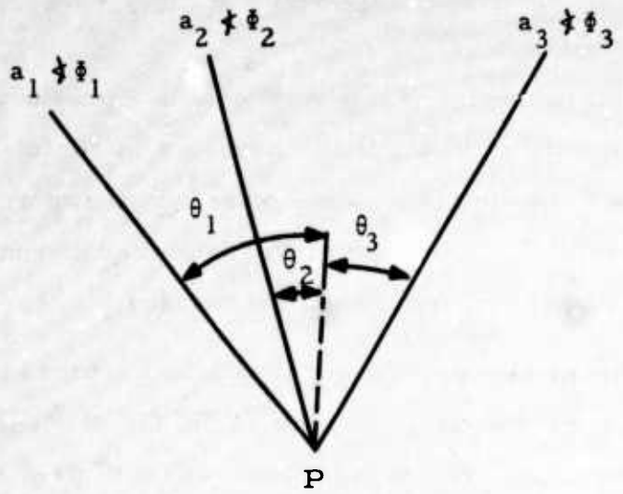

FIGURE D-1 MULTIPLE SOURCE DISCRIMINATION

$a_1, a_2, a_3, \ldots$ are the amplitudes of the sources, and $\Phi_1, \Phi_2, \ldots$ are the phases of the sources, upon arrival at point P. Thus $\Phi_1, \Phi_2, \ldots$ are affected not only by the relative phase differences between each of the sources, but also by the differences in path lengths from each source to P. The phase angles are all given with respect to a phase reference at P.

Two methods of determining $\theta_1, \theta_2, \theta_3, \ldots$ suggest themselves. One is to move the point P and investigate a segment of the radiation field of the source distribution. If a large enough sample of the radiation field is chosen, it should be possible to calcualte what source

distribution produced it. This method, however, presents practical difficulties in that an adequate sample may be many wavelengths long and at low frequencies may require motion over considerable distances.

The other method will be explored here. It involves placing a directional antenna at P, rotating it about its phase center, and examining the output as a function of aiming angle. From knowledge of the antenna's response to a point source and of the measured pattern, it is possible to deduce what the source distribution is. This may be done in either of two ways:

1. The response of the antenna to a great variety of source distributions, amplitudes, and phase angles may be calculated and the measured response compared to each of these. The calculated response most closely corresponding to the measured response will give the source distribution.

2. An analysis of the measured pattern based on its Fourier expansion will give directly the values of θ_1, θ_2, ... This analysis is presented in this Appendix.

It should be emphasized that the analysis which follows is superfluous if the antenna placed at P has a sufficiently large aperture. For then the antenna will possess sufficient resolution to distinguish between various sources. The following calculations are necessary for large beamwidth antennas only.

Now assume the antenna at P has a field response of $A(\theta)$. Then the response of the antenna to a unit magnitude point source at θ_1 is

$A(\theta - \theta_1)$. Hence, the signal received by the antenna placed at P of Figure D-1 can be represented in the phasor diagram shown in Figure D-2.

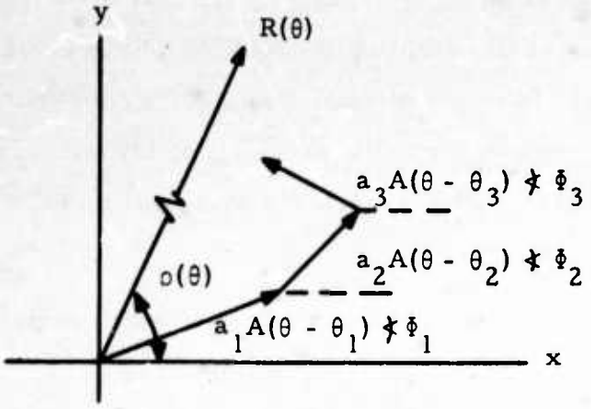

FIGURE D-2 ADDITION IN THE COMPLEX PLANE

The orientation of the x and y axes is chosen arbitrarily as a phase reference. The x-component of the resultant phasor is

$$R_x(\theta) = R(\theta) \cos o(\theta) = \sum_{i=1}^{n} a_i A(\theta - \theta_i) \cos \Phi_i \qquad \text{(Eq. D-1)}$$

and the y-component of the resultant phasor is

$$R_y(\theta) = R(\theta) \sin o(\theta) = \sum_{i=1}^{n} a_i A(\theta - \theta_i) \sin \Phi_i \qquad \text{(Eq. D-2)}$$

In complex notation, Equations D-1 and D-2 become

$$\tilde{R}(\theta) = R(\theta)\, e^{j\rho(\theta)} = \sum_{i=1}^{n} a_i\, A(\theta - \theta_i)\, e^{j\Phi_i} = \sum_{i=1}^{n} \tilde{a}_i\, A(\theta - \theta_i)$$

(Eq. D-3)

Note that $\tilde{R}(\theta)$ is a measurable quantity since $R(\theta)$ and $\rho(\theta)$ are measurable.

Clearly $\tilde{R}(\theta)$ is a periodic quantity, with period = 2π. Hence it may be expanded in a Fourier series:

$$\tilde{R}(\theta) = \sum_{k=-\infty}^{\infty} \tilde{\beta}_k\, e^{jk\theta} \qquad \text{(Eq. D-4)}$$

where

$$\tilde{\beta}_k = \frac{1}{2\pi} \int_0^{2\pi} \tilde{R}(\theta)\, e^{-jk\theta}\, d\theta \qquad \text{(Eq. D-5)}$$

We know that $A(\theta)$ is periodic also, hence it has the Fourier expansion

$$A(\theta) = \sum_{k=-\infty}^{\infty} \tilde{\alpha}_k\, e^{jk\theta} \qquad \text{(Eq. D-6)}$$

where

$$\tilde{\alpha}_k = \frac{1}{2\pi} \int_0^{2\pi} A(\theta)\, e^{-jk\theta}\, d\theta \qquad \text{(Eq. D-7)}$$

Hence, the right-hand side of Equation D-3 may be written

$$\sum_{i=1}^{n} \tilde{a}_i\, A(\theta - \theta_i) = \sum_{i=1}^{n} \tilde{a}_i \sum_{k=-\infty}^{\infty} \tilde{\alpha}_k\, e^{jk(\theta - \theta_i)}$$

$$= \sum_{k=-\infty}^{\infty} \tilde{\alpha}_k\, e^{jk\theta} \sum_{i=1}^{n} \tilde{a}_i\, e^{-jk\theta_i} \qquad \text{(Eq. D-8)}$$

Finally, from Equations D-4 and D-8, we have

$$\frac{\tilde{\beta}_k}{\tilde{\alpha}_k} = \tilde{\delta}_k = \sum_{i=1}^{n} \tilde{a}_i\, e^{-jk\theta_i} \qquad \text{(Eq. D-9)}$$

Equation D-9 represents a set of nonlinear simultaneous equations, one for each value of k. The left-hand side of Equation D-9 is known, since it is computed from the known quantities $A(\theta)$ and $\tilde{R}(\theta)$. Since there are 2n unknown quantities, $\tilde{a}_1 \ldots \tilde{a}_n$ and $\theta_1 \ldots \theta_n$, we expect that only 2n of Equation D-9 will be independent, and we can choose the most convenient set for the solution of the problem.

If we pick $k = +(n-1), \ldots +1, 0, -1, \ldots, -n$, and make the substitutions $S_i = e^{+j\theta_i}$ we get the equations

$$\tilde{\delta}_{n-1} = \tilde{a}_1 S_1^{-(n-1)} + \tilde{a}_2 S_2^{-(n-1)}, \ldots, + \tilde{a}_m S_n^{-(n-1)}$$

$$\tilde{\delta}_{n-2} = \tilde{a}_1 S_1^{-(n-2)} + \tilde{a}_2 S_2^{-(n-2)}, \ldots, + \tilde{a}_m S_n^{-(n-2)}$$

$$\vdots \qquad \vdots \qquad \vdots \qquad \vdots$$

$$\tilde{\delta}_o = \tilde{a}_1 + \tilde{a}_2 , \ldots, + \tilde{a}_n$$

$$\vdots \qquad \vdots \qquad \vdots \qquad \vdots$$

$$\tilde{\delta}_{-(n-1)} = \tilde{a}_1 S_1^{n-1} + \tilde{a}_2 S_2^{n-1} , \ldots, + \tilde{a}_n S_n^{n-1}$$

$$\tilde{\delta}_{-n} = \tilde{a}_1 S_1^{n} + \tilde{a}_2 S_2^{n} , \ldots, + \tilde{a}_n S_n^{n} \quad \text{(Eq. D-10)}$$

This set of equations can be solved by the following procedure:

a. Multiply the equation for $k = +(n-1)$ by S_1 and subtract it from the equation for $k = +(n-2)$ to form the first equation of a new set.

b. Multiply the equation for $k = +(n-2)$ by S_1 and subtract it from the equation for $k = +(n-3)$ to obtain the second equation of a new set.

c. Repeat the process for $(2n-1)$ pairs of equations. There will result $(2n-1)$ new equations with $\tilde{a}_1$ eliminated.

d. Repeat the entire process on the new set of $(2n-1)$ equations, multiplying by S_2 to obtain a third set of $(2n-2)$ equations

with $\tilde{a}_1$ and $\tilde{a}_2$ eliminated. The process is continued until all the $\tilde{a}_i$'s are eliminated.

The procedure results in the set of n equations

$$\begin{aligned}
&\tilde{\delta}_{-n} + \tilde{\delta}_{-(n-1)}U_1 + \tilde{\delta}_{-(n-2)}U_2, \ldots, + \tilde{\delta}_o U_n = 0 \\
&\tilde{\delta}_{-(n-1)} + \tilde{\delta}_{-(n-2)}U_1 + \tilde{\delta}_{-(n-3)}U_2, \ldots, + \tilde{\delta}_{+1}U_n = 0 \\
&\quad\vdots \qquad\qquad \vdots \qquad\qquad \vdots \qquad\qquad \vdots \\
&\tilde{\delta}_{-1} + \tilde{\delta}_o U_1 + \tilde{\delta}_{+1}U_2, \ldots, + \tilde{\delta}_{+(n-1)}U_n = 0
\end{aligned}$$

(Eq. D-11)

where

$$\begin{aligned}
U_1 &= -(S_1 + S_2 + S_3 + S_4, \ldots, + S_n) \\
U_2 &= +(S_1S_2 + S_2S_3, \ldots, + S_{n-1}S_n) \\
&\vdots \\
U_n &= (-1)^n (S_1S_2, \ldots S_n)
\end{aligned}$$

(Eq. D-12)

From Equations D-11 it is possible to solve directly for the U_i. Once the U_i are known, the S_i can be computed by the following technique:

a. Add S_1 to both side of the first of Equations D-12.

b. Multiply each of Equations D-12 by S_1^{n-m}, where m is the numerical subscript of U.

c. Add the resulting equations to yield the following polynomial

$$S_1^n + \tilde{\gamma}_1 S_1^{n-1}, \ldots, + \tilde{\gamma}_{n-1} S_1 + \tilde{\gamma}_n = 0 \qquad \text{(Eq. D-13)}$$

where $\tilde{\gamma}_i$ are the (complex) solutions for U_i arrived at from Equations D-11.

The elimination procedure leading to Equation D-3 might just as easily have used any of the S_i. From this, it follows that the n complex roots of Equation D-3 are the values of S_i, i=1, ..., n. Having found S_1, S_2, ..., S_n (the numbering is obviously arbitrary) we can substitute into any n of Equations D-10 to find the $\tilde{a}_1$, $\tilde{a}_2$, ..., $\tilde{a}_n$ associated with each of them. The amplitude, phase, and angular position of each source of Figure D-1 have now been completely determined.

The choice of +(n-1), ..., + 1, 0, -1, ..., -n for the values of k preceding Equations D-10 is the result of the desire to require as few harmonics as possible in the Fourier expansion of the antenna pattern. Thus it is necessary to have at least as many harmonics as sources. An interesting consequence of this statement is that the ability of an antenna satisfying this criterion to distinguish between various sources is limited only by the accuracy with which $\tilde{R}(\theta)$ and $A(\theta)$ can be measured. The solution presented above is the same regardless of whether two sources are 1° apart or 90° apart in angular position. Thus, if the initial measurement were exact, the antenna system described (antenna plus computation equipment) would, in effect, possess infinite resolving power.

As an example of this procedure, suppose that the antenna pattern is

$$A(\theta) = 1 + \cos\theta + \cos 2\theta \qquad \text{(Eq. D-14)}$$

The half-power beamwidth is 72°. By the method presented in this appendix, such an antenna should be capable of resolving two sources $\tilde{\alpha}_1$ and $\tilde{\alpha}_2$ at angular positions θ_1 and θ_2 respectively. In other words, Equation D-13 should reduce to an identity for $S = e^{j\theta 1}$ or $e^{j\theta 2}$. From D-14 we have

$$\tilde{\alpha}_2 = \tilde{\alpha}_2 = \frac{1}{2}$$

$$\tilde{\alpha}_1 = \tilde{\alpha}_1 = \frac{1}{2} \qquad \text{(Eq. D-15)}$$

$$\tilde{\alpha}_o = 1$$

The response of the antenna to the two sources is

$$\tilde{R}(\theta) = 1 + \tilde{\alpha}_1 \cos(\theta - \theta_1) + \tilde{\alpha}_2 \cos(\theta - \theta_2)$$

$$+ \tilde{\alpha}_1 \cos 2(\theta - \theta_1) + \tilde{\alpha}_2 \cos 2(\theta - \theta_2) \qquad \text{(Eq. D-16)}$$

From which

$$\tilde{\beta}_{-2} = \frac{1}{2}\left(\tilde{a}_1 e^{2j\theta_1} + \tilde{a}_2 e^{2j\theta_2}\right)$$

$$\tilde{\beta}_{-1} = \frac{1}{2}\left(\tilde{a}_1 e^{j\theta_1} + \tilde{a}_2 e^{2j\theta_2}\right)$$

$$\tilde{\beta}_o = \tilde{a}_1 + \tilde{a}_2$$

$$\tilde{\beta}_1 = \frac{1}{2}\left(\tilde{a}_1 e^{-j\theta_1} + \tilde{a}_2 e^{-j\theta_2}\right)$$

$$\tilde{\beta}_2 = \frac{1}{2}\left(\tilde{a}_1 e^{-2j\theta_1} + \tilde{a}_2 e^{-2j\theta_2}\right) \qquad \text{(Eq. D-17)}$$

From D-15 we have

$$\tilde{\delta}_{-2} = 2\tilde{\beta}_{-2}$$

$$\tilde{\delta}_{-1} = 2\tilde{\beta}_{-1} \qquad \text{(Eq. D-18)}$$

$$\tilde{\delta}_o = \tilde{\beta}_o$$

$$\tilde{\delta}_1 = 2\tilde{\beta}_1$$

which, following D-10, are all we need.

The solutions to D-11 are

$$\tilde{\gamma}_1 = \frac{\begin{vmatrix} -\tilde{\delta}_{-2} & \tilde{\delta}_o \\ -\tilde{\delta}_{-1} & \tilde{\delta}_1 \end{vmatrix}}{\Delta} \qquad \text{(Eq. D-19)}$$

$$\tilde{\gamma}_2 = \frac{\begin{vmatrix} \tilde{\delta}_{-1} & -\tilde{\delta}_{-2} \\ \tilde{\delta}_o & -\tilde{\delta}_{-1} \end{vmatrix}}{\Delta}$$

$$\Delta = \tilde{\delta}_{-1}\tilde{\delta}_1 - \tilde{\delta}_o^2$$

which, when the values of $\tilde{\delta}_i$ are substituted, become

$$\tilde{\gamma}_1 = \frac{\tilde{a}_1\tilde{a}_2 e^{j\theta_1}\left(1 - e^{j(\theta_1 - \theta_2)}\right) + \tilde{a}_1\tilde{a}_2 e^{j\theta_2}\left(1 - e^{j(\theta_2 - \theta_1)}\right)}{\Delta}$$

$$\tilde{\gamma}_2 = \frac{\tilde{a}_1\tilde{a}_2 e^{2j\theta_1}\left(1 - e^{j(\theta_2 - \theta_1)}\right) + \tilde{a}_1\tilde{a}_2 e^{2j\theta_2}\left(1 - e^{j(\theta_1 - \theta_2)}\right)}{\Delta}$$

$$\Delta = \tilde{a}_1\tilde{a}_2\left(1 - e^{j(\theta_1 - \theta_2)}\right) - \tilde{a}_1\tilde{a}_2\left(1 - e^{j(\theta_2 - \theta_1)}\right) \quad \text{(Eq. D-20)}$$

After some algebra, it can can be seen that the roots of

$$S^2 + \tilde{\gamma}_1 S + \tilde{\gamma}_2 = 0$$

are $S_1 = e^{j\theta_1}$, $S_2 = e^{j\theta_2}$ (Eq. D-21)

REFERENCES

Chapter 1

1. L. L. Libby, "Special Aspects of Balanced Shielded Loops," Proc. IRE, Vol. 34, pp. 641-646, September 1946

2. F. Adcock, "Some Early Observations on Aircraft with the Four-Aerial Direction-Finder," JIEE, Vol. 64, pp. 837-838, March 1926

3. T. Heiligtag, "Uber der Grunde der Missweisungen beim Richtungempfang," Jahrbuch Zeitschrift for Drahtlose Telegraphie und Telephonie, Vol. 21, p. 77, 1923

4. E. C. Hayden, "Some Basic Problems in the Determination of the Direction of Arrival of Radio Waves," Ph.D. Dissertation, University of Illinois, 1958

5. W. R. LePage, et al, "A Study of Directional Antenna Systems for Radio D/F Purposes," Syracuse University, Institute of Industrial Research, Report No. 5, TIP No. U10968, ca. September 1948

6. C. W. Earp, and R. M. Godfrey, "Radio Direction-Finding by the Cyclical Differential Measurement of Phase," JIEE, Vol. 94, Part IIIA, pp. 705-721, March 1947

7. B. Kovit, "Commutated-Antenna DF Meets Civil and Military Needs," Space/Aeronautics, Vol. 34, pp. 223-225, October 1960

8. A. D. Bailey, "An Investigation of the Direction of Arrival of Radio Waves," Ph.D. Dissertation, University of Illinois, 1954

9. E. C. Hayden, op. cit.

10. R. F. Donnelly, D. G. Detert, and A. D. Bailey, "A Study of High-Frequency Directional Propagation Over a 450 Kilometer East to West Path," University of Illinois, Radiolocation Research Laboratory, RRL No. 254, ASTIA No. AF-625-413; November 1965

REFERENCES (continued)

11. E. C. Hayden, "Propagation Studies using Direction-Finding Techniques," J. Res. Nat. Bur. Stand., Vol. 65D, No. 3, p. 197, May-June 1961

12. B. M. Bramley, "Directional Observations on H. F. Transmissions over 2100 Km," Proc. IEE, Vol. 103, Part B, No. 9, pp. 295-300, May 1956

13. W. C. Bain, "On the Rapidity of Fluctuations in Continuous-Wave Radio Bearings at High Frequencies," Proc. IEE, Paper 1715R; Publ. October 1954

14. S. B. Smith and H. G. Hopkins, "H.F. Directive-Finding," Wireless Engr., Vol. 13, pp. 11-14, January 1954

15. R. Silberstein, "Radio Propagation Effects on High-Frequency Direction-Finders; Phase I, Experimental," National Bureau of Standards, Central Radio Propagation Laboratory Quarterly Report No. 5, Contract No. 55055-PH-47-91 (6753), (TIP No. U2930), June 1948

16. W. M. Sherrill and D. N. Travers, "Shipboard Siting of Direction Finders for the 3 to 30 Mc Range," Southwest Research Institute, San Antonio, Texas, Report No. SR-19, Project No. SF001-0801, Contract No. Nobsr-89167, ASTIA No. AD-615-172, April 1965

17. H. Kunze and H. Rattei, "Terrain-Dependent Bearing Errors and Their Avoidance With VHF Rotating Adcock," Telefunken Ztg., Vol. 34, pp. 215-220, September 1961

18. W. Ross and F. Horner, "The Siting of Direction-Finding Stations," Radio Research Special Report No. 22, HMSO, also Nature, Vol. 169, p. 875, and U. S. Department of Commerce PB106738, May 1952

19. C. W. McLeish and R. S. Roger, "An Investigation of High Frequency Direction-Finding Errors Caused by Nearby Vertical Reradiators," Proc. IEE, Vol. 106B, pp. 58-60, January 1959

20. C. H. Brenner and G. A. Thiele, "Pattern Handbook: Volumes I-VI," Ohio State University Research Foundation, Columbus, Ohio, Report Nos. 1522-11 through 1522-16, ASTIA Nos. AD463370, AD467888, AD467893, AD468701, AD470818, and AD470819, 1 March 1965 to 1 August 1965

21. R. Bateman, E. F. Florman, and A. Tait, "A Source of Error in Radio Phase-Measuring Systems," Proc. IRE, Vol. 38, pp. 612-614, June 1950

22. H. G. Hopkins and F. Horner, "Direction-Finding Site Errors at Very High Frequencies," Proc. IEE, Part III, Vol. 96, pp. 321-332, July 1949

23. F. Horner, "The Scattering of Radio Waves by Metal Wires and Sheets," Proc. IEE, Part III, Vol. 96, pp. 333-340, July 1949

24. C. Crampton, R. T. P. Whipple, and H. H. Mugridge, "The Errors in Bearings of a High-Frequency Direction Finder Caused by Reradiation from a Nearby Vertical Mast," JIEE, Part IIIA, Vol. 94, pp. 815-822, March 1947

25. M. A. Ross, "Fundamental Problems in Radio Direction Finding at High Frequencies (3-30 Mc/s)," JIEE, Vol. 94, Part IIIA, pp. 154-165, March 1947

Chapter 2

1. W. Ross, "Site and Path Errors in Short-Wave Direction-Finding," JIEE, Part III, Vol. 94, pp. 108-114, March 1947

2. P. Beckmann and A. Spizzichino, "The Scattering of Electromagnetic Waves from Rough Surfaces," Pergamon Press, Chapter 7, pp. 119-151, 1963

3. M. Siddiqui, "Statistical Inference for Rayleigh Distributions," J. Res. NBS, Vol. 68D, pp. 1005-1010, September 1964

4. H. Cramer, "Mathematical Methods of Statistics," Princeton University Press, 1951

5. H. Cramer, op. cit., p. 141

6. J. A. Greenwood and D. Durand, "The Distribution of the Length and Components of the Sum of n Random Unit Vectors," Ann. Math. Stat., Vol. 26, pp. 233-246, June 1955

7. S. O. Rice, "Mathematical Analysis of Random Noise," Bell Syst. Tech. J., Vol. 23, pp. 282-332, 1944 and Vol. 24, pp. 46-157, 1954

8. P. Beckmann and A. Spizzichino, op. cit., pp. 120-129

9. ibid., p. 207

10. J. A. Greenwood and D. Durand, op. cit.

Chapter 3

1. P. Beckmann and A. Spizzichino, op. cit., p. 50

2. R. W. P. King and T. T. Wu, "The Scattering and Diffraction of Waves," Harvard University Press, Appendix, p. 213, 1959

3. R. F. Harrington, "Time-Harmonic Electromagnetic Fields," McGraw-Hill, Chapter 6, p. 293-294, 1961

4. R. W. P. King and T. T. Wu, op. cit., p. 209

Chapter 5

1. "IRE Standards on Navigation Aids: Direction Finder Measurements, 1959," Proc. IRE, Vol. 47, pp. 1350-1371, August 1959

Appendix B

1. H. Cramer, op. cit., pp. 424-426

2. M. M. Siddiqui, "Some Problems Connected with Rayleigh Distributions," J. Res. NBS, Vol. 66D, pp. 167-174, March-April 1962

3. K. A. Norton, L. E. Vogler, W. V. Mansfield, and P. J. Short, "The Probability Distribution of the Amplitude of a Constant Vector Plus a Rayleigh-Distributed Vector," Proc. IRE, Vol. 43, pp. 1354-1361, October 1955

General

1. L. A. Lyons and A. T. Adams, "A Statistical Analysis of Siting Error in Radio Direction-Finding," paper presented before URSI Fall Meeting, Palo Alto, California, December 1966

2. D. N. Travers and S. M. Hixon, "Abstracts of the Available Literature on Radio Direction-Finding, 1899-1965," Southwest Research Institute, San Antonio, Texas, Task Report No. XXI, Contracts No. NObsr-64585, NObsr-85086, NObsr 8916, July 1966

BIOGRAPHICAL DATA

NAME:	Laurence Anthony Lyons
DATE AND PLACE OF BIRTH:	June 5, 1939 Boston, Massachusetts
EDUCATION:	
Elementary School	Richard Olney School Boston, Massachusetts Graduated, 1950
High School	Boston Latin School Boston, Massachusetts Graduated, 1956
College	Harvard University Cambridge, Massachusetts A. B., 1960
Graduate Work	Syracuse University Syracuse, New York Graduate Research Assistant M. E. E., 1964
OTHER EXPERIENCE:	International Business Machines Corporation, 1960-1962 Syracuse University Research Corporation, 1965-1966

UNCLASSIFIED

Security Classification

DOCUMENT CONTROL DATA - R&D

(Security classification of title, body of abstract and indexing annotation must be entered when the overall report is classified)

1. ORIGINATING ACTIVITY (Corporate author) Defense Systems Division Syracuse University Research Corporation Box 26, University Station, Syracuse, New York 13210	2a. REPORT SECURITY CLASSIFICATION UNCLASSIFIED 2b. GROUP NONE

3. REPORT TITLE

A STATISTICAL ANALYSIS OF SITING ERROR IN RADIO DIRECTION-FINDING

4. DESCRIPTIVE NOTES (Type of report and inclusive dates)

Interim Report

5. AUTHOR(S) (Last name, first name, initial)

Lyons, Laurence A.

6. REPORT DATE	7a. TOTAL NO. OF PAGES	7b. NO. OF REFS
30 August 1967	148	45

8a. CONTRACT OR GRANT NO. NOnr 4798(00)	9a. ORIGINATOR'S REPORT NUMBER(S) DSD R-161
b. PROJECT NO. R and D Project CS 454 and CS 471	9b. OTHER REPORT NO(S) (Any other numbers that may be assigned this report) NONE
c. d.	

10. AVAILABILITY/LIMITATION NOTICES

DISTRIBUTION OF THIS DOCUMENT IS UNLIMITED

11. SUPPLEMENTARY NOTES	12. SPONSORING MILITARY ACTIVITY
NONE	Office of Naval Research Department of the Navy

13. ABSTRACT

A statistical model has been developed for a direction-finding site at HF (1 - 30 MHz). The model was used to analyze the effects of extended re-radiators on D/F accuracy and was examined both theoretically and experimentally.

An explicit expression is obtained for the probability density distribution of the electric field amplitude as a function of each of two quantities; azimuthal position of the transmitter and transmitter frequency. The distribution is shown to be a one-parameter Rice distribution in each case. The parameter may be obtained by sampling over either azimuthal angle or frequency.

It is suggested that this parameter be used as a single-number criterion for the evaluation of D/F sites.

DD FORM 1 JAN 64 1473

UNCLASSIFIED

Security Classification

14. KEY WORDS	LINK A		LINK B		LINK C	
	ROLE	WT	ROLE	WT	ROLE	WT
Direction Finding						
High Frequency						
Statistics						

INSTRUCTIONS

1. **ORIGINATING ACTIVITY:** Enter the name and address of the contractor, subcontractor, grantee, Department of Defense activity or other organization *(corporate author)* issuing the report.

2a. **REPORT SECURITY CLASSIFICATION:** Enter the overall security classification of the report. Indicate whether "Restricted Data" is included. Marking is to be in accordance with appropriate security regulations.

2b. **GROUP:** Automatic downgrading is specified in DoD Directive 5200.10 and Armed Forces Industrial Manual. Enter the group number. Also, when applicable, show that optional markings have been used for Group 3 and Group 4 as authorized.

3. **REPORT TITLE:** Enter the complete report title in all capital letters. Titles in all cases should be unclassified. If a meaningful title cannot be selected without classification, show title classification in all capitals in parenthesis immediately following the title.

4. **DESCRIPTIVE NOTES:** If appropriate, enter the type of report, e.g., interim, progress, summary, annual, or final. Give the inclusive dates when a specific reporting period is covered.

5. **AUTHOR(S):** Enter the name(s) of author(s) as shown on or in the report. Enter last name, first name, middle initial. If military, show rank and branch of service. The name of the principal author is an absolute minimum requirement.

6. **REPORT DATE:** Enter the date of the report as day, month, year; or month, year. If more than one date appears on the report, use date of publication.

7a. **TOTAL NUMBER OF PAGES:** The total page count should follow normal pagination procedures, i.e., enter the number of pages containing information.

7b. **NUMBER OF REFERENCES:** Enter the total number of references cited in the report.

8a. **CONTRACT OR GRANT NUMBER:** If appropriate, enter the applicable number of the contract or grant under which the report was written.

8b, 8c, & 8d. **PROJECT NUMBER:** Enter the appropriate military department identification, such as project number, subproject number, system numbers, task number, etc.

9a. **ORIGINATOR'S REPORT NUMBER(S):** Enter the official report number by which the document will be identified and controlled by the originating activity. This number must be unique to this report.

9b. **OTHER REPORT NUMBER(S):** If the report has been assigned any other report numbers *(either by the originator or by the sponsor)*, also enter this number(s).

10. **AVAILABILITY/LIMITATION NOTICES:** Enter any limitations on further dissemination of the report, other than those imposed by security classification, using standard statements such as:

(1) "Qualified requesters may obtain copies of this report from DDC."

(2) "Foreign announcement and dissemination of this report by DDC is not authorized."

(3) "U. S. Government agencies may obtain copies of this report directly from DDC. Other qualified DDC users shall request through _____."

(4) "U. S. military agencies may obtain copies of this report directly from DDC. Other qualified users shall request through _____."

(5) "All distribution of this report is controlled. Qualified DDC users shall request through _____."

If the report has been furnished to the Office of Technical Services, Department of Commerce, for sale to the public, indicate this fact and enter the price, if known.

11. **SUPPLEMENTARY NOTES:** Use for additional explanatory notes.

12. **SPONSORING MILITARY ACTIVITY:** Enter the name of the departmental project office or laboratory sponsoring *(paying for)* the research and development. Include address.

13. **ABSTRACT:** Enter an abstract giving a brief and factual summary of the document indicative of the report, even though it may also appear elsewhere in the body of the technical report. If additional space is required, a continuation sheet shall be attached.

It is highly desirable that the abstract of classified reports be unclassified. Each paragraph of the abstract shall end with an indication of the military security classification of the information in the paragraph, represented as *(TS), (S), (C), or (U)*.

There is no limitation on the length of the abstract. However, the suggested length is from 150 to 225 words.

14. **KEY WORDS:** Key words are technically meaningful terms or short phrases that characterize a report and may be used as index entries for cataloging the report. Key words must be selected so that no security classification is required. Identifiers, such as equipment model designation, trade name, military project code name, geographic location, may be used as key words but will be followed by an indication of technical context. The assignment of links, rules, and weights is optional.